Overtopping of Seawalls

Research and Development

Project Record
W5/006/5

ENVIRONMENT AGENCY

All pulps used in production of this paper is sourced from sustainable managed forests and are elemental chlorine free and wood free

Overtopping of Seawalls

R&D Project Record W5/006/5

P Besley

Research Contractor:

H R Wallingford Ltd

Further copies of this report are available from:
Environment Agency R&D Dissemination Centre, c/o
WRc, Frankland Road, Swindon, Wilts SN5 8YF

tel: 01793-865000 fax: 01793-514562 e-mail: publications@wrcplc.co.uk

Publishing Organisation
Environment Agency
Rio House
Waterside Drive
Aztec West
Almondsbury
Bristol
BS32 4UD

Tel: 01454 624400 Fax: 01454 624409

ISBN 1 85705 070 3

Dissemination Status
Internal: Released to Regions
External: Released to Public Domain

Statement of Use
This document provides full details of the project on overtopping of sea defences and provides the background to the production of Technical Report W178 – Wave Overtopping of Seawalls: Design and Assessment Manual.

Research Contractor
This document was produced under Environment Agency R&D Project W5-006 by:

HR Wallingford Ltd
Howbery Park
Wallingford
Oxfordshire
OX10 8BA

Tel: 01491 835381 Fax: 01491 832233

Environment Agency's Project Manager
The Environment Agency's Project Manager for R&D Project W5-006 was:
Keith Slaney - North East Region

R&D Project Record W5/006/5

CONTENTS

page

LIST OF FIGURES iii

LIST OF TABLES iv

NOTATION v

EXECUTIVE SUMMARY vii

1. INTRODUCTION 1

1.1 Introduction 1

1.2 Objectives and Methodology 1

1.3 Report outline 2

2. METHODS OF PREDICTING MEAN OVERTOPPING DISCHARGE 3

2.1 Introduction 3

2.2 Sloping structures 3

2.3 Vertical structures 8

2.4 Composite structures 12

2.5 Conclusions and recommendations 13

3. METHODS OF PREDICTING PEAK OVERTOPPING EVENTS 15

3.1 Introduction 15

3.2 Proportion of waves overtopping a structure 15

3.3 Maximum individual volume 17

3.4 Effect of angled wave attack 17

3.5 Conclusions 18

4. REVIEW OF SITE-SPECIFIC OVERTOPPING DATA 19

4.1 Introduction 19

4.2 Collation of details of overtopping studies 19

4.3 Assessment of the importance of the data 20

4.4 Assessment of gaps in data 22

4.5	Data analysis	22
4.6	Conclusions	25
5.	**CREST WALLS LOCATED ON ROCK-ARMOURED SEAWALLS**	**26**
5.1	Introduction	26
5.2	Crest wall discharge coefficients	26
5.3	Bradbury et al's data	27
5.4	Owen and Steele's method	27
5.5	Discharge factors for walls on permeable slopes	29
5.6	Effect of recurved wall on discharge factors	29
5.7	Effect of crest berm width on discharge factors	30
5.8	Design chart	30
5.9	Conclusions	31
6.	**ANALYSIS OF WAVE BY WAVE OVERTOPPING**	**32**
6.1	Introduction	32
6.2	Experimental technique	32
6.3	Number of waves overtopping	33
6.4	Maximum individual overtopping event	36
6.5	Effect of angled wave attack on number of waves overtopping	38
6.6	Relationship between peak events and mean discharge	39
6.7	Peak flow rates	40
6.8	Conclusions	40
7.	**THE EFFECT OF CREST BERM WIDTH ON OVERTOPPING DISCHARGES**	**41**
7.1	Introduction	41
7.2	Previous work	41
7.3	Model tests	42
7.4	Test results	43

7.5 Design guideline 44

7.6 Conclusions 45

8. TOLERABLE OVERTOPPING LIMITS 46

8.1 Introduction 46

8.2 Model studies 46

8.3 Prototype experiences and observations 46

8.4 Mean discharges 49

8.5 Specification of tolerable overtopping 49

LIST OF FIGURES

Figure 2.1 Owen (1980) relationship for impermeable simple slopes
Figure 2.2 Wave return wall
Figure 2.3 Wave return wall design chart (Owen and Steele(1991))
Figure 2.4 Goda's (1985) graphical design method
Figure 2.5 Overtopping of vertical wall (Allsop et al (1995))
Figure 2.6 De Waal's (1994) vertical wall overtopping data
Figure 2.7 Vertical wall under impacting wave attack (Allsop et al (1995)
Figure 2.8 Composite structure

Figure 4.1 Overtopping of simply sloping smooth structure
Figure 4.2 Overtopping of SHED armoured slopes with and without crest berm
Figure 4.3 Overtopping of Antifer armoured slopes with crest berms
Figure 4.4 Overtopping of rock armoured slopes with crest walls
Figure 4.5 Overtopping of Accropode armoured slopes
Figure 4.6 Effect of slope roughness on overtopping
Figure 4.7 Vertical seawall at Colwyn Bay
Figure 4.8 Overtopping of vertical seawall at Colwyn Bay

Figure 5.1 Sections tested by Bradbury et al
Figure 5.2 Owen and Steele's (1991) design chart
Figure 5.3 Overtopping of section 14
Figure 5.4 Discharge factors of recurved wall on rock armoured slope
Figure 5.5 Discharge factors of crest walls on rock armoured slopes
Figure 5.6 Discharge factors for crest wall on rock armoured slope, $W_*h = 3.73$
Figure 5.7 Discharge factors for crest wall on rock armoured slope, $W_*h = 2.64$
Figure 5.8 Discharge factors for crest wall on rock armoured slope, $W_*h = 2.09$
Figure 5.9 Discharge factors for crest wall on rock armoured slope, $W_*h = 1.55$
Figure 5.10 Discharge factors for crest wall on rock armoured slope, $W_*h = 1.32$
Figure 5.11 Discharge factors for crest wall on rock armoured slope, $W_*h = 0.94$
Figure 5.12 Discharge factors for crest wall on rock armoured slope, $W_*h = 0.74$
Figure 5.13 Discharge factors for crest wall on rock armoured slope, $W_*h = 0.55$
Figure 5.14 Discharge factors for crest wall on rock armoured slope, $W_*h = 0.40$
Figure 5.15 Discharge factors for crest wall on rock armoured slope, $W_*h = 0.20$

Figure 5.16 Discharge factors for crest walls on rock armoured slopes, selected values of W*h
Figure 5.17 Effect of recurved wall on discharge factors
Figure 5.18 Effect of crest berm on discharge factors
Figure 5.19 Discharge factors for crest walls on rock armoured slopes, selected values of W*h
Figure 5.20 Design chart

Figure 6.1 Number of waves overtopping a vertical wall, deep and shallow water
Figure 6.2 Number of waves overtopping a vertical wall, impacting waves only
Figure 6.3 Number of waves overtopping simple armoured slopes
Figure 6.4 Number of waves overtopping sloped structures, all structural types
Figure 6.5 Distribution of individual overtopping volumes, reflecting waves
Figure 6.6 Distribution of individual overtopping volumes, impacting waves
Figure 6.7 Predicted and measured maximum volume
Figure 6.8 Relationship between mean discharge and peak event, (reflecting waves)
Figure 6.9 Relationship between mean discharge and peak event (impacting waves)
Figure 6.10 Relationship between mean discharge and peak event (Structure A)
Figure 6.11 Relationship between mean discharge and peak event (Structure B)

Figure 7.1 Effect of crest width on overtopping, Lowe (1991)
Figure 7.2 Accropode armoured structure
Figure 7.3 Rock armoured structure
Figure 7.4 Overtopping without crest berm (Accropode armoured structure)
Figure 7.5 Overtopping without crest berm (rock armoured structure)
Figure 7.6 Effect of crest width on overtopping (Accropode armoured structure)
Figure 7.7 Effect of crest width on overtopping (rock armoured structure)
Figure 7.8 Effect of crest width on overtopping (dimensionless data)

Figure 8.1 Tolerable mean discharges

LIST OF TABLES

Table 2.1 A and B coefficients : simply sloping seawalls
Table 2.2 A and B coefficients : bermed structures
Table 2.3 Roughness coefficients

Table 4.1 Overtopping studies included in the review
Table 4.2 Type of overtopping measurements

Table 5.1 Geometric parameters of sections tested by Bradbury et al
Table 5.2 Regression analysis to equation of form $D_f = X A_{*c}^{Y}$
Table 5.3 Regression analysis to equation of form $D_f = X Q_{*b}^{Y}$

Table 7.1 Herbert & Reeves (1991) overtopping results
Table 7.2 Lowe (1991) overtopping results
Table 7.3 Overtopping test wave conditions
Table 7.4 Overtopping test results

NOTATION

a,b	empirically determined coefficients (Franco, vertical walls)
A,B	empirically determined coefficients (Owen, slopes)
A,B,C	Weibull fitting coefficients
A_c	Armour crest freeboard
A_{*c}	Dimensionless armour crest freeboard = $A_c / (T_m (g H_s)^{0.5})$
c,C	empirically determined coefficients
C_f	crest berm reduction factor
Cw	Crest berm width
d	depth of water over mound of composite structure
D_f	return wall discharge factor
h_*	wave breaking parameter = $(h/H_s) (2\pi h/gT_m^2)$
h	water depth at the toe of the seawall
H_s	significant wave height at the toe of the seawall
H_{so}	offshore significant wave height
L_o	deep water wave length
N_{ow}	number of waves overtopping
N_w	number of waves in sequence
O_r	overtopping ratio for angled wave attack
P(V)	probability of non-exceedance of individual volume, V
q_b	peak discharge at point of wave breaking
Q_b	mean overtopping base discharge (Owen and Steele)
Q_*	dimensionless mean discharge (Owen, slopes) = $Q / (gT_mH_s)$
Q_{*v}	dimensionless mean discharge (van der Meer and de Waal, slopes) = $Q / (s_{op}/(g H_{so}^3 \tan\alpha))^{0.5}$
$Q^{\#}$	dimensionless mean discharge (Franco, vertical walls) = $Q / (gH_s^3)^{0.5}$
$Q^{\#G}$	dimensionless mean discharge (Goda, vertical walls) = $Q / (2gH_{so}^3)^{0.5}$
Q_h	dimensionless mean discharge (Allsop et al, vertical walls) = $Q/(gh^3)^{0.5}/ h_*^2$
Q_d	dimensionless mean discharge (Allsop et al, composite structures) = $Q/(gd^3)^{0.5} / d_*^2$
Q	mean overtopping discharge per unit length of seawall
Q_w	mean discharge measured at a distance of w behind crest
r	roughness coefficient
R_*	dimensionless crest freeboard (Owen, slopes) = $R_c / (T_{mi}(gH_s)^{0.5})$
R_{*v}	dimensionless crest freeboard (van der Meer and de Waal, slopes) = $R_c (s_{op})^{0.5}/ (H_{so} \tan\alpha)$
R_h	dimensionless crest freeboard (Allsop et al, vertical walls) = $(R_c/H_s) h_*$
R_d	dimensionless crest freeboard (Allsop et al, composite structure) = $(R_c/H_s)(d/H_s)d_*$
R_c	crest elevation above still water level
s_m	nominal wave steepness = H_s/L_o
s_{op}	offshore sea steepness = $2\pi H_{so}/gT_{po}^2$
T_m	mean zero crossing wave period at the toe of the seawall
T_{mo}	offshore mean zero crossing period
T_p	peak wave period at the toe of the seawall
T_{po}	offshore peak wave period
V	individual overtopping volume
V_{bar}	average individual overtopping volume

V_{max}	maximum individual overtopping volume
Wh	wave return wall height
W*h	dimensionless wave return wall height
α	angle of the seawall slope to the horizontal
β	angle of wave attack to the normal
δ	ratio of wave height to water depth at breaking
γ	reduction factor for angled wave attack (Franco, vertical walls)
γ_t	total reduction factor = $\gamma_b,\gamma_f,\gamma_\beta,\gamma_h$ (van der Meer and de Waal, slopes)
γ_b	reduction factor for berms
γ_f	reduction factor for roughness
γ_β	reduction factor for oblique short crested wave attack
γ_h	reduction factor for depth-limited wave attack
γ_x	reduction factor for structural type (Franco)
γ_{pow}	reduction factor for number of waves overtopping
Γ	Gamma function
ξ_{op}	surf similarity parameter = $\tan\alpha / (s_{op})^{0.5}$

EXECUTIVE SUMMARY

Man-made defences, predominantly in the form of seawalls protect approximately 860 kilometres (23%) of the English coast. These defences range from simple earth embankments through vertical concrete walls and onto more complex composite structures often involving wave return walls and/or rock armouring. Regardless of structural type, the purpose of a seawall is usually to prevent erosion of the coastline and to limit the risk of marine inundation of the hinterland.

Over the past twenty years much research has been undertaken in the UK and elsewhere into the overtopping performance of seawalls and related structures. In the UK the Ministry of Agriculture, Fisheries and Food under Commission FD02 has funded most of this research effort.

The research has concentrated on providing techniques for predicting the mean overtopping discharge, and hence consequent flood volumes and drainage requirements, for a range of commonly occurring seawall types. Little, or no attention, has been paid to either the peak individual (wave-by-wave) overtopping discharge or to the number of waves likely to overtop a particular defence, despite the importance of these two parameters in determining the overall standard of performance of a sea defence.

It is now recognised that :-

- peak overtopping discharges represent the most hazardous events for pedestrians and vehicles moving behind the wall, and that for certain seawall designs the peak individual discharge may also be the event initiating damage to, or failure of, the defence
- the number of waves overtopping a seawall is the most easily recorded indicator of overtopping performance, being amenable to both visual observation and capture on video cameras etc. As such, if suitable relationships can be established, the number of overtopping waves provides the most obvious means of calibrating prediction techniques defined in terms of either mean or peak individual discharge.

This project record draws together and summarises previous research into the overtopping performance of seawalls. Data is re-analysed to provide a set of consistent design techniques, representing the most reliable approach to the assessment of seawall overtopping by wave action. The empirical formulae presented in the Wave Overtopping of Seawalls Design and Assessment Manual, R & D Technical Report W178, is based on the data described within this project record.

The manual is intended to be used by flood and coastal defence engineers responsible for the design of new seawalls or the assessment and possible remediation of existing structures.

KEY WORDS

Flood control works, coastal structures, breakwaters, vertical seawalls, sloping seawalls, mean and peak overtopping discharges, tolerable discharge, normal and oblique wave attack.

1. INTRODUCTION

1.1 Introduction

Over the last ten years MAFF have funded a long-term research programme into methods to predict overtopping discharges over different types of sea defences. The performance of many structures such as embankments and vertical walls has been analysed for a range of conditions, under both normal and oblique wave attack. In addition, complimentary work has been carried out in Holland and Italy, for dyke and composite caisson structures.

The objective of this project is to bring together results of all relevant work carried out to date and to present them in the form of a design manual. Traditionally, design for the overtopping of seawalls has been concerned with the mean overtopping discharge. It has recently become acknowledged, however, that peak discharges are of greater significance to the safety of users of a seawall than mean discharges. The design methods presented in the manual will therefore provide means of calculating not just mean overtopping discharges but also peak overtopping discharges, expressed in terms of the largest volume contained in a single overtopping wave. The manual will also make recommendations concerning tolerable overtopping limits in terms of peak discharges.

This project record describes the work involved in formulating the design methods recommended in the manual. It includes a review and assessment of research previously conducted by HR Wallingford and other organisations, as well as descriptions of research conducted especially for the purposes of this project. The manual, which summarises the work described in this report, is published as Wave Overtopping of Seawalls R&D Technical Report W178.

1.2 Objectives and Methodology

The principal objective of the project was to collate and compile in an integrated format all the appropriate information regarding the overtopping of seawalls. The work and methods used in the project are described below:-

(i) A thorough review of all the available information regarding the overtopping of seawalls was carried out. This included data in the possession of HR Wallingford as well as other sources. The source data was largely in the form of physical model test results, but also included results acquired from prototype monitoring programmes and on-site observations. All aspects of overtopping were examined, including mean and peak discharges and tolerable limits.

(ii) Some aspects of overtopping have been the subject of a considerable number of investigations and there are inevitable differences in their methodologies and conclusions. Where data sources or design methods contradicted one another, the most appropriate for inclusion in the manual had to be identified.

(iii) Areas in which data was regarded as insufficient were identified. Where appropriate, these gaps in the knowledge were filled by additional experiments or by re-analysis of existing data.

(iv) The data was compiled in an integrated format which would form the basis of the new manual.

1.3 Report outline

The project record outline is described below: -

Chapter 2 provides a review of the most widely accepted methods of predicting mean overtopping discharges of seawalls. A variety of types of structure are examined, which include sloped and vertical seawalls. The effect of both normal and angled wave attack is considered. Where two or more calculation procedures are available their merits are discussed and the most appropriate method recommended.

Chapter 3 examines methods to predict peak overtopping events. Results are presented for a variety of structural types. This area has been the subject of considerably less research than mean discharges.

Chapter 4 examines site-specific data, i.e., that which is concerned with a specific structure rather than a structural type. Such data can be used to validate, and in some cases extend, prediction methods. As well as looking at model tests, Chapter 4 also examines the results of a prototype monitoring programme conducted on a vertical seawall.

The next three Chapters each examine in detail an aspect of overtopping design which was identified in the review as potentially benefiting from additional research or analysis. Chapter 5 looks at the effectiveness of crest walls on permeable slopes, by re-examining an existing data set. A modified design method is proposed as a result.

Chapter 6 presents analysis of peak individual overtopping volumes. Model test data held by HR Wallingford in which individual wave-by-wave overtopping volumes were measured is re-examined. The relationships between mean and peak discharges are examined for a variety of structures.

Chapter 7 looks at the effect of a permeable crest berm on mean overtopping discharge, an area which is not sufficiently considered in existing design methods. A programme of model tests was commissioned and carried out. The results of these tests form the basis of a new design rule.

Chapter 8 examines tolerable overtopping limits in terms of peak events. The source data includes observations, experiences and video records from prototype seawalls under storm conditions.

2. METHODS OF PREDICTING MEAN OVERTOPPING DISCHARGE

2.1 Introduction

This chapter reviews the most widely accepted methods for predicting the overtopping of seawalls. A variety of structural forms are examined, including sloped seawalls, vertical seawalls, composite seawalls and seawalls with return walls. The effect of both normal and angled wave attack is examined. In each case the merits of the various methods are discussed and recommendations made as to the most appropriate for inclusion in the manual. All the methods discussed here apply to mean discharges only. Prediction of maximum individual overtopping volume is dealt with in Chapter 3.

2.2 Sloping structures

2.2.1 Normal wave attack

A considerable number of studies have been undertaken into the overtopping performance of seawalls. Many of these earlier studies were completed in the USA and used regular wave physical model studies. Subsequently, a number of authors have produced design methods to predict mean overtopping discharge. The most comprehensive series of random wave studies was completed by Owen (1980), who investigated the performance of simply sloping and bermed structures. More recently van der Meer and de Waal (1992) have proposed an alternative set of equations. This section examines both of these methods in detail.

Owen (1980) carried out a number of physical model tests to study overtopping and determined a relationship linking the height of the seawall and the overtopping discharge. A method was developed for predicting overtopping discharge utilising relatively simple, straightforward formulae.

In Owen's (1980) equation the height of the seawall and the discharge are expressed in terms of the dimensionless freeboard and the dimensionless discharge. The dimensionless freeboard, R_*, is defined as :-

$$R_* = R_c / (T_m(gH_s)^{0.5}) \qquad (2.1)$$

where R_c is the crest elevation above still water level
T_m is the mean zero crossing wave period at the toe of the seawall
H_s is the significant wave height at the toe of the seawall

Note that wave conditions are defined at the toe of the seawall. The numerical value of R_* is small when a low seawall is attacked by large or long period waves. The physical significance of R_* is perhaps best appreciated if it is re-written in the following form :-

$$R_* = (R_c / H_s)\,(s_m/2\pi)^{0.5} \qquad (2.2)$$

where s_m is the nominal wave steepness ($= H_s/L_o$).
L_o is the deep water wave length

The second definition indicates that, for waves of constant steepness, R_* is simply related to the ratio of the crest freeboard to the wave height.

The dimensionless discharge, Q_*, is defined as :-

$$Q_* = Q / (gT_mH_s) \quad (2.3)$$

where Q is the mean overtopping discharge in terms of discharge per unit length of seawall.

Again the physical significance of Q_* is perhaps best illustrated by re-writing it as :-

$$Q_* = (Q / (gH_s^3)^{0.5}) (s_m/2\pi)^{0.5} \quad (2.4)$$

For waves propagating onto a beach or up a sloping seawall the peak discharge, q_b, at the point of the wave breaking is given approximately by :-

$$q_b = (gH_s^3)^{0.5} / (2\,\delta^{0.5}) \quad (2.5)$$

where δ is the ratio of the wave height to the water depth at breaking.

It can be seen therefore that Q_* can be re-written as :-

$$Q_* = (Q / q_b) (s_m/2\pi)^{0.5} / (2\,\delta^{0.5}) \quad (2.6)$$

or in other words, for constant wave steepness and breaking ratio, Q_* is simply related to the ratio of the overtopping discharge to the wave breaking discharge.

Owen's (1980) physical model tests led to an experimental formula linking the dimensionless overtopping discharge to the dimensionless freeboard for a simple seawall :-

$$Q_* = A \exp (- B R_*/r) \quad (2.7)$$

where $Q_* = Q / (gT_mH_s)$
$R_* = R_c / (T_m(gH_s)^{0.5})$
r = roughness coefficient
A and B are empirically determined coefficients

A seawall is thus defined by its crest freeboard, and the gradient and roughness of its slope. The wave climate is defined by the mean period and significant waveheight at the toe of the structure.

Owen (1980) derived, or interpolated, values of A and B for simple seawalls ranging in slope angle from 1:1 to 1:5. Figure 2.1 plots equation 2.7 for a selection of simply sloping impermeable seawalls. Owen (1980) also found that the equations derived for simply sloping seawalls could equally be applied to the bermed structures tested in the study, albeit with modified empirical coefficients. The original coefficients proposed by Owen (1980) have recently been revised as further research has become available. Tables 2.1 and 2.2 give the recommended values for simply sloping and bermed structures respectively. The values of A and B were determined experimentally within the following range of parameters :-

$$0.05 < R_* < 0.30$$
$$10^{-6} < Q_* < 10^{-2}$$
$$1.5 < h/H_s < 5.5$$
$$0.035 < H_s/L_o < 0.055$$

where h is the water depth at the toe of the seawall

Owen (1980) produced typical values of the roughness coefficient based upon the relative run-up performance of alternative types of construction. Results are given in Table 2.3.

Work on structures armoured with concrete units (Besley et al (1996)), suggests that the Owen (1980) formula, although giving an acceptable estimate of the hydraulic performance, does not accurately predict the overtopping discharge over a wide range of R_*. Data suggest that the point at which the prediction line intersects the Q_* axis depends on the type of armouring. Equation 2.7 can not account for this through variation of r alone. The intersection on the Q_* axis is given by the coefficient A, which should be a function of the structure slope only.

To predict the overtopping performance of a structure armoured with concrete units with confidence it is therefore recommended that model tests should be carried out. Where this is not possible, model results from a similar configuration to that of the proposed design may be used to estimate the mean overtopping discharge, using a regression based on A, B and r=1. Where no model data is available the Owen (1980) formulae using published values of A, B and a roughness coefficient will give an estimate of the mean overtopping discharge acceptable for use during the preliminary design stage.

An important factor affecting the performance of permeable seawalls is the width of the crest berm. Very little data concerning the effect of permeable crest berms on overtopping discharges is available. A variety of site-specific model tests had suggested that the overtopping discharge reduces by a factor of 10 for every 10m landward of the top of the slope. This factor has been adopted as an approximate design rule. It was felt, however, that a more precise relationship could be determined. A programme of model tests was commissioned and carried out for this purpose. The results are described in Chapter 7 of this report.

The Owen (1980) method has been extended by Owen and Steele (1991) to include the influence of wave return walls (Figure 2.2) located on impermeable seawalls. The effect of the return wall was described by an empirically determined discharge factor, D_f. The discharge factor of a return wall is the ratio of the overtopping discharge over a seawall with the return wall in place to that over the same seawall without a return wall. Results were produced for a variety of seawall slopes and return wall heights and presented in the form of a graphical design method (Figure 2.3). The Owen and Steele (1991) method isolated the effect of the height of the return wall from that of the seawall on which it was based. The discharge factor determined for a particular height of return wall could be thus be applied to other situations.

Bradbury et al (1988) derived an alternative method to describe the performance of return walls on permeable slopes. Overtopping performance was described in terms of the freeboard of the overall structure. This approach does not therefore address the question of the efficacy of raising the crest wall as compared to raising the armour crest level. The

performance of wave return walls on permeable slopes was one of the areas identified as requiring additional analysis for the purposes of the manual. An examination of Bradbury et al's (1988) original data set suggested that, with re-analysis, it could form the basis of an improved design method. This method is presented in Chapter 5 of this report.

Recently van der Meer and de Waal (1992) have proposed an alternative series of equations to estimate overtopping for simply sloping and bermed seawalls. Wave overtopping is expressed by one of two formulae, the choice of which depends on whether the structure is subject to plunging (breaking) or surging (non-breaking) waves. Plunging waves are defined as those where the surf similarity parameter, ξ_{op}, < 2, whilst for surging waves $\xi_{op} \geq 2$.

The surf similarity parameter is defined as :-

$$\xi_{op} = \tan\alpha / \sqrt{(s_{op})} \qquad (2.8)$$

where α is the angle of the seawall slope to the horizontal
s_{op} is the offshore sea steepness ($=2\pi H_{so}/gT_{po}^2$)
H_{so} is the offshore significant wave height
T_{po} is the offshore peak wave period.

For plunging waves the crest freeboard and discharge are non-dimensionalised as follows :-

$$R_{*v} = R_c \sqrt{s_{op}} / (H_{so} \tan\alpha) \qquad (2.9)$$

$$Q_{*v} = Q\sqrt{(s_{op} / (g H_{so}^3 \tan\alpha))} \qquad (2.10)$$

These equations are related using :-

$$Q_{*v} = 0.06 \exp(-5.2 R_{*v} / \gamma) \qquad (2.11)$$

where
γ is the total reduction factor $= \gamma_b \gamma_f \gamma, \gamma_h$
γ_b is the reduction factor for berms
γ_f is the reduction factor for roughness
γ_β is the reduction factor for oblique short crested wave attack
γ_h is the reduction factor for depth-limited wave attack

For surging waves the parameters are non-dimensionalised as follows :-

$$R_{*v} = R_c / H_{so} \qquad (2.12)$$

$$Q_{*v} = Q / \sqrt{(g H_{s\,o}^3)} \qquad (2.13)$$

and are related by :-

$$Q_{*v} = 0.2 \exp(-2.6 R_{*v} / \gamma) \qquad (2.14)$$

The equations of Owen (1980) and van der Meer and de Waal (1992) both have advantages and disadvantages for the designer. The Owen (1980) equation is simple to use but requires numerous empirical coefficients in order to study different wall profiles. Alternatively the van der Meer and de Waal (1992) equations are more complicated to use, but do not use

different empirical coefficients for alternative seawall profiles. The drawback of reducing to one the number of empirical coefficients in the van der Meer and de Waal (1992) equations is that a significant amount of averaging has been applied in the derivation of the equations. This has resulted in a loss of definition in the calculated overtopping discharges for any particular seawall profile.

Furthermore the work of Owen (1980) uses input wave conditions derived at the toe of the seawall. This is in contrast to van der Meer and de Waal (1992) who use deep water wave conditions as input and then allow for wave breaking through the use of γ_h. The method of calculating γ_h proposed by van der Meer and de Waal (1992) is strictly only applicable to foreshore slopes of 1:100. This may significantly influence the results on, say, UK shingle beaches backed by a seawall. Under extreme conditions the shingle beach may be completely submerged and form a steep foreshore slope for the incident waves.

After much deliberation the authors have concluded that the method proposed by Owen (1980) is presently the most appropriate means of estimating overtopping discharges at smooth simply sloping and bermed seawalls around the UK coastline. It is considered that the use of a large number of empirical coefficients is a minor drawback in comparison to the increased accuracy of the results.

2.2.2 Angled wave attack

The work described above applies to normal wave attack only. A variety of authors have investigated the influence of angled wave attack on overtopping discharge.

Owen (1980) and de Waal and van der Meer (1992) investigated the performance of simply sloping and bermed seawalls under angled wave attack. Under long crested waves Owen (1980) noted that overtopping could increase, compared to normal wave attack, for attack angles of up to 30° to the normal with the maximum increase occurring at 15°.

De Waal and van der Meer (1992) derived equations to describe the reduction factor for overtopping under oblique wave attack, γ_β. It is intended that this factor be used in the van der Meer and de Waal equations (1992) described above (equations 2.11 and 2.14). For long-crested waves :-

$$\gamma_\beta = \cos^2 (\beta\text{-}10^\circ) \qquad (2.15)$$

where β is the angle of wave attack to the normal in degrees.

Equation 2.15 is valid for $\gamma_\beta \geq 0.60$. When $0^\circ \leq \beta \leq 60^\circ$ then $\gamma_\beta = 1$.

For short-crested waves the reduction factor is given by :-

$$\gamma_\beta = 1 - 0.0033\ \beta \qquad (2.16)$$

Banyard and Herbert (1995) have reported separate equations to describe the behaviour of simply sloping and bermed seawalls in short-crested seas. These equations enable the overtopping ratio, O_r, to be calculated where O_r is defined as the ratio of overtopping at a given wave angle to that predicted under normal wave attack. For simply sloping seawalls :-

$$O_r = -0.000152\,\beta^2 + 1 \qquad (2.17)$$

and for bermed seawalls:-

$$O_r = 1.99 - 1.93\left[1.0 - \left(\frac{\beta - 60.0}{69.8}\right)^2\right]^{0.5} \qquad (2.18)$$

The behaviour of the two types of seawall differed considerably, with the bermed structure exhibiting a greater reduction in overtopping, for a given wave angle, than the simply sloping seawalls. The difference in performance was particularly noticeable at small angles of wave attack. Banyard and Herbert (1995) also found that the overtopping at angled attack was in all cases less for long-crested seas that for short-crested. The above equations can thus be applied conservatively to long-crested seas.

The authors concluded that the Banyard and Herbert (1995) method was most appropriate for inclusion in the manual. The de Waal and van der Meer (1992) equation and the Banyard and Herbert (1995) equations show similar trends and have a similar range of applicability. The de Waal and van der Meer (1992) equation, however, is intended for use with van der Meer and de Waal's (1992) overtopping equations (2.11 and 2.14). As the overtopping manual will use Owen's (1980) equation to calculate normal mean discharge, the Banyard and Herbert (1995) method is considered more appropriate.

The behaviour of recurved walls located on top of sloped seawalls under angled wave attack was also investigated by Banyard and Herbert (1995). They related the overtopping reduction factor to the discharge factor, D_f, by the following equation :-

$$O_r = -1.18\,\mathrm{Ln}(D_f) - 0.4 \qquad (2.19)$$

This equation is valid for all angles up to and including 45° and is applicable to both short and long-crested seas. The general trend of the data showed that overtopping at angled wave attack is greater than that at normal wave attack (i.e. $O_r > 1$) for values of D_f less than 0.31.

This contrasts with the results of Franco (1996) who found that, as with other structures, the overtopping of a recurve wall on a slope tended to reduce as the angle of attack increased. However, it is felt that the relative height of the wave return wall (and hence D_f) may be an important factor in this phenomenon. The authors therefore recommend that the method of Banyard and Herbert (1995) be adopted even though it may be overly conservative.

2.3 Vertical structures

2.3.1 Normal wave attack

Vertical or near vertical seawalls protect a significant length of the UK coastline. These seawalls are common in urban areas and are often sited behind shingle or sandy beaches. A number of authors have studied the overtopping of vertical walls.

Goda (1985) investigated the overtopping performance of plain vertical seawalls for approach slopes of 1:10 and 1:30 and offshore sea steepnesses, $s_{om} = 2\pi H_{so}/gT_{mo}^2$ (where H_{so} and T_{mo} are respectively the offshore significant wave height and period) ranging from 0.012 to 0.036.

Goda (1985) proposed a design method based on a graphical format. For a given approach bathymetry and offshore sea steepness, a dimensionless discharge, $Q^{\#G}$, was plotted on the y-axis against h/H_{so} on the x-axis. H is the depth of water at the toe of the structure and $Q^{\#G}$ is given by :-

$$Q^{\#G} = Q / (2gH_{so}^3)^{0.5} \quad (2.20)$$

Lines of constant relative freeboard, R_c/H_{so}, were illustrated on each graph, where R_c is the height of the crest of the wall above still water level. Figure 2.4 shows an example.

The wave conditions and bathymetry considered by Goda (1985) are generally unrepresentative of conditions around the UK coastline where storm sea steepnesses are greater and approach slopes are shallower. Consequently, work was carried out by Herbert (1993) to confirm and extended the work of Goda (1985) to typical UK conditions. Conditions were varied to cover approach bathymetries of 1:10, 1:30 and 1:100 and offshore sea steepnesses of $0.017 < s_{om} < 0.060$, where $s_{om} = 2\pi H_{so}/gT_{mo}^2$. The measured overtopping data gave good agreement with the work of Goda (1985).

The weakness of the work of Goda (1985) and Herbert (1993) is that significant interpolation is required. The influence of the offshore bathymetry must be assessed by selecting the nearest simple seabed slope whilst graphs are only available for a limited number of offshore sea steepnesses.

Analysis by Besley et al. (1994) suggested that the prediction method developed by Owen (1980) for slopes could be applied to vertical walls if inshore values of wave height and mean period were used. Overtopping of a wall in relatively shallow waters depends on the inshore wave height, period and form of breaking. Analysis of the tests on simple vertical walls completed at HR Wallingford in 1994 using the inshore wave conditions gave the following relationship between Q_* and R_* :-

$$Q_* = 0.002 \exp(-26.76\, R_*) \quad (2.21)$$

Franco (1993) conducted physical model studies to investigate the effects of overtopping on vertical structures. Eventually a formally similar approach to Goda (1985) was produced, using an exponential relationship linking the height of the structure and the overtopping discharge. However the formula was expressed in terms of different dimensionless parameters.

The dimensionless parameter that accounts for the influence of the structure freeboard on overtopping is simply expressed as the ratio of the freeboard to the inshore wave height, R_c/H_s.

The numerical value of R_c/H_s is small when a low seawall is attacked by large waves. The parameter does not take account of the wave steepness and therefore assumes that the process of overtopping is not directly influenced by the wave period.

The dimensionless parameter, $Q^{\#}$, that accounts for the mean overtopping discharge is expressed as :-

$$Q^{\#} = Q / (gH_s^3)^{0.5} \quad (2.22)$$

The significant difference between Owen's (1980) equation and Franco's (1993) equation resides in the omission of any direct wave period or steepness term in the Franco (1993) parameters. A better correlation was generally achieved when fitting data to the Franco (1993) parameters, reflecting the low dependence on wave period of run-up on vertical walls.

Numerous physical model tests led to an experimental formula that links the overtopping discharge to the structure freeboard :-

$$Q^{\#} = a \exp(-b(R_c/H_s)/\gamma_x) \qquad (2.23)$$

Where a and b are experimental constants

γ_x is a reduction factor which accounts for structural type

The reduction factor γ_x is applied for a wide range of structures including simple vertical walls, retreated (shifted) crest walls, curved parapet walls, perforated front wall (wave screen) or rubble mound protection. Values of a and b have been proposed by a number of authors. The following is a brief summary.

Franco et al (1994) and Franco (1996, 1998) investigated the overtopping of vertical breakwaters in deep water only. The following equation was derived for relative freeboards ranging from $0.9 < R_c/H_s < 2.2$:-

$$Q^{\#} = 0.082 \exp(-3.0R_c/H_s) \qquad (2.24)$$

Allsop et al (1995) have derived an empirical equation of the same form as that of Franco as follows:-

$$Q^{\#} = 0.03 \exp(-2.05 R_c/H_s) \qquad (2.25)$$

This equation, which covers a range of relative freeboards of $0.03 < R_c/H_s < 3.2$, is applicable to vertical walls in both deep and shallow water.

The data of Allsop et al (1995) is plotted with equations 2.24 and 2.25 in Figure 2.5. If equation 2.24 is extrapolated to higher values of relative freeboard, R_c/H_s, it under-predicts the overtopping discharge. As the bathymetry and the crest level of the models used were fixed, high values of relative freeboard correspond to shallower water depths and thus the presence of breaking waves.

The data from a separate study conducted by de Waal (1994) is shown in Figure 2.6. It can be seen that Allsop et al's (1995) equation 2.25 and de Waal's (1994) data set correspond quite closely.

At higher values of relative freeboard, Figure 2.6 suggests that there is considerably more scatter in the data. As explained above, these results correspond to conditions in which breaking waves predominate. Further analysis of the combined data sets of Allsop et al (1995) and de Waal (1994) has identified that the overtopping performance of vertical walls is dependent upon the type of incident wave conditions. In deep water waves hit the structure and are generally reflected back seawards (so called reflected waves). However, as the waves become limited by the available water depth, they are prone to break over the seawall (so

called impacting waves) causing a change in the overtopping performance. Overtopping equations were subsequently derived for both types of wave action.

A wave breaking parameter, h_*, was defined which dictates whether waves at the structure are dominated by impacting or reflecting waves. h_* is defined by :-

$$h_* = (h/H_s)\ (2\pi h/gT_m^2) \qquad (2.26)$$

Reflecting waves dominate when $h_* > 0.3$. Impacting waves dominate when $h_* \leq 0.3$. The formulation of h_* reflects the fact that waves are more likely to break if the wavelength or the wave height is large compared to water depth.

Separating their data according to h_*, Allsop et al (1995) determined that, for $h_* > 0.3$, the mean overtopping discharge was accurately described by an equation of the form of equations 2.23 to 2.25, but with new a and b parameters :-

$$Q^{\#} = 0.05 \exp (-2.78\ R_c/H_s) \qquad (2.27)$$

For $h_* \leq 0.3$, however, a different relationship was determined. To reflect the importance of wave breaking, new dimensionless discharge and freeboard parameters, both incorporating h_*, were defined thus :-

$$Q_h = q / (gh^3)^{0.5} / h_*^2 \qquad (2.28)$$

$$R_h = (R_c/H_s)\ h_* \qquad (2.29)$$

Examination of all the results from both Allsop et al's (1995) and de Waal's (1994) data sets for which $h_* \leq 0.3$ produced the following relationship :-

$$Q_h = 1.37 \times 10^{-4}\ R_h^{-3.24} \qquad (2.30)$$

The data and the prediction line is shown in Figure 2.7. Equation 2.30 therefore provides a good prediction of the mean overtopping discharge of a vertical wall subject to breaking waves.

The goodness of fit of the data was superior to all previous equations and, for this reason, equations 2.27 and 2.30 are recommended for use with vertical walls.

2.3.2 Angled wave attack

The influence of wave angle on the overtopping performance of a vertical wall in short-crested and long-crested seas has been studied by Banyard and Herbert (1995). Overtopping under oblique waves was found to be up to eight times greater than the value for normal wave attack.

The value of the overtopping ratio, O_r, (defined above) was found to be dependent upon on relative freeboard, R_c/H_s. The overtopping ratio increased as the relative freeboard increased, i.e., the greatest increases in overtopping were for conditions in which the normal wave attack discharge was expected to be small. Banyard and Herbert (1995) calculated the overtopping ratio on the basis of a predicted normal discharge rather than a directly measured

one. This allows considerable scope for inaccuracy, particularly in cases where the predicted normal discharge is small.

Further work on the overtopping performance of vertical walls under angled wave attack was carried out by Franco (1996). The overtopping equations of the form given above, were modified by the incorporation of a factor, γ, thus :-

$$Q^{\#} = a \exp(-bR_c/H_s/\gamma) \quad (2.31)$$

γ has the effect of changing the slope of the plot of $Q^{\#}$ against R_c/H_s. Values of γ were determined for a variety of wave approach angles and for short and long crested waves and different wave steepnesses. For vertical walls the most severe case was found to be long crested waves. γ was found to decrease linearly from 1 to 0.72 up to angles of 45°, after which it remained approximately constant up to an angle of 60°

The results were in contrast to those of Banyard and Herbert (1995) in that discharges were found to be lower under angled attack compared to under normal attack. It must be borne in mind that Franco's results were obtained from a direct comparison between measured discharges at normal and angled attack. Furthermore they were backed up by those of other researchers (Danish Hydraulics Institute, reference not available) who achieved very similar results. For these reasons the method of Franco (1996) is recommended for use with vertical walls.

2.4 Composite structures

2.4.1 Normal wave attack

A composite structure is a hybrid of a vertical wall and a rubble mound. An example is shown in Figure 2.8. Such structures are not common in the UK, although the methods described here can be applied to vertical structures repaired or improved by the addition of a rubble mound to the toe. Composite walls were examined by Allsop et al (1995) and it was discovered that the overtopping discharge was significantly affected by the relative size of the mound. In order to account for this the wave breaking parameter is re-defined using the depth of water over the mound, d, as well as h, as follows :-

$$d_* = (d/H_s)\,(2\pi h/gT_m^2) \quad (2.32)$$

This parameter can be used to decide whether the mound is "small" or "large". When $d_* > 0.3$ the mound is defined as small and has little effect on the incident waves. In this case the structure behaves as a plain vertical wall and, since $h_* > d_*$, reflected wave conditions apply. The overtopping discharge is then described by equation 2.27.

When $d_* \leq 0.3$, however, the mound is larger and begins to affect the incident waves. The dimensionless discharge and freeboard are then defined in a similar manner to those of vertical walls (equations 2.28 and 2.29) as follows :-

$$Q_d = q / (g\,d^3)^{0.5} / d_*^2 \quad (2.33)$$

$$R_d = (R_c/H_{si})\,(d/H_{si})\,d_* \quad (2.34)$$

Note the use of d, rather than h, in the dimensionless parameters. Fitting an equation to all the data for which $d_* \leq 0.3$ produced the following equation :-

$$Q_d = 4.63 \times 10^{-4} R_d^{-2.79} \quad (2.35)$$

In this situation both reflected and impacting waves may occur. No method of determining which type dominates has yet been developed. Equation 2.35 applies strictly only to impacting waves. However as the overtopping resulting from impacting waves was greater than that resulting from reflecting waves, equation 2.35 can be applied conservatively to the reflecting wave case.

A third case is when the mound is emergent, i.e., its crest is above still water level. This can occur with a large mound at low tide levels. The structure should then be treated as an armoured slope with a crest wall and analysed using the methods described in the section on sloped structures, above.

Allsop et al (1995) identified a final category of composite structure with a small relative freeboard, i.e., those with $R_c/H_s < 1.5$. It was found that the performance of these structures is unaffected by the presence of the mound and is best described by Allsop et al's (1995) equation for vertical structures in all water depths, i.e. equation 2.25.

Most design methods for composite vertical walls, whether the caisson is supported on a natural rock reef or on dredged fill, recommend that the foundations should not cause waves to break onto the structure. Allsop et al (1996) provided a decision chart to guide engineers away from designs likely to cause breaking onto vertical walls. Although the chart was intended to define wave loading, it is also relevant for wave overtopping. The method of Allsop et al (1996) will also be invaluable during the rehabilitation of deteriorating seawalls.

2.4.2 Angled wave attack

No data could be identified to describe the effect of angled wave attack on composite structures. In the absence of definitive data it is recommended that, when considering angled wave attack, composite structures with small mounds ($d_* > 0.3$) should be treated as vertical walls. When the mound is emergent the structure is treated as an armoured slope with a crest wall. No recommendation can yet be made for composite structures with large mounds ($d_* \leq 0.3$).

2.5 Conclusions and recommendations

2.5.1 Sloped structures

The method proposed by Owen (1980) is considered to be the most appropriate means of estimating overtopping discharges at simply sloping and bermed seawalls around the UK coastline. The Owen (1980) equation uses different empirical coefficients in order to study different wall profiles. The van der Meer and de Waal (1992) equations have fewer empirical coefficients. A significant amount of averaging has been applied in the derivation of the equations. This has resulted in a loss of definition in the calculated overtopping discharges for any particular seawall profile.

Furthermore the work of Owen (1980) uses wave conditions defined at the toe of the seawall, whereas van der Meer and de Waal (1992) uses as input deep water wave conditions and then

allows for wave breaking through the use of a correction factor. The method of calculating this factor proposed by van der Meer and de Waal (1992) is strictly only applicable to foreshore slopes of 1:100. This may significantly influence the results on steeper foreshore slopes which are found on many UK coastlines.

When angled wave attack occurs the reduction factors of Banyard and Herbert (1995) are recommended. Other methods (which give similar results) are available but are compatible only with the van der Meer and de Waal (1992) method of predicting overtopping discharge.

To predict the overtopping performance of a structure armoured with concrete units with confidence it is recommended that model tests should be carried out. Where this is not possible, model results from a similar configuration to that of the proposed design may be used to estimate the mean overtopping discharge. Where no model data is available the Owen (1980) formulae will give an estimate of the mean overtopping discharge acceptable for use during the preliminary design stage.

Two areas of interest were identified as potentially benefiting from further analysis. The first was the performance of crest walls sited on permeable armoured slopes. It was decided that the data set of Bradbury and Allsop (1988) should be re-analysed in an attempt to produce a new design method.

A second area of interest is that of permeable crest berms. A programme of model tests was proposed to investigate the effect of permeable crest width on mean overtopping discharge.

2.5.2 Vertical structures

Of the two most widely known approaches to vertical walls, that of van der Meer (1993) and Franco (1993) is recommended over that of Goda (1985) and Herbert (1993). The principal weakness of the Goda (1985) and Herbert (1993) method is that a considerable degree of interpolation is required to use the graphical methods. In addition the van der Meer (1993) / Franco (1993) method benefits from using wave conditions defined at the toe of the structure, rather than offshore.

Several variations on the van der Meer (1993) and Franco (1993) method have been proposed. Of these, the method of Allsop et al (1995) is recommended. It incorporates the further refinement of being able to distinguish between breaking and non-breaking conditions and has been (in part) confirmed by other independent research work.

The effect of angled wave attack is best accounted for by the use of the reduction factors determined by Franco (1996). These results were found to give very close agreement with those of independently conducted tests.

2.5.3 Composite structures

The method developed by Allsop et al (1995) is recommended for predicting the overtopping of composite seawalls. The method can identify various types of composite structure, categorised according to the extent to which the mound influences the overtopping performance.

Data on the effect of angled wave attack on composite walls is unavailable. However, limited recommendations can be made based upon observed similarities in behaviour with other structural types.

3. METHODS OF PREDICTING PEAK OVERTOPPING EVENTS

3.1 Introduction

As described in the previous Chapter, data concerning mean overtopping discharges is plentiful. Consequently most overtopping design methods are based upon the estimation of mean discharge. This is a rational approach to take when designing coastal structures for flood prevention. Recently, however, it has become acknowledged that when addressing the safety of pedestrians, or the prevention of damage to buildings located behind a coastal structure, peak overtopping events are more critical than average discharges. Peak events can be expressed in one of two ways. Firstly there is the maximum discharge rate. This approach was taken by Endoh and Takahashi (1994). Maximum flow rate is however, a difficult quantity to measure and research has therefore concentrated on determining the maximum volume associated with a single overtopping wave. Experiments which measure individual wave by wave overtopping are more complex to conduct than those which merely measure mean discharge. Consequently there is still relatively little data available on this topic, and as yet no widely established design method. This Chapter provides a review of published work in this field.

Methods for predicting peak overtopping volume generally consist of two phases; the first to predict the number of waves which overtop the structure, the second to probabilistically describe the distribution of individual overtopping volumes and hence to predict the largest in the sequence.

3.2 Proportion of waves overtopping a structure

One of the earlier studies was conducted by Franco et al (1994). Franco et al (1994) measured wave by wave overtopping over a variety of structural forms, including vertical walls. The number of waves overtopping each structure was counted and the individual wave-by-wave overtopping volumes measured. Franco et al (1994) determined that the proportion of waves overtopping a vertical wall could be described by the following equation:-

$$N_{ow}/N_w = \exp\left(-(R_c/H_s)^2 / (0.91)^2\right) \qquad (3.1)$$

where N_{ow} = number of waves overtopping.
N_w = number of waves in sample.
R_c = crest freeboard
H_s = inshore significant wave height

Equation 3.1 was developed on the basis of the results of tests conducted in relatively deep water. The form of equation 3.1 can be interpreted by considering the fact that the number of waves overtopping the structure equates to the number of run-up events exceeding the crest level. Run-up level on a vertical wall is strongly dependent on wave height. The individual run-up levels (like the wave heights) are thus Rayleigh distributed. The expression for the number of waves overtopping the structure in deep water (equation 3.1) is thus in the form of a cumulative Rayleigh distribution.

Equation 3.1 was formulated from the results of tests conducted in relatively deep water only. Subsequent analysis conducted at HR Wallingford found that it does not apply to shallow water where wave breaking is predominant. This work is outlined in detail in Chapter 6 of this report.

In addition to examining overtopping volumes Franco et al (1994) also made recommendations concerning the tolerable peak discharges. These are described in Chapter 8 of this report.

Smith et al (1994) followed a similar approach to Franco et al (1994) when considering the number of waves overtopping grass dykes, i.e., :-

$$N_{ow}/N_w = \exp\left(-(R_c/H_s)^2 / c^2\right) \qquad (3.2)$$

Where c is given by :-

$$c = 0.81\ \gamma_f\ \xi_{op} \qquad (3.3)$$

where ξ_{op} is the surf similarity parameter defined by :-

$$\xi_{op} = \tan\alpha / \sqrt{(s_{op})} \qquad (3.4)$$

where α is the angle of the seawall slope to the horizontal
s_{op} is the offshore sea steepness ($=2\pi H_{so}/gT_{po}^2$)

γ_f is the roughness of the slope, which in the case of grass dykes is between 0.8 and 0.9. The inclusions of ξ_{op} and γ_f in the expressions reflect the influence of wave period, slope angle and roughness on the run-up levels (as opposed to the vertical wall case where only wave height is considered). As with vertical walls, however, the expression for proportion of waves overtopping a slope (equation 3.3) is of Rayleigh form.

Owen (1992) took a similar approach when considering the proportion of waves overtopping a smooth impermeable slope, but using the dimensionless parameters formulated by Owen (1980). It was found that :-

$$N_{ow}/N_w = \exp\left(-C\ R_*^2\right) \qquad (3.5)$$

Where R_* is the dimensionless freeboard given by $R_c / (T_m (gH_s)^{0.5})$
T_m is the mean wave period
H_s is the inshore significant wave height
C is a coefficient which depends on the slope

Again, the importance of period and slope angle is reflected in the formulation of the parameters. Slope roughness and permeability was not varied in Owen's (1992) study. For the purposes of this report, however, Owen's (1992) equation was compared with data from experiments conducted on various types of armoured slopes and the effect of roughness examined. The results are described in Chapter 6.

3.3 Maximum individual volume

Given that the number of overtopping events and the mean discharge can be predicted using the methods described above and in Chapter 2, it is possible to estimate the magnitude of the largest individual overtopping event.

Franco et al (1994) and Smith et al (1994) found that distribution of the volumes of individual overtopping events, V, can be described by the Weibull distribution :-

$$P(V) = 1 - \exp(-((V-C)/A)^B) \quad (3.6)$$

where P(V) = probability of non-exceedance
A, *B* and *C* are fitting parameters.

The fitting parameter *C* represents the lower limit of the data. In this case this represents the minimum individual overtopping volume which the experimental method employed can distinguish.

If equation 3.6 is re-arranged, the maximum expected individual overtopping volume, V_{max}, in a sequence of N_{ow} overtopping events is then given by :-

$$V_{max} = C + A\,(\ln(N_{ow}))^{1/B} \quad (3.7)$$

Franco et al (1994) determined values of *A* and *B* for overtopping of a vertical wall in relatively deep water, finding that :-

$A = 0.84V_{bar}$, where V_{bar} is the average individual overtopping volume.
$B = 0.75$

One of the most important facts to emerge from Franco et al's (1994) work was that the relationship between mean and peak discharge is not constant, but that it varies with structural type and wave climate.

Smith et al (1994) examined the maximum individual overtopping volume on a grass dyke. It was assumed that the shape of the distribution of individual volumes was identical to that produced by Franco et al (1994), i.e. $A = 0.84\ V_{bar}$, $B = 0.75$. This assumption was validated by the test results.

In Chapter 6 of this report distributions of individual volumes are analyzed for other cases.

3.4 Effect of angled wave attack

Franco (1996) examined the effect of angled wave attack on the proportion of waves overtopping a vertical wall. It was found that the number of waves overtopping reduced under angled wave attack. Franco et al's (1994) equation (3.1) was modified thus :-

$$N_{ow}/N_w = \exp(-(R_c/H_s)^2 / C^2) \quad (3.8)$$

Where C is a parameter which varies as a function of angle of attack. Franco (1996) determined values of C for angles of up to 60°, for both short and long-crested seas and for differing values of wave steepness.

Franco (1996) found that for normal wave attack with long-crested seas that C = 0.91, in agreement with Franco et al (1994), and for angled wave attack C < 0.91. Similar reductions were noted for short crested seas.

For sloped structures, Franco (1996) determined reduction factors to be incorporated in Smith et al's (1994) equation for the number of waves overtopping a slope (equation 3.2), thus :-

$$N_{ow}/N_w = \exp\left(- (R_c/H_s)^2 / \gamma_{pow}\, c^2\right) \qquad (3.9)$$

Franco (1996) produced very similar results to Smith et al (1994) for long crested waves with normal attack (finding that $\gamma_{pow} = 0.94$ rather than 1) and finding that $\gamma_{pow} < 1$ for angled attack.

3.5 Conclusions

Most overtopping design methods are based upon the estimation of mean discharge. When addressing the safety of users of a coastal structure, or the prevention of damage to buildings located behind a coastal structure, peak overtopping events are more critical than average discharges. Prediction methods for individual overtopping volumes are less well established than that those for mean discharges.

In order to predict the maximum individual overtopping volume it is generally necessary to estimate the number of waves which overtop the structure. This can be achieved by considering the run-up of the individual waves. Probabilistic methods can then be employed to estimate the largest individual volume in the waves which overtop the structure. The Weibull distribution has been shown to be suitable for this purpose.

4. REVIEW OF SITE-SPECIFIC OVERTOPPING DATA

4.1 Introduction

A review of methods for estimating mean and peak overtopping events were presented in Chapters 2 and 3. Those methods were generally based upon model studies which were generic in nature, i.e. they represented a structural type rather than a specific structure or site. There is, however, a large amount of data available which is site-specific. This data can be used to validate and, in some cases extend, the design methods. This Chapter examines site-specific results and compares them with the methods reviewed in Chapter 2.

The review of available data was conducted in two parts. The first task was to establish which physical model studies have included measurement of wave overtopping and to collate details of each of them. Secondly, an assessment of the quantity and importance of the data in each study was made to establish which data sets were most appropriate for use in further analysis.

As well as looking at model test data this Chapter also examines the results of a prototype monitoring programme conducted on a vertical seawall.

4.2 Collation of details of overtopping studies

A comprehensive list of studies carried out at HR and other European laboratories, was compiled from various sources.

Details of each study were extracted from the study reports and from data sets held electronically. The type of structure, the wave conditions and the type of overtopping measurement were noted. Further information on each of these categories is given below. A summary of all relevant studies is given in Table 4.1.

Type of structure

The sea defences were divided into four types: smooth sloping revetments, rock armoured revetments, concrete armour unit revetments and vertical walls. Each of these categories covers a range of structures and so further details of the construction were noted for each study.

Wave conditions

For assessment of the data sets it was important to know the depth of water at the structure relative to the wave height, and whether wave spreading and wave obliquity had been modelled.

Type of overtopping measurement

Overtopping in physical models is generally measured in one or more of the following ways. The type of measurement was noted in Table 4.2.

(i) The number of waves overtopping the defences (N_{ow}) may be counted, either by eye or by installing probes at strategic points on the crest of the structure. The number of waves overtopping is divided by the number of incident waves to find the proportion of waves overtopping. The number of incident waves is generally found from the duration of the test event divided by the mean wave period (T_m).

(ii) The total volume which overtops a length of sea defence during a predetermined time may be collected. The volume is divided by the time and the length of the structure under consideration to find the mean overtopping discharge, Q.

(iii) The volume of water collected behind the sea defence is measured continuously throughout testing. This provides a record of the wave by wave overtopping, and therefore a description of the individual overtopping volume distribution. Prediction of the peak wave overtopping discharge for a particular storm duration may be made from these results.

4.3 Assessment of the importance of the data

Once details of the existing wave overtopping studies had been collated, the importance of the data was assessed. To form a database for comparison of the overtopping performance of different structures it is important to know whether the structural type and range of wave conditions are covered by existing design methods. If the test conditions were not covered by existing design methods, and also where little information exists, the assessment was conducted with reference to the following criteria:

(i) The position of the wave condition calibrations
The wave conditions generated in a physical model are generally calibrated against the conditions required using wave probes. The computer input signal to the wave paddle is adjusted until the conditions are satisfactory. The wave probe(s) used for calibration may be placed at any point on the model bathymetry for which the required wave conditions are known. Calibration may therefore be conducted offshore, in intermediate ($0.5 < h/L < 0.02$), or deep water. Alternatively calibration may be conducted at the position of the structure before it is constructed in the model.

When the wave overtopping performance of a structure is being investigated in the physical model, it is relatively unimportant if the waves are calibrated offshore, nearshore or at the structure. If the waves are calibrated offshore then the physical model bathymetry is being used to transform the waves to their inshore state. If the waves are calibrated at the structure then a numerical model will have been used to predict the wave transformation prior to the physical model study.

The effect of the bathymetry on the incident wave conditions must be taken into account when comparing data from different model studies. This has been achieved in previous design methods by providing different design charts for different gradients of seabed, for example Goda (1985), or by providing a design method which applies ostensibly to a single gradient of approach bathymetry. Where the wave conditions have been calibrated at the structure the effect of the approach bathymetry may be ignored, since it will have no effect on the comparison of the inshore wave height to the hydraulic performance of the structure. It is, therefore important to identify where the wave conditions have been calibrated, since the comparison of results from models calibrated inshore with models calibrated offshore will clearly lead to erroneous findings.

(ii) Measurements made
The most common type of overtopping measurement made in physical model studies is the mean overtopping discharge. Extensive research into the relationship between

the structural form of the sea defence, the wave condition and the mean discharge has been conducted previously and is reviewed in Chapter 2. Since the design methods based on this research are well established, most of the recent physical model testing has been conducted where the proposed structure is not covered by existing design methods. The data from such testing can therefore be used to revise and extend the existing methods.

Fewer studies include measurement of the number of waves overtopping. A limited number of studies include the measurement of both the mean overtopping discharge and the number of waves overtopping. This data is more useful since it allows verification of previous design methods and also allows a direct comparison between the two methods of measurement.

Wave by wave overtopping measurement allows analysis of the distribution of wave overtopping, which may be used to relate mean discharge to peak discharge. Unfortunately, since the equipment and testing procedures required to conduct such experiments is more expensive, relatively few studies have used this method.

(iii) Types of structure

The most common type of structure to be tested is the rubble mound with rock armour. Although concrete armour units are also tested frequently, there are many different types of armour unit. Consequently, only a few data sets are available for each type. Physical model testing of plain sloping and vertical walls have also been carried out.

(iv) Obliquity / wave spreading

Most structures are tested from only one wave direction, usually the predominant wave direction for the study site. Where a number of wave directions are required an investigation of the overtopping performance under oblique wave attack may be conducted in a wave basin. Wave flume studies are only used for studying normal wave attack on sea defences.

The waves generated in physical models are generally long-crested, where successive wave crests are parallel and the wave energy propagates in one direction only. These conditions are generated using a wave paddle which extends the full width of the model. Under certain circumstances, short-crested waves are used, where spreading of the wave energy is simulated. Such conditions are created using a wave machine with short paddle segments, which are individually controlled by the wave generation computer. Short-crested waves provide a more realistic simulation of the wave conditions which occur where winds are locally generated.

(v) Improvement of quality of data

If only offshore wave conditions were available and the foreshore bathymetry was known, inshore wave conditions were calculated at the toe of the structure. Inshore wave conditions were calculated using the HR Wallingford WENDIS model which represents the physical processes of shoaling due to depth variation, and energy dissipation due to bed friction and wave breaking. The model has been calibrated against physical model data sets. The model was also compared to design curves from the wave energy decay model ENDEC, and to computations using Goda's

equations. There was good agreement between all three models for bathymetry slopes steeper than 1:100.

4.4 Assessment of gaps in data

Generally many of the structures studied in physical model tests are located in deep water or close to steeply shoaling bathymetry. Where the wave conditions are severe, such structures are often armoured with large concrete armour units. These types of structure are often seen at new port developments around the UK, however, they are not representative of numerous small embankments and vertical walls backing beaches and protecting low lying land.

Many of these smaller scale embankments are often faced with concrete or grass, and many are armoured with rock. As space is at a premium around the coast many new embankments are now constructed with recurve walls at the crest.

Previously unused data describing the wave by wave overtopping performance of structures armoured with concrete cubes and vertical walls has been analysed during this study. In addition a small number of 2-dimensional physical model tests were carried out to study the wave by wave overtopping performance of smooth and rock armoured structures with wave walls.

4.5 Data analysis

4.5.1 Simply sloping structures

As described in Chapter 2 of this report, the most widely used relationship to predict overtopping for simply sloping structures is the correlation between the non-dimensional discharge Q_* and the non dimensional crest freeboard R_* :-

$$Q_* = A \exp (- B R_*/r) \qquad (4.1)$$

where R_* is given by :-

$$R_* = R_c / (T_m(gH_s)^{0.5}) \qquad (4.2)$$

and Q_* is given by :-

$$Q_* = Q / (gT_mH_s) \qquad (4.3)$$

where R_c is the crest elevation above still water level
T_m is the mean zero crossing wave period at the toe of the seawall
H_s is the significant wave height at the toe of the seawall
Q is the mean discharge

A, B and r are empirical coefficients dependent on structure slope and roughness. Knowing the dimensions of the structure and the incident wave conditions the graphs can be used to calculate the mean overtopping discharge over embankment crests. Physical model data can be used to make up these diagrams. A number of Q_* against R_* graphs for various structures are shown in Figures 4.1 to 4.5.

The first figure in the series, Figure 4.1, shows the relationship between the mean overtopping discharge and the non dimensional crest freeboard R_* for a simply sloping smooth structure assessed by Owen (1980). The graph shows that for a given value of R_* the performance of 1:1.5 and 1:2 slopes are very similar. Reducing the slope of the structure to 1:4, for instance, significantly reduces the overtopping discharge.

Owen's (1980) method of analysis can be applied to armoured structures by use of the roughness coefficient, r. The performance of two single layer hollow cube structures is shown in Figure 4.2. The structures are very similar (slopes = 1:1.5 and 1:1.33 respectively). The only major difference is the crest detail. The 1:1.5 sloping structure had a 5m wide rock berm at the crest, the other structure had no berm. Also plotted is the Owen (1980) prediction line with r = 0.55 (the generally accepted figure for hollow cube armour units). The upper set of data, relating to the structure without a berm, compares extremely well with the Owen prediction for a simply sloping armoured structure with r = 0.55.

It is interesting to note that the slopes of the 2 regression lines through each set of data are very similar, however, the lines are offset. The presence of the 5m rock berm at the crest of the other structure significantly reduces the overtopping discharge, moving the data set down the Q_* axis.

The performance of four Antifer cube armoured structures is illustrated in Figure 4.3. Each has a small horizontal berm (approximately 4m wide) at the crest. The performance of the 1:2 sloping structure appears to be better that the 1:1.5 slope. This result does not agree with Owens data for smooth slopes where the performance of 1:1.5 and 1:2 slopes were similar. The general trend is clear however; their performance is better than that predicted by Owen's (1980) equation with r = 0.55. This is, again, a result of the crest berms.

Tests such as those described above have led an approximate rule being adopted; that for every 10m landward of the top of the slope the mean overtopping discharge may be reduced by a factor of approximately 10. It was decided that this rule should be confirmed (or modified) by a new set of model tests. Chapter 7 describes this work in detail.

The performance of four similar rock armoured structures is shown in Figure 4.4. All the slopes lie between 1:1.5 and 1:3. However, each structure also has a wave return wall located on its crest. The data is scattered due to the various slope angles and configurations of the wave wall. However, a trend can be seen. The data all lies below the Owen (1980) prediction for a 1:2 sloping structure with r = 0.55 as applicable to 2 layers of rock armour. The better performance is due to the recurve walls located behind the armour crest.

It was decided on the basis of this data to re-examine the performance of wave return walls on permeable armoured slopes. This work is described in detail in Chapter 5 of this report.

Recent tests suggest that the two most efficient concrete armour units are Dolos (two layers) and Accropodes (single layer). The performance of two Accropode structures is compared in Figure 4.5. Comparing this data with that of the other structures the performance of the Accropode structure improves significantly at larger values of R_*. The Owen (1980) equation with r = 0.3 is also plotted in Figure 4.5. The regression line passes through the data set, however, it is only appropriate over a small range of R_*. As the roughness of the structure increases the applicability of the Owen regression reduces.

The final graph in the series (Figure 4.6) illustrates the effect of increasing the roughness of the armouring for structures having slopes of 1:1.5 and 1:2. Note, reducing the steepness of the slope reduces the mean overtopping discharge. As the roughness of the armour increases from a smooth slope to the most effective 2 layer Dolos structure the mean overtopping discharge reduces significantly. For example, assuming $R_* = 0.1$ the non-dimensional discharge Q_* reduces from $2x10^{-3}$ for a smooth slope to 2×10^{-6} for the Dolos armoured structure ($r = 0.3$), a factor of 1000. As long as the slope and roughness of the structure can be defined and compared with one of the known armouring units then a rough estimate of the mean overtopping discharge may be made from the data provided in Figure 4.6.

The data above shows that the Owen (1980) method, based on coefficients A and B and roughness coefficient, r, gives an acceptable first estimate of the mean overtopping discharge. The data, however, shows that both the slope of the regression line, given by B/r, and also the location at which the regression line cuts the Q_* axis, given by the constant A, can vary depending on the type of structure. Some of these discrepancies are a result of structural details such as crest berms and return walls, which are not explicitly taken into account by Owen's (1980) equation but can significantly affect overtopping performance. Owen's (1980) equation also becomes less accurate for structures with very low roughness coefficients.

Where more accuracy is required, and model data is available for a similar structure, an alternative approach is to assume $r = 1$ and fit a regression line through the data to find values of A and B.

4.5.2 Vertical walls

Site-specific data on vertical walls is rarer than that concerning sloped structures. However, one study of a prototype seawall is available.

A vertical wall at Colwyn Bay in North Wales frequently suffers significant overtopping during storms from the north and north-east (Herbert 1996). The structure affords protection to a promenade and roadway immediately behind its crest. The coastline is characterised by a sandy lower beach with some patches of cobbles and an upper shingle beach, the width of which varies along the frontage. A vertical stone-faced seawall, approximately 3m high is sited at the rear of the beach. A typical cross section is illustrated in Figure 4.7. Overtopping measurements were undertaken in a series of short-term deployments during storm events in late January 1994. Storm events were predicted by identifying spring tidal dates and monitoring the Meteorological Office Weathercall forecasting system during periods of storm activity.

A wave/tide recorder was used to measure the inshore wave conditions and water levels. A large calibrated tank captured overtopping water. Each series of overtopping measurements was completed over about three hours during periods of high tides.

The data from the wave/tide recorder was filtered using high and low pass filters to separate the wave component (high frequency) from the water level record (low frequency). The wave record was analysed using spectral methods to give the inshore significant wave height, H_s, and mean and peak wave periods, T_m and T_p. At the shoreline the direction of wave energy was perpendicular to the axis of the seawall (within $\pm 10°$). Analysis of the wave conditions at the site indicated a mean wave period of approximately 5-6 seconds so an averaging interval of 10 minutes was equivalent to about 100 waves.

The mean overtopping discharge derived using the empirical formulae described in Chapter 2 were compared with the measurements from the field. Equation 2.26 assessed the form of the wave reaching the structure, and it was found that the wave breaking parameter, h_*, was less than 3.0 for all but one of the analysis intervals, which suggested that impacting waves dominate. For impacting waves the non-dimensional overtopping discharge Q_h is given by equation 2.30. The field data and the trend line by given equation 2.30 are compared in Figure 4.8, with relatively good agreement. A best fit line is also shown.

4.6 Conclusions

A selection of site-specific data has been examined with reference to the design methods presented in Chapter 2. The design methods presented for armoured slopes and vertical walls have generally been validated by the site-specific data. In some cases however the results have highlighted the need for design methods to account for structural details, such as crest berms and return walls. In the case of crest berms, it was decided that a programme of model tests should be commissioned to investigate in more detail than was previously available their affect on overtopping discharges.

5. CREST WALLS LOCATED ON ROCK-ARMOURED SEAWALLS

5.1 Introduction

One of the areas identified in Chapter 2 as requiring additional analysis was the effectiveness of crest walls located on top of armoured seawalls. Bradbury et al (1988) carried out a set of experiments to investigate the performance of such structures. Owen and Steele (1991) conducted similar experiments using smooth, impermeable slopes and developed an empirical design method on the basis of their results. The method developed by Owen and Steele was extremely flexible and allowed the performance of a wide range of return walls to be predicted. An examination of Bradbury et al's original data set suggested that, with re-analysis, it could form the basis of a similar design method.

5.2 Crest wall discharge coefficients

Owen and Steele (1991) examined the problem of the effectiveness of recurved crest walls located on top of smooth, impermeable slopes. A crest wall discharge coefficient, D_f, was defined as:-

$$D_f = Q/Q_b \qquad (5.1)$$

where Q is the overtopping discharge over a seawall section with a crest wall and Q_b is the base discharge, i.e., the overtopping discharge over the same section, under identical conditions, but with the crest wall removed. D_f should always take a value between 0 and 1. This expression of crest wall effectiveness differs from the definition used by other authors, e.g. Bradbury et al (1988), which relates the discharge over a section with a crest wall to the discharge over the same section if the crest wall were removed and the slope were continued to the same level as the top of the crest wall. Owen and Steele adopted the definition of equation 5.1 so that a more direct measure of the effectiveness of the crest wall alone can be made rather than that of the seawall / crest wall combination. The results can therefore be more readily applied to other situations.

Owen and Steele evaluated D_f for various combinations of seawall slopes and crest wall dimensions. The results are presented in the form of a design chart. It is intended that the overtopping rate of the seawall in the absence of the return wall is first estimated and that the appropriate value of D_f is then applied from the design chart.

Bradbury et al examined the problem of crest walls on armoured slopes. The overtopping was examined in terms of the freeboard of the overall structure. Bradbury et al computed new values of A and B coefficients for use in Owen's (1980) method. It was intended that designers use the values of A and B relevant to the model which their structure most closely resembled. This approach did not fully address the question of the efficacy of raising the crest wall as compared to raising the armour crest level. To rectify this Owen and Steele extended their method to rough, permeable slopes by applying it to the data of Bradbury et al. The results follow the same general trends as those from the smooth, impermeable wall tests, although with considerably more scatter in the data. It was concluded that return walls on permeable slopes are more effective than those on impermeable slopes.

Only a small sub-section of Bradbury et al's data set which deals with recurved walls was used for this purpose, the same subsection of data was used by Owen and Steele to make a direct comparison with their own data.

This Chapter applies the analysis method developed by Owen and Steele to a more extensive selection of Bradbury et al's data set in an attempt to develop design curves for the effectiveness of wave return walls on rough permeable slopes.

5.3 Bradbury et al's data

The data used in the calculation of the discharge coefficients are based on the results of a series of model tests conducted by Bradbury et al (1988). Included in the series of tests were measurements of overtopping of a variety of crest walls on top of simple rock slopes. The geometries of the model sections whose performance is examined in this report are shown in Figure 5.1. The principle parameters of the models along with the test codes used in the original study are shown in Table 5.1.

All the results are from tests conducted with rock slopes of 1:2. The armour layer in all cases consisted of 2 layers of rock. The majority of the test sections had crest berm widths, Cw, of 0.15m and armour crest levels, A_c, of 1.555m, the principal geometric variable being the crest wall height, Wh. There are, however, several exceptions. One section (11) had a wider crest berm width of 0.3m so that the effect of the berm width could be investigated. A further section (13) had a recurved (rather than a simple rectangular) crest wall.

5.4 Owen and Steele's method

Smooth Impermeable Slopes

The discharge factors presented by Owen and Steele (1991) relate the overtopping of a crest wall on top of a seawall, Q, to the overtopping of the same seawall in the absence of a crest wall, Q_b. Q_b can also be considered as the discharge which arrives at the base of the crest wall. For the purposes of calculating D_f, Q_b was not measured, but estimated using the method of Owen (1980), whereby the dimensionless overtopping, Q_{*b}, is related to the dimensionless crest freeboard, $A_{*}c$, by the following equation:-

$$Q_{*b} = A \exp(-B\, A_{*c} / r) \qquad (5.2)$$

where $Q_{*b} = Q_b / (T_m\, g\, H_s)$

$A_{*c} = A_c / (T_m\, (g\, H_s)^{0.5})$

and A, B and r are empirically determined coefficients, describing the slope and roughness of the seawall (see Chapter 2 of this report). H_s and T_m are the significant wave height and mean period, both defined at the toe of the seawall, respectively.

For variOus combinations of smooth, impermeable seawalls and crest walls Owen and Steele calculated D_f based on measured values of Q and values of Q_b estimated from equation 5.2, using a value of A_{*c} equal to the freeboard of the armour slope crest. The results were presented in the form a design chart which plots D_f against adjusted dimensionless crest berm freeboard, X_*, for various values of dimensionless crest wall height, W_*h, given by :-

$$W_*h = Wh/A_c \qquad (5.3)$$

X_* is a modified value of A_{*c}, adjusted with empirically determined factors for crest berm width and seawall slope. Figure 5.2 shows Owen and Steele's final design chart. One of the principal conclusions of the study was that :-

"..the discharge factor increases as the dimensionless crest elevation decreases: in other words the wave return wall is more effective when there is less water arriving at its base. When very large quantities of water arrive at the return wall it becomes "drowned", and has very little effect on the overtopping discharge."

This is reflected in the trends shown in Figure 5.2.

Rough permeable slopes

Owen and Steele used the results from section 13 of Bradbury et al's data to estimate the discharge coefficients of crest walls on rock slopes. Section 13 was selected as it had a recurved wall similar in profile to the one used in the original work on smooth slopes.

Whilst considering equation 5.2 adequate to estimate Q_b for smooth, impermeable slopes, Owen and Steele carried out additional tests (designated section 14) to provide an direct measurement of Q_b for the rock slopes. Section 14 had similar dimensions to the other sections used by Bradbury et al but with no crest wall. This feature allows Q_b to be calculated for the other structures. Thus for each structure an accurate estimate can be made of the overtopping performance in the absence of a crest wall.

If equation 5.2 is used to estimate Q_b the empirical coefficients, for 2 layers of rock armour at a slope of 1:2, are as follows :-

$$A = 9.39 \times 10^{-3}$$
$$B = 21.6$$
$$r = 0.55$$

The measured overtopping performance of section 14, along with the predicted result from equation 5.2 is shown in Figure 5.3. As can be seen equation 5.2 overestimates the overtopping discharge. This is in part a result of the presence of the permeable crest berm. A more accurate method is to fit a form of equation 5.2 to the data by setting r equal to 1 and, by plotting $\ln Q_{*b}$ against A_{*c} and determining A and B from the least squares method. The results are also plotted on Figure 5.3.

The result of this analysis is that the overtopping discharge which the model sections would experience in the absence of their crest walls can be described by the equation :-

$$Q_{*b} = 0.01608 \exp(-67.92\, A_{*c}) \qquad (5.4)$$

This allows the crest wall discharge factors to be accurately calculated.

The estimate of Q_b thus determined was then used in the calculation of D_f for section 13. Figure 5.4 shows the results for section 13 along with those for the equivalent smooth, impermeable slope. D_f is plotted against A_{*c}, as in the original work of Owen and Steele. As each section was tested at two water levels, each provides two sets of data when grouped according to W_*. It can be seen that, for a constant level of A_{*c}, the crest wall on a rough, permeable slope is more effective than one on a smooth, impermeable slope.

It was suggested that :-

"As the wave runs up the slope and onto the crest, its forward progress is arrested by the return wall, increasing the depth of water on the crest. For an impermeable slope the remainder of the wave runup to some extent rides over this cushion of water and a fraction overtops the wave return wall. On a permeable slope the increased depth of water on the crest causes a greater head difference from the crest to the bottom of the slope, increasing the reverse drainage down through the armour layer and, to a lesser extent, the underlayer. The remainder of the runup therefore finds it more difficult to overtop the wave return wall."

5.5 Discharge factors for walls on permeable slopes

The discharge factors for the walls on sections 4, 5, 6, 7, 8 and 9 were calculated using equation 5.1, where Q_b is given by equation 5.4. Graphs showing D_f against A_{*c} for all of the sections tested are shown in Figure 5.5. The data are grouped according to constant values of $W_{*}h$. The general trend of the data can be seen to follow that predicted by Owen and Steele (1991). This accords with the conclusion that the effectiveness of the wall decreases as the quantity of water reaching it increases.

Owen and Steele's method of analysis involved plotting $\ln(D_f)$ against $\ln(A_{*c})$ and fitting a straight line to the data points, effectively fitting to the data an equation of the form :-

$$D_f = X\, A_{*c}^{\ Y} \qquad (5.5)$$

The slope of the line will give the parameter Y, whilst the intersection with the $\ln(D_f)$ axis will provide the parameter X.

Initially the full data set was grouped in data groups of $W_{*}h$. The results are shown in Figures 5.6 to 5.15 and the coefficients X and Y, along with the r^2 correlation factor of the fit are given in Table 5.2. As can be seen there is a considerable degree of scatter in all of the data groups, with generally low values of r^2. The lowest values of r^2 arise from groups with a small number of data points and a limited range of A_{*c}, e.g. the results for $W_{*}h = 1.32$ and $W_{*}h = 0.94$. This results in calculated values of the slope constant, Y, which are inconsistent with the overall trends. It was decided, therefore, to discard groups with $r^2 < 0.25$.

A further problem arises at high levels of $W_{*}h$ (i.e., >1.5) where the results are less sensitive to changes in $W_{*}h$. The results for $W_{*}h = 2.64$, 2.09 and 1.55 produce very similar relationships. It was decided, therefore, to combine these data sets and to designate $W_{*}h$ for the combined group as the weighted average of all three, i.e., 1.96.

The resulting curves are plotted in Figure 5.16. Results are shown for $W_{*}h = 3.73$, 1.96 and 0.4. The result for $W_{*}h = 0.2$ is also included to provide a lower limit to the data set. It can be seen that the general behaviour of the crest walls on permeable slopes is similar to those on impermeable slopes.

5.6 Effect of recurved wall on discharge factors

Section 13 was the only section tested which had a recurved wall profile rather than a simple rectangular wall profile. Other than the wall profile the section dimensions were identical to those of models 6 and 9. These sections were tested at two water levels each, so two groups

of W_*h data are available. The results of models 6, 9 and 13 are plotted in Figure 5.17. It can be seen that the effect of the recurved wall is to reduce the discharge factors compared to those of the simple rectangular walls. When the relative wall height is low ($W_*h = 0.55$) the recurved wall makes a greater difference at higher values of A_{*c}. This is to be expected as at low values of A_{*c} the wall will become "drowned" and its profile will be of less significance. In the case of the greater relative wall height ($W_*h = 1.55$) there is little difference between the two data sets.

5.7 Effect of crest berm width on discharge factors

A wider crest berm provides a larger permeable surface through which the water building up against the crest wall can drain. Crest walls on wider bermed structures would be expected to be more efficient. However, the effect of the berm width on the discharge factors is difficult to determine precisely as no direct data is available on the discharge, Q_b, of the wider bermed section (model 11). Chapter 7 of this report presents a new method for estimating the effect of the crest berm on overtopping discharge. An equation was derived thus :-

$$C_f = 3.06 \exp(-1.48 (Cw/H_s)) \qquad (5.6)$$

where C_f = crest width reduction factor
Cw = crest width
H_s = inshore significant wave height

C_f is the ratio of the discharge behind a crest berm of width Cw to that with no crest berm present. The discharge with no crest berm present was estimated using Owen's equation (5.2) with the appropriate empirical factors. This figure was then used to estimate the crest wall discharge factor, D_f, for section 11. The results are plotted on Figure 5.18, along with those of sections 6 and 9 which had identical crest walls. It can be seen that there is practically no difference between the D_f values of the sections with and without the wider crest berm for the higher relative wall height. The differences at the lower relative wall height are small. It must be stressed that this comparison cannot be made with the same degree as accuracy as others in this chapter, since Q_b was not directly measured.

5.8 Design chart

Owen and Steele (1991) concluded that the efficiency of the crown wall is primarily a function of the volume of water arriving at its base, Q_b. As slope roughness was not a factor in Owen and Steele's experiments, armour crest freeboard and slope angle were the only parameters affecting Q_b. D_f was therefore described as a function of A_{*c} and slope by the parameter X_*. When considering armoured slopes however the roughness must also be taken into account. Determining a direct relationship between D_f and Q_{*b} should therefore make the results more generally applicable.

For this purpose a similar approach was taken as for the determination of relationships between D_f and A_{*c}. For each group of constant W_*h an equation of the following form was fitted to the data:-

$$D_f = X Q_{*b}^{\ Y} \qquad (5.7)$$

Q_{*b} was estimated from equation 5.4. As before, there was a considerable amount of scatter, and problems arose with those groups which have a small number of data points and a limited

range of Q_{*b}. Parameters X and Y are given in Table 5.3 along with the regression analysis data. Values of r^2 are similar to the equivalent fit of D_f to A_{*c}.

Regression lines were plotted for $W_{*}h$ = 3.73, 1.96, 0.4 and 0.2. The results are plotted in Figure 5.19. In order to produce a more convenient design chart, interpolation between these values then produces a design chart, Figure 5.20. Given that the base discharge, Q_b, can be estimated, Figure 5.20 can be used to determine the reduction factor, D_f, for any height of crest wall. When a crest berm is present allowance must be made for it in the calculation of Q_b, using the method outlined in Chapter 7 of this report.

5.9 Conclusions

A revised method of estimating the effect of a crest wall on a rock-armoured slope has been presented. The data of Bradbury et al (1988) was re-analysed using the method proposed by Owen and Steel (1991). A design chart has been produced which provides a more flexible method of estimating the effectiveness of a wide range of crest walls.

6. ANALYSIS OF WAVE BY WAVE OVERTOPPING

6.1 Introduction

In situations where the safety of personnel is of primary interest, overtopping limits are best defined in terms of peak events rather than average discharge. The most effective way of defining the peak event is by the maximum individual volume of water which overtops the structure during the course of a storm. This Chapter describes the analysis of the results of model tests in which the wave-by-wave overtopping volumes were individually measured. Such data is available for a variety of structural types. This Chapter starts with a description of the experimental technique employed at HR Wallingford for this type of test. Very similar methods have been employed at other laboratories. The statistical methods employed in analysing the results are then described. The Chapter concludes with recommendations for predicting the peak-overtopping event for a variety of structural forms and wave conditions.

6.2 Experimental technique

Tests were run for a duration equivalent to approximately 1000 waves. The length of the wave sequence (the time taken before the wave record begins to repeat) was considerably longer than the actual test length, thus ensuring that any particular group of waves only occurred once. All data were collected at 20Hz and saved to disk.

All water overtopping the structures was collected in a series of tanks positioned behind the model. Water levels in the tanks were measured continuously using either electromagnetic float gauges or load cells. When measurement was by float gauge the tanks were split into sections of different plan area to allow the accurate measurement of low discharge. The continuous measurements allowed the volume of water overtopping the seawall per wave to be assessed. Readings from the float gauges or load cells were noted before and after each test, enabling the mean overtopping discharge over the test length to be determined.

During each test the number of waves overtopping the structure was counted using overtopping probes positioned at the structure's crest. As an overtopping wave passes the structure, an electronic voltage pulse is triggered.

All wave overtopping data was recorded for post analysis using WARP, a real time wave recording and analysis package developed at HR Wallingford. This program allows the time varying voltage of an instrument to be recorded at a specified time interval and the digitally converted data to be stored. In most cases three or four channels of overtopping data were recorded i.e., two probes on top of the structure measuring the number of waves overtopping and either a load cell or one probe in each of the measuring tanks recording the change in level of the rising water. A typical recording interval was 0.05s for each channel of data. The test length varied between 20-40 minutes in the model.

To translate the raw data a separate computer program was written to assess the number of overtopping waves which actually produced enough water to be measured with sufficient accuracy in the tank, and to assess the individual volume of those waves. The logic of the program is described below.

The first step was to pick out overtopping waves measured by one of the two overtopping probes. This consisted of searching through the raw data until a deviation from the base

signal was found. This indicated the start of an overtopping wave, although not necessarily one which would add significantly to the overall volume. The data file consisted of the time value of the start of each pulse and is referred to as the spike file. The second step was to search through the raw data of the overtopping tank level to find the change in level between two successive overtopping waves as indicated on the spike file. This was achieved by allowing for the time delay between the overtopping event and the increase in level in the tank. When a level gauge was used in the tank it recorded an oscillation after every overtopping event. To allow for this effect, an average of the tank readings over the last few seconds before the arrival of the next wave was taken as the baseline. A similar baseline was found for the next event and the volume of the wave was calculated from the difference in these two averaged readings.

Allowances were made in the program for those tests where two tanks were used and water overflowed from one to the other. Threshold parameters were set by the operator (for both the spike file and the tank level file) to reject waves considered to be caused by noise on the signal. A further parameter, which could be set by the operator, was the length of time over which the averaging of the baseline between overtopping waves was calculated. This method allowed full control of the data to achieve the best results from various test results.

Output from the program consisted of a data file, listing the following parameters:

1. the input parameters
2. the volume of each overtopping wave and its time of entry
3. the total volume of water collected (litres per metre) as calculated from the summation of the individual waves
4. the overall volume as calculated from the start and end readings of the tank file(s)
5. the average discharge in l/s/m

Data from this file was then imported into spreadsheets in which wave by wave overtopping volume distributions were calculated. During the tests a check was made on the number of overtopping waves actually occurring on the model. There was a very good comparison with the number of overtopping events defined by the program giving confidence in the overall assessment of the procedure.

6.3 Number of waves overtopping

6.3.1 Vertical walls

Franco et al (1994) conducted experiments, using methods similar to those described above, to investigate wave by wave overtopping of a vertical wall. The following equation was developed to predict the number of waves overtopping the wall :-

$$N_{wo}/N_w = \exp\left(-\left(R_c/H_s / 0.91\right)^2\right) \qquad (6.1)$$

where N_{wo} is the number of waves overtopping.
N_w is the number of waves in the sample.
R_c is the crest freeboard.
H_s is the inshore significant waveheight.

The tests were conducted in relatively deep water so that non-breaking wave conditions predominated (see Chapter 3 of this report).

The number of waves overtopping the structure equates to the number of run-up events exceeding the crest level. As run-up level is closely dependent on wave height, the distribution of overtopping events is of Raleigh form.

A similar series of tests was conducted at HR Wallingford (Allsop et al (1995)). The main difference between HR Wallingford's tests and those conducted by Franco et al (1994) were that HR Wallingford's tests incorporated both shallow and deep-water conditions. The results concerning the proportion of overtopping waves are plotted in Figure 6.1, along with the prediction line given by equation 6.1. The data labels indicate values of h/H_s, where h is the water depth at the toe of the structure. Values of $h/H_s > 3.0$ indicate relatively deep water. It can be seen that equation 6.1 offers a reasonable approximation to the results for $h/H_s > 3.0$. Fitting an exponential relationship to the deep water data only produces the following equation :-

$$N_{wo}/N_w = \exp(-(R_c/H_s / 0.909)^2) \quad (6.2)$$

Although the data set is rather limited in size, it produces a very similar result to that of Franco et al (1994).

When the water is shallow and breaking waves predominate, this equation under-predicts N_{wo}. There are two principle reasons for this. Firstly, where waves break in significant numbers the distribution of individual wave heights diverges from the Raleigh form. Secondly, the mechanism by which individual waves overtop the structure is altered; being no longer dominated by simple run-up. Waves which break onto the face of the structure generate a different (and more chaotic) water motion than those which reflect and run up it. It is clear that the results for breaking conditions must be distinguished from those for non-breaking conditions, and that they require a different method of analysis.

It is useful at this point to return to the analysis of mean discharge (Chapter 2). The influence of shallow water on mean overtopping discharges over vertical walls was examined by Allsop et al (1995). For simple vertical walls constructed on a shallow sloping bathymetry a wave breaking parameter, h_*, was defined which dictates whether waves at the structure are dominated by impact (breaking) waves or by reflecting/pulsating (non-breaking) waves. h_* is defined by :-

$$h_* = (h/H_s)(2\pi h/gT_m^2) \quad (6.3)$$

where T_m is the inshore mean wave period

Reflecting waves were found to dominate when $h_* > 0.3$. Impacting waves dominate when $h_* \leq 0.3$. The formulation of h_* reflects the fact that waves are more likely to break if the wavelength or the wave height is large compared to water depth.

Allsop et al (1995) found that when $h_* > 0.3$, the overtopping discharge is well described by an equation relating it to R_c/H_s. When $h_* \leq 0.3$, however, it was found that the overtopping discharge was better described by relating it to a parameter which took account of the degree of wave breaking. The new parameter, R_h, was defined as :-

$$R_h = (R_c/H_s)\, h_* \quad (6.4)$$

The data of Allsop et al (1995) concerning the number of waves overtopping, N_{wo}, was examined in terms of R_h (Ref. Madurini). Values of N_{wo} are plotted against R_h for all results with $h_* \leq 0.3$ in Figure 6.2, and produce the following equation :-

$$N_{ow}/N_w = 0.031\ R_h^{-0.99} \qquad (6.5)$$

Equation 6.5 shows good correlation with the data over a range of R_h. It is interesting to note that the proportion of waves overtopping is most over-predicted when $h_* = 0.26$, close to the upper limit of $h_* \leq 0.3$.

On the basis of the above analysis it is recommended that when $h_* > 0.3$, the proportion of waves overtopping the structure should be estimated using equation 6.1. When $h_* \leq 0.3$ equation 6.5 should be used.

6.3.2 Sloped structures

Owen (1992) showed that for smooth slopes, as for vertical walls, the number of waves overtopping was approximately equal to the number of waves with a calculated run-up greater than the crest elevation, i.e. :-.

$$N_{ow}/N_w = \exp(-C\ R_*^2) \qquad (6.6)$$

where N_{ow} is the number of waves overtopping
N_w is the number of waves in the sequence
C is a parameter which depends on the seawall slope
R_* is the dimensionless freeboard given by, $R_c / (T_m (gH_s)^{0.5})$

It is reasonable to assume that the same will hold for armoured slopes. The proportion of overtopping waves is plotted against R_*^2 for a selection of seawalls in Figure 6.3. All the structures have slopes of 1:1.5 but have various types of armour, i.e., CBs, Antifers and Dolos. Also plotted is a line representing a smooth slope, produced by interpolating a value of C between Owen's results for 1:1 and 1:2 slopes. As expected, the results for the armoured slopes have fewer overtopping waves than the smooth slope for a given level of R_*.

Since the run-up level of waves is a function of slope roughness, the number of waves overtopping an armoured slope is expected to be :-

$$N_{ow}/N_w = \exp(-C\ (R_*/r)^2 \qquad (6.7)$$

A series of lines representing equation 6.7 with different values of roughness, r, is plotted on Figure 6.3, using r = 0.3 for the Dolos units, r = 0.5 for the Antifers and r = 0.8 for the CB's. There is a good correlation between the data points and the lines produced by equation 6.7.

Unfortunately the amount of data available from studies with slopes other than 1:1.5 is limited. This is a result of the fact that the majority of tests of armoured structures are conducted on site-specific models. The structures generally have features such as berms and return walls which equation 6.7 cannot account for. It must be remembered that equation 6.7 is applicable only to simple slopes.

Various methods of analysis were investigated in an attempt to predict the number of waves overtopping more complex types of sloped structures. However, no satisfactory method was

developed for accounting for the various structural details. Eventually it was decided that the proportion of waves overtopping could best be described by relating it to the dimensionless mean overtopping discharge, Q_*. An equation was fitted to the data as follows :-

$$N_{ow}/N_w = 55.41 Q_*^{0.634} \quad \text{for } 0 < Q_* < 0.0008 \qquad (6.8a)$$

$$N_{ow}/N_w = 2.502 Q_*^{0.199} \quad \text{for } 0.0008 \leq Q_* > 0.01 \qquad (6.8b)$$

$$N_{ow} = N_w \quad \text{for } Q_* \geq 0.01 \qquad (6.8c)$$

where N_{ow} is the number of waves overtopping
N_w is the number of waves in the sequence
Q_* is the dimensionless overtopping discharge, given by $Q_* = Q / (T_m g H_s)$

The data, prediction lines and 95% confidence limits for $Q^* < 0.0008$ are shown in Figure 6.4. As expected there is a considerable degree of scatter. This is probably due to the variation in structural forms and wave conditions which occur in the data.

6.3.3 Composite structures

No data is available to describe the number of waves overtopping composite structures. It is therefore suggested that rules developed for other structural types be applied. Structures with a small mound could be treated as vertical walls subject to reflecting waves. Structures with a large mound could be treated as vertical walls subject to impacting waves. The distinction between structures with large and small mound is made using the d_* parameter, given by equation 2.32.

6.4 Maximum individual overtopping event

6.4.1 The Weibull distribution

Given that the number of overtopping events N_{wo} can be predicted using the methods described above, and that the mean discharge is known (see Chapter 2) it is now possible to estimate the magnitude of the largest individual overtopping event.

The volumes of individual overtopping events, V, can be described by a Weibull distribution:-

$$P(V) = 1 - \exp(-((V-C)/A)^B) \qquad (6.9)$$

where P(V) = probability of non-exceedance and A, B and C are empirical coefficients. The coefficient C represents the lower limit of the data, representing the minimum individual volume that the experimental method can distinguish. A and B are determined by fitting the Weibull equation to the experimental data.

The maximum expected individual overtopping volume, V_{max}, in a sequence of N_{wo} overtopping waves is then given by :-

$$V_{max} = C + A (\ln(N_{wo}))^{1/B} \qquad 6.10)$$

6.4.2 Vertical walls

Franco et al (1994) determined values of A and B for overtopping of a vertical wall in relatively deep water, giving an expression for A in terms of V_{bar} the average individual overtopping volume :-

$$A = 0.84V_{bar}, \text{ and } B = 0.75 \qquad (6.11)$$

A two parameter Weibull distribution (assuming $C = 0$) was fitted to the results of the HR Wallingford data. Sample probability plots of V/V_{bar} for impact and reflecting conditions are shown in Figures 6.5 and 6.6 respectively. The results correspond well with the Weibull distribution, except at low values of V/V_{bar}, where there is a divergence. Accurate prediction of discharges at low probabilities of non-exceedance is of little interest to the present study. At high probabilities of non-exceedance, the inclusion of C makes little difference to the shape of the distribution as C is very small for all the data sets used. It was therefore decided that the Weibull distribution should be fitted to values of $V > V_{bar}$ only, as this gives the most reliable estimate of V_{max}.

The average value of B for reflected waves in the HR Wallingford data set ($B = 0.754$) was very similar to Franco et al's (1994) result of B=0.75. For impact dominated waves B was found to average 0.854.

Values of A can be determined from the relation:-

$$V_{bar} = C + A\,\Gamma\,(1 + 1/B) \qquad (6.12)$$

Where Γ is the Gamma function that can be found in mathematical tables. For reflecting waves A= 0.843 V_{bar} (compared with A = 0.84 V_{bar} from Franco et al (1994)), but for impacts, A=0.922 V_{bar}.

When reflected waves predominate (i.e., when $h_* > 0.3$) the maximum individual overtopping volume, V_{max}, in a series of N_{wo} overtopping waves, is therefore given by :-

$$V_{max} = 0.843\ V_{bar}\ (\ln(N_{wo}))^{1/0.754} \qquad (6.13)$$

When impact waves predominate (i.e., when $h_* < 0.3$) the maximum individual overtopping is given by :-

$$V_{max} = 0.922 V_{bar}\ (\ln(N_{wo}))^{1/0.854} \qquad (6.14)$$

Values of V_{max} estimated from equations 6.13 and 6.14 (using measured V_{bar} and N_{ow}) are presented in Figure 6.7, plotted against measured values of V_{max} from the HR Wallingford data set. A reasonable correlation is obtained.

Franco (1996) determined values of B for vertical walls and found that B was dependent on wave steepness and on whether the waves were short-crested or long-crested. For a wave steepness of 0.02 Franco (1996) found that B = 0.66 and 0.72 for long-crested and short-crested waves respectively. For a steepness of 0.04 the corresponding results were 0.82 and 0.94. As small values of B indicate larger maximum volumes, these results will be recommended in the manual as a conservative approach.

6.4.3 Sloped structures

Individual wave overtopping volumes were analysed from a variety of tests on sloped structures, including both site-specific and generic model studies. The overtopping events are distributed in a similar way to those of a vertical wall, i.e., they follow a Weibull distribution for $V > V_{bar}$. At lower levels of V there is a divergence from the Weibull distribution, so as before the Weibull parameters were calculated for $V > V_{bar}$ only. There was generally more variation in the parameters *A* and *B* than in the case of the vertical structures. This is to be expected as the structures included in the study incorporated a variety of features, such as berms and crest walls etc. However, no distinct pattern emerged to enable particular values to be associated with specific structural types or sea conditions. If the averages of all values of *A* and *B* are taken, then the equation describing the maximum individual overtopping volume for a sloped structure is :-

$$V_{max} = 0.921 V_{bar} (\ln(N_{ow}))^{1/0.853} \qquad (6.15)$$

Franco (1996) also examined sloped structures and found that values of *B* were generally 0.1 higher than the equivalent vertical wall results.

6.4.4 Composite structures

No data is available describing the distribution of individual waves overtopping composite structures. It is therefore suggested that rules developed for other structural types be applied. Structures with a small mound could be treated as vertical walls subject to reflecting waves. Structures with a large mound could be treated as vertical walls subject to impacting waves.

6.5 Effect of angled wave attack on number of waves overtopping

Chapter 3 describes Franco's (1996) reduction factors for predicting the number of waves overtopping a vertical wall under angled wave attack. The reduction factors are intended for use in Franco et al's (1994) equation (6.1 above) which applies only to non-breaking waves. There is at present no satisfactory method for predicting the effect of angled wave attack on the number of waves overtopping a vertical wall when breaking waves predominate.

Franco (1996) also determined reduction factors for sloped structures. These factors are intended for use with Smith et al's (1994) equation for predicting the number of waves overtopping a slope, which was based upon the van der Meer and de Waal (1992) expressions for run-up and overtopping. As explained in Chapter 2 of this report it was decided that the manual would utilise the Owen (1980) method for calculating mean discharges over sloped structures and that the Banyard and Herbert (1995) equations would be used to describe effect of angled attack. Banyard and Herbert (1995) did not measure the number of waves overtopping. However, Franco (1996) concluded that as a result of angled attack the mean discharge was reduced. Similarly the number of waves overtopping were reduced but to a lesser extent. It should be noted that a particular level of mean discharge distributed over a smaller number of waves gives larger values of individual volume, therefore a conservative approach is to under-predict the number of waves overtopping. It is recommended that the same reduction factor calculated for the mean discharge be applied to the number of waves overtopping.

6.6 Relationship between peak events and mean discharge

6.6.1 Vertical walls

Reflecting waves
The analysis presented above may be used to develop relationships between mean discharge and peak events.

Reflecting waves are those for which $h_* > 0.3$. Given a description of the structure and the wave climate the mean overtopping discharge, Q, of a vertical wall in reflecting waves can be estimated using the methods described in Chapter 2. The proportion of overtopping waves, N_{wo} / N_w, can then be calculated using equation 6.1. The average volume, V_{bar}, per overtopping wave can then be calculated. The volume of the largest overtopping event in a sequence of waves can then be estimated using equation 6.13.

Measured values of V_{max} are plotted against measured values of Q for the HR Wallingford tests in Figure 6.8. Each data point represents the largest overtopping event in a test with a duration corresponding to 1177 wave periods. A nominal scale has been applied to present the data as prototype equivalent values. Incident wave height, H_s, ranged from 0.7m to 0.5m.

Also plotted on Figure 6.8 is the relationship between Q and V_{max} predicted using equations 6.1 and 6.13 along with the method for predicting mean discharge given in Chapter 2. Prediction lines are given for wave heights of H_s = 0.7m and 1.5m. It can be seen that for a given value of Q, the predicted maximum individual overtopping volume increases significantly with increasing H_s. This is in accordance with the findings of van der Meer & Janssen (1995) for overtopping of sloping dykes and demonstrates that specifying safety limits only in terms of mean discharge can be misleading.

The results of Franco et al's (1994) tests using 1000 waves are also plotted in Figure 6.8. The wave heights varied from 3m to 5m, considerably higher than those used in this study. The values of V_{max} measured are accordingly higher. The general trend, however, follows that of the HR Wallingford results.

Impacting waves
Impacting waves are those with $h_* \leq 0.3$. The mean overtopping discharge, Q, can be estimated using the method described in Chapter 2, and the proportion of overtopping waves using equation 6.5. The average volume, V_{bar}, per overtopping wave can then be calculated. The volume of the largest overtopping event in a sequence of waves can then be estimated using equation 6.14.

The results of the impacting waves using HR Wallingford data are shown in Figure 6.9. The incident wave conditions ranges from H_s = 0.16m to 0.2m, T_m = 1.59s to 2.5s, and h from 0.34m to 0.43m. The h_* parameter, which governs the "breaking performance" of the waves, varies from 0.1 to 0.26. Also plotted on Figure 6.9 is a prediction line valid between h_*= 0.1 to 0.26. The predicted value of V_{max} is fairly insensitive to changes in h_*.

6.6.2 Sloping structures

A similar exercise was carried out using two sets of site-specific results for armoured seawalls. Results are shown in Figures 6.10 and 6.11. Equation 2.3 from chapter 2 along with equations 6.8 and 6.15 from this chapter were used to estimate the relationship between mean discharge, Q, and peak event, V_{max}. As can be seen the equations predict the general trend of the data, although there is some divergence. This may in part be due to the uncertainties in equation 6.8 and the *A* and *B* parameters discussed above.

6.7 Peak flow rates

Model tests suggest the time over which the peak individual volume is discharged is approximately 40% of the mean wave period. This relation can be used to estimate the peak flow if required.

6.8 Conclusions

The method proposed by Franco et al (1994), based on a Rayleigh distribution of run-up levels, provides an accurate estimate of the number of waves which overtop a vertical wall in predominantly non-breaking conditions. When wave breaking predominates however, different processes occur. The waves are non-Rayleigh distributed and run-up levels are affected by interaction of the breaking waves with the wall. A method has been described which takes account of these factors.

The Rayleigh distribution of run-up levels also provides a reasonable estimate of the number of waves which overtop a simply sloped structure. For more complex types of sloped structure however, such as those with berms and crest walls, no reliable method of predicting the number of waves overtopping a structure from run-up levels could be determined. The most effective way of estimating the number of waves overtopping is to relate it to the mean discharge rate.

The distribution of overtopping volumes can be represented by a Weibull distribution. The parameters of the distribution vary with structural type and wave conditions. Parameters have been presented for various situations.

The relationship between mean discharge and maximum event is not constant, but varies with wave climate and type of structure. When specifying overtopping limits for safety it is therefore important to try and estimate the largest overtopping volume.

7. THE EFFECT OF CREST BERM WIDTH ON OVERTOPPING DISCHARGES

7.1 Introduction

This Chapter describes a series of physical model tests conducted at HR Wallingford in order to investigate the effect of crest berm width on the mean overtopping discharge of an armoured seawall. This is an area which has not been the subject of much previous research, and yet experience has shown the crest berm width to be a major influence on the performance of seawalls and breakwaters. One method to assess the performance of crest berms was formulated from the results of several site-specific model tests. The rule of thumb suggests that for every 10m back from the crest, the overtopping will reduce by a factor of 10. This Chapter briefly examines the data on which this rule was based. A revised design guideline is then presented, based on the results of new tests conducted specifically to examine the effect of crest berm width.

7.2 Previous work

The existing guideline was formulated from the results of several site-specific model studies conducted at HR Wallingford. Two of the most significant of these were Herbert & Reeves (1991) and Lowe (1991). This section examines the data from the two studies and suggests ways in which the work could be extended.

Two sea defence structures, both rock-armoured slopes, were assessed by Herbert & Reeves (1991). The tests were designed to investigate rock armour stability, the level of wave reflections and the overtopping discharge for a number of extreme conditions. Overtopping was measured in a calibrated tank immediately behind the top of the armour slope. The tests were intended to investigate how much of the airborne overtopping water would reach a distance of 10m behind the top of the armour slope. For this reason, the tank was split into two compartments so that any airborne water landing further back than 10m from the crest could be measured separately. Measurements were taken throughout the whole 6 hour prototype test duration. The data collected are shown in Table 7.1, which gives the total discharge measured in both sections of the tank, Q_0, and the discharge measured only in the rearward section, Q_{10}. Wave conditions were defined offshore.

The effectiveness of a crest berm of width, Cw, in reducing overtopping discharge can be quantified by a reduction factor, C_f, given by the ratio of the overtopping discharge measured behind the crest berm to that measured when the berm is not present, i.e.,

$$C_f = Q_w / Q_0 \qquad (7.1)$$

where Q_w = measured discharge at distance Cw behind crest
Q_0 = measured discharge with no berm

In the case of these tests, the overtopping measured in the rearward tank can be considered equal to that which would be experienced behind a 10m wide crest berm. The sum of the discharge in both tanks will be the discharge experienced if no berm is present. It must be remembered that these values only apply to airborne water. On a real structure some overtopping water will reach a distance of 10m by flowing over the crest berm.

Values of C_f for the Herbert & Reeves (1991) data are given in Table 7.1. C_w generally falls between 0.07 and 0.33 and averages 0.15.

More detailed experiments were carried out on a model armoured seawall by Lowe (1991). The purpose of the tests was to determine the degree of movement or displacement of the armour and to determine the overtopping experienced at certain distances behind the crest.

Overtopping of the seawall was measured using a collecting tank placed directly behind the top of the armour slope. The collecting tank had five compartments separated by walls set at 5.0, 6.3, 8.0, 11.0 and 20m from the top of the slope. Test results are shown in Table 7.2. As with the Herbert & Reeves (1991) data, wave conditions are defined offshore. The discharge given for a particular distance in Table 7.2 refers to the total discharge which was measured beyond that distance.

The reduction factor, C_f, (as defined above) is plotted in Figure 7.1 for each distance. Results are divided according to rock armour size. There is a considerable degree of scatter in the data. The average reduction factor for a crest width of 10m is approximately 0.06 and for a 20m crest width 0.003. Some variation in reduction factor can be seen with rock size. The fact that the results for 6.8t rocks generally lie between those for 2.5t and 5t however, suggests this is not an important parameter and that the scatter is more likely to be due to other factors or simply to the inherent inaccuracies in the method.

These two sets of results were, in part, the basis of the design rule quoted in the introduction. Because of the way in which the tests were conducted only airborne water was collected at a number of locations behind the crest. This does not accurately reflect the behaviour of water flowing over a crest berm. Consequently a new programme of tests was conducted which accurately represented this effect. The results are described in the following section.

7.3 Model tests

7.3.1 Facilities

The physical model tests were carried out in HR Wallingford's deep random wave flume. The flume is 52m long and has an operating range of water depths at the paddle of between 1.3m and 1.7m. For most of its length the flume is split into 1.2m wide central test channel and two side absorption channels. Splitter walls of graduated porosity between the central and side channels are designed to minimise the level of re-reflected waves. The central channel terminates in a 10m long 'finger flume'. The test section is constructed close to the end of the finger flume and is bounded on both sides by glass walls. The wave paddle is a buoyant sliding wedge driven by a double acting hydraulic ram. A computer, using software developed at HR Wallingford, controls the paddle enabling either regular or random waves to be produced.

7.3.2 Test sections

The models were constructed to a scale of 1:31.8. The bathymetry (seabed profile) was constructed at a slope of 1:70 and was manufactured from a layer of cement mortar overlying a compacted sand fill. The bathymetry was placed to within a vertical accuracy of +/-0.05m and a horizontal accuracy of +/- 0.1m.

Two separate sections were tested; an Accropode-armoured section and a rock-armoured section with slopes of 1:1.5 and 1:2 respectively. The cross section of the Accropode structure is shown in Figure 7.2. The Accropodes were hand placed to a specific laying pattern by a qualified member of personnel. Both the core and underlayer rock were designed to reproduce a realistic level of porosity. A small crest wall was located behind the top row of Accropodes, at a level equivalent to 9.0m OD. The crest berm was armoured with 6-8t rock armour placed behind the crest wall. A rock toe was also used to ensure stability of the Accropodes.

The rock-armoured structure (Figure 7.3) had a slope of 1:2 to maintain consistency with the data of Lowe (1991). Rock armour of 10 – 12t was used on the front face and for the crest berm. The toe was constructed of 6-8t rock.

7.3.3 Test procedures

The same wave conditions were used to test both structures, these are shown in Table 7.3. The wave conditions used were designed to cause a wide range of overtopping discharges. All wave conditions were calibrated in the flume before any structure was built. A shingle-spending beach located at the end of the flume ensured that reflections during calibration were reduced to a minimum. Twin wire resistance type wave gauges were used at the calibration point, which was at the toe of the structure, to measure the wave height and period.

Each test consisted of the running of one wave condition for a period equivalent to 1000 waves. The length of the wave sequence (the time taken before the wave record begins to repeat) was considerably longer than the actual test length. This safeguards against any group of waves being repeated.

Each test was repeated with varying crest widths, starting with no crest berm and increasing in 5m increments up to 20m. Water overtopping the structure was collected on a chute, located behind the crest berm. The chute ran into a calibrated tank in which the mean overtopping discharge was measured electronically. The crest berm reduction factor, C_f, was calculated as the ratio of measured overtopping with a berm to that without a berm.

7.4 Test results

7.4.1 Comparison with Owen's equation

The overtopping results for both structures are shown in Table 7.4. A plot of dimensionless overtopping, Q_*, against dimensionless crest freeboard, R_*, for the Accropode and rock-armoured structures are shown in Figures 7.4 and 7.5 respectively. These graphs are compiled with data for seawalls with no crest berms. Q_* and R_* are defined by equations 2.3 and 2.1 from Chapter 2 of this report. Also plotted in each case is the predicted relationship between Q_* and R_* from equation 2.7, using the appropriate values of A and B from Table 2.1 with r = 0.55 for the rock-armoured structure and r = 0.4 for the Accropode structure. A good correlation is obtained in the case of the rock armoured structure. For the Accropode structure the correlation is acceptable, although, as noted in Chapter 4 of this report, the slope of the line is not accurately reproduced by the A and B coefficients.

7.4.2 Effect of berm width

Values of C_f for both structures are given in Table 7.4. C_f is plotted against crest width in Figure 7.6 for the Accropode-armoured structure. An exponential trend line has been fitted to each test data set. There is very little variation in the trend of C_f with crest width from test to test. The results show that the crest berm is more effective on this structure than the design rule quoted above suggests. An average reduction factor of approximately 0.03 results from a 10m crest width, compared to the previously estimated value of 0.10.

The reduction factors are plotted against crest width for the rock armoured structure in Figure 7.7. As with the Accropode tests there is very little variation with wave condition. For a crest width of 10m C_w is approximately 0.1, a similar result to that obtained in the previous studies. Visual observations suggest that the majority of water arriving at the collection chute is in fact airborne.

The performance of the crest berm on the rock-armoured structure is not as good as that of the Accropode-armoured structure, despite the fact that the berms were armoured with rock in both cases. There could be several explanations for this. The increased roughness of the Accropodes may influence the patterns of flow at the crest. Alternatively the design of the Accropode seawall itself may be influencing the results. A small concrete seawall is located just behind the crest of the Accropodes (Figure 7.2). This wall helps to hold the Accropodes in place, thus making them more secure. It also has the effect of reducing the amount of water that passes through the armour at the crest, and diverts flow upwards, possibly increasing the effectiveness of the crest berm.

7.5 Design guideline

The results described above have been used to formulate a revised formula for predicting the effect of crest berms on overtopping discharges. The first point to note is that the Accropode structure generally demonstrated a more efficient crest berm than the rock structure. The reasons for this are not entirely clear, although it is possible that it is due to differences in the details of the models. In order to take a conservative approach the design recommendation will therefore be made on the basis of the rock structure results only.

Clearly the most important parameter is the crest width. The most appropriate way of non-dimensionalising the crest width is by calculating its ratio to the incident wave height at the toe of the structure, H_s.

A plot of C_f against dimensionless crest width, Cw/H_s, for both the rock and Accropode structures is shown in Figure 7.8. There appears to be a good correlation in both cases, with relatively little scatter. Equations were fitted to both sets of data, as follows :-

For Accropode armoured structures: $C_f = 4.35 \exp(-2.1\ Cw/H_s)$ (7.2)

For rock armoured structures: $C_f = 3.06 \exp(-1.5\ Cw/H_s)$ (7.3)

The equations result in values of C_f of 1 when $Cw/H_s = 0.7$ and 0.75 for the Accropode and rock-armoured structures respectively. This may suggest that a berm with a width C_w less than $H_s \times 0.7$ will be relatively ineffective.

7.6 Conclusions

The effectiveness of crest berms in reducing mean overtopping discharges has been investigated by a new set of model tests. The results are broadly in agreement with previous studies. The previously accepted design rule was that the overtopping discharge reduced by a factor of 10 every 10m behind the top of the slope. This rule has been confirmed for crest widths up to 20m wide. The new tests are a more realistic reflection of prototype structures. Results have been expressed in a non-dimensional form which can be incorporated in design methods. The berm behind the Accropode-armoured structure was more effective than that behind the rock-armoured structure. It is not entirely clear whether this is due to minor difference in crest detail or any inherent properties of the armour units. Consequently the results from the rock-armoured structure have been used, so that a conservative approach is taken.

8. TOLERABLE OVERTOPPING LIMITS

8.1 Introduction

Overtopping limits have traditionally been specified in terms of mean discharge rates. The generally accepted limits (Simm (1991)) are reproduced in Figure 8.1. This is a rational approach to take when designing for flood prevention. When attempting to assess safety levels however, this approach is questionable, as the maximum individual event is expected to be of greater significance. The analysis presented in chapter 3 of this report, demonstrates that, for a given level of mean discharge, the volume of the largest overtopping event will vary with wave conditions and structural type. It is thus inconsistent to specify safety levels with sole reference to mean discharge levels.

8.2 Model studies

Data correlating individual overtopping events with hazard levels are rare. One of the few studies was carried out by Franco et al (1994), who conducted experiments which investigated safe overtopping limits for pedestrians and vehicles. It was demonstrated, by means of model tests and experiments on volunteers, that the danger level which an individual overtopping event represents can be directly related to its volume. A volume was defined as "safe" if it created a less than 10% chance of the individual who is subjected to it falling over. An event was defined as "very dangerous" if it created a greater than 90% chance of the individual subjected to it falling over.

Franco et al (1994) discovered that the "safe" limit varied with structural type. A given volume overtopping a vertical structure was found to be more dangerous than the same volume overtopping a sloped, armoured structure. The "safe" limit for a vertical wall was found to be $0.1m^3/m$, whilst for a sloped, armoured structure it was $0.75m^3/m$. For the same structures, the "very dangerous" limits were $0.75m^3/m$ and $2m^3/m$ respectively. However, Franco et al (1994) also noted that a volume as low as $0.05m^3/m$ could unbalance an individual when striking their upper body without warning. The latter figure was determined from experiments on volunteers rather than from model tests and can thus be considered more realistic.

Franco et al (1994) determined very different limits for different types of structure. It is thought that such differences may be due to the structure's crest detail, in particular the height of any parapet wall, if present. This factor determines how the overtopping water jet impacts upon the individual.

8.3 Prototype experiences and observations

8.3.1 Full scale grass dyke tests

Smith et al (1994) reported on full-scale tests conducted on grass dykes. An observer stood on the crest of the dyke as it was being tested. One of the objects of the experiment was to determine safe overtopping limits for personnel carrying out inspection and repair work. Smith et al (1994) concluded that work was unsafe when the mean discharge exceeded 10 l/s/m. From an examination of Smith et al's (1994) data this corresponded to a maximum individual volume, V_{max}, of approximately $1.6m^3/m$. This is between the "safe" and "very dangerous" limits for the sloped, armoured structure determined by Franco et al (1994), and accords with their observation that safe limit of V_{max} varies with structural type. One reason

for this variation may be the different way in which the water strikes the individual. Smith et al (1994) reported that the vast majority of the overtopping discharge acted on the observer's legs only. It must also be borne in mind that the safety limits for trained personnel (such as the observer in Smith et al's (1994) tests) working on a structure and anticipating overtopping are higher than those for other users.

8.3.2 Colwyn Bay vertical wall

Information on prototype safety is available from Herbert (1996) who monitored overtopping at a vertical seawall at Colwyn Bay, Wales. During the installation and operation of the apparatus it was noted that personnel could work safely on the crest of the wall during mean discharges of up to 0.1 l/s/m. When the mean discharges exceeded 0.1 l/s/m it was considered unsafe. This limit is considerably lower than that given by Smith et al (1994). Individual overtopping volumes were not measured, however, the methods described in the preceding chapters of this report can be used to provide an estimate of V_{max}, given that the mean discharge and the incident wave conditions are known. This process results in an estimated V_{max} of approximately $0.04m^3/m$ for the sea state which caused the 0.1 l/s/m mean discharge. This is in close agreement with Franco et al's (1994) estimate of the volume which could cause someone to lose their balance.

Herbert (1994) also noted that overtopping became a danger to vehicles when the mean discharge exceeded 0.2 l/s. Using the process described above it was determined that this corresponds to a V_{max} of approximately $0.06m^3/m$.

8.3.3 Endoh & Takahashi

An alternative approach to defining safety limits of individual overtopping events is to look at them in terms of peak discharge. Endoh and Takahashi (1994) conducted experiments on volunteers to determine the peak flow rates which would be dangerous to pedestrians. Using a similar method to Franco et al (1994) they subjected volunteers to high rates of flow and determined the point at which they were unbalanced. Instead of total volume however, they measured flow rates. They also developed a numerical model based on the computed drag forces on a person. Good agreement was found between the predicted and measured flow rates at which the person fell over. They extended the study to predict flow rates which would carry people over handrails and barriers.

The way in which the water struck the volunteer was, as in the experiments of Smith et al (1994), on the legs only. From an examination of Endo and Takahashi's (1994) results it would seem that, typically, a flow rate of 0.8 to $1m^3/s/m$ unbalanced the volunteer. Assuming the duration of the flow in a prototype wave would be several seconds, this corresponds to an individual overtopping volume of approximately 2 to 3 m^3/m. This accords reasonably well with the result of Smith et al (1994).

8.3.4 Orkney Islands Churchill Barriers

For the purposes of this report observations of overtopping at three sites have been made using video footage recorded on-site. The three locations were Churchill Barriers in the Orkney Islands, Sidmouth on the south coast of England and Towyn on the north Wales coast. Of these only the Churchill Barrier site gave enough data to provide a full analysis. The methods described in the preceding chapters of this report were used in conjunction with information from the video tapes to estimate the mean and peak overtopping rates.

Footage of a storm occurring on 5th – 6th of January 1996 was available at the Churchill Barrier site. An extensive sequences of video was taken from one location at the southern end of the site. A knowledge of the site from earlier studies allowed the incident wave conditions and water levels to be estimated.

The conditions used in the analysis were as follows. The Barrier consists of a sloping, concrete block armoured 1:1 gradient slope with a flat-topped crest, carrying a two lane road, at about 5.08m ODN. There is a crash barrier at the edge of each carriageway. The sea bed level at the toe was taken as – 4.67m ODN. The estimated water level during the storm was 1.39m ODN, which is the same as the predicted high tide at Wick on 5th January. This gave a water depth of 6.06m. Depth limited wave conditions were assumed to be occurring during the storm. The depth limited significant wave height is given by 0.55 x water depth, and is therefore 3.33m. From the video the wave period was estimated at 7.2 seconds, giving a sea steepness of 0.041. Also, and most importantly, an estimate was made from the video of the proportion of overtopping waves. This was found to be 40%. This value can be used to estimate the dimensionless discharge, Q_*, (using equations 6.8(a) to 6.8(b)) as 4.2×10^{-4}.

From the definition of Q_* (equation 2.3)

$$Q = Q_* T_m g H_s = 0.0989 \text{ m}^3/\text{s/m} \qquad (8.1)$$

The video lasted 2040 seconds, giving a total overtopping volume of $202\text{m}^3/\text{m}$. The number of overtopping waves, N_{ow}, is 113. The average volume per overtopping wave, V_{bar}, is therefore $1.79\text{m}^3/\text{m}$. Finally, equation 6.15 gives the maximum overtopping volume in the sequence :-

$$V_{max} = 0.921 \, V_{bar} \, (\ln N_{ow})^{1/0.853} = 10.2\text{m}^3/\text{m} \qquad (8.2)$$

To confirm this figure the mean discharge was estimated using equation 2.7 with the appropriate values of A and B from Table 3.1 and assuming r = 0.55. This results in Q = $0.070\text{m}^3/\text{s/m}$ and $V_{max} = 7.15\text{m}^3/\text{m}$. The differences in these predictions are well within the accuracy limits of the methods involved.

Whether considered in terms of mean or peak discharges, the overtopping experienced during this storm was well in excess of safety limits suggested by all the relevant studies. For example, Herbert (1996) considered a mean discharge of 0.2 l/s/m to be hazardous to traffic. However, throughout the sequence used for estimating the number of overtopping waves, vehicles continued to pass across the barrier in both directions, despite the large amounts of water both on the road and in the air. (At one time a learner motorcyclist on a 50cc moped was seen to cross!). It was noted that several of the vehicles were hit by the spray from overtopping waves. About two hours after the start of filming a blue flashing light on a police car can be seen on the far side of the barrier, which was then closed to further traffic.

From the video it was clear that most of the overtopping discharge was in the form of spray rather than green water. This fact would reduce hazard levels to some extent, as it seems reasonable to assume that discharge in this form is less dangerous than green water discharge. It is, however, difficult to predict with any degree of certainty whether the overtopping discharge on a particular structure will be in the form of spray or not. The possibility of overtopping being in the form of spray does not therefore justify the upward revision of overtopping limits.

This video footage, combined with knowledge of the site, gave a valuable data set from which likely discharges could be estimated using the methods presented in this report. For this procedure to be used the minimum requirements are a knowledge of the inshore wave conditions and water level and the design of the structure. In this case depth limited waves were assumed and water level was estimated from tide tables. The wave period was estimated from the video footage. Secondly, although video footage for a number of sites was investigated, it became clear that often such material is inadequate. If this procedure is to be used successfully then several minutes worth of video from a fixed location is required to give an adequate estimate of both N_{wo}, the number of overtopping waves, and the incident wave period.

8.4 Mean discharges

Whilst maximum individual volumes are recommended for use in specifying limits for safety of personnel and vehicles, mean discharge is more appropriate in other areas of interest. These include the integrity of the seawall itself, where damage tends to be progressive rather than resulting from a single severe event. For this reason the current limits (Figure 8.1) are recommended. It may have been appropriate to examine damage to building in terms of maximum volume. Unfortunately no data is available. The current limits are therefore retained.

8.5 Specification of tolerable overtopping

Data concerning overtopping limits in terms of individual volumes is available from a variety of sources. Although various values have been proposed for safe overtopping limits, most of this variation can be attributed to differences in the structure under consideration. Most results indicate that tolerable discharges can be higher when water strikes an individual on the lower legs than on the upper body. Overtopping is also more dangerous when in the form of a concentrated jet rather than spray. The authors consider that the most dangerous mode of water striking a pedestrian could occur on any structural type. Franco et al's (1994) data indicate that, when this occurs, a volume of as little as $0.05m^3/m$ can cause an individual to fall over. Prototype measurements indicated an almost identical figure of $0.04\ m^3/m$. This figure was therefore recommended for inclusion in the manual. A limit of $0.06\ m^3/m$ was adopted as the limit for vehicles.

Any situation in which the limits given above are exceeded is likely to be potentially hazardous to pedestrians and vehicles. These limits imply that many situations in which even a single green water overtopping event occurs are potentially hazardous. In these cases safety can only be assured when no overtopping takes place. Because of the random nature of waves it is difficult to specify a situation in which overtopping events are completely eliminated. A probabilistic approach is therefore required. The probability of an individual wave overtopping is given by N_{ow}/N_w. The probability that no waves will overtop during a sequence of N_w waves is therefore :-

$$P(\text{no overtopping}) = (1-N_{ow}/N_w)^{Nw} \qquad (8.3)$$

and the probability that there will be at least one overtopping event during the sequence is given by :-

$$P(\text{overtopping}) = 1- (1-N_{ow}/N_w)^{Nw} \qquad (8.4)$$

The acceptable risk of an overtopping event occurring may depend on the use of the structure in question. It is therefore recommended that when analysis of individual overtopping volumes indicates that very small numbers of overtopping events create unsafe conditions the structure should be optimised by limiting the probability of an overtopping event taking place to an acceptable level. When overtopping events do occur, discharges must be limited to the values given above.

References

Allsop, N.W.H., Besley, P., and Madurini, L., Overtopping Performance of Vertical and Composite Breakwaters, Seawalls and Low Reflection Alternatives, Paper 4.6 in Final Proceedings of MCS Project, published by University of Hanover, 1995.

Allsop, N.W.H., McKenna, J.E., Vicinanza, D., and Whittaker, T.J.T., New Design Methods for Wave Impact Loadings on Vertical Breakwaters and Seawalls, Proceedings of 25th ICCE, Orlando, published by ASCE, 1996.

Banyard, L., and Herbert, D.M., The Effect of Wave Angle on the Overtopping of Seawalls, HR Wallingford, Report SR 396, 1995.

Besley P., Allsop, N.W.H, Colombo, D., and Madurini L., Overtopping Performance of Vertical Walls and Low Reflection Alternatives : Results of Wave Flume Tests, Paper presented to 3rd MCS Workshop, Emmeloord, 1994.

Besley, P., Reeves, M.K., and Allsop, H., Single Layer Armour Unit Research Club, Random Wave Physical Model Tests : Overtopping and Reflection Performance, HR Wallingford, Report IT 384, 1996.

Bradbury, A.P., Allsop, N.W.H. and Stephens, R.V., Hydraulic Performance of Breakwater Crown Walls, HR Wallingford, Report SR 146, 1988.

de Waal, J.P., Wave Overtopping of Vertical Coastal Structures : Influence of wave Breaking and Wind, Paper presented to 2nd MCS Workshop, Milan, 1994.

de Waal, J.P., and van der Meer, J.W., Wave Run-up and Overtopping on Coastal Structures, Proceedings 23rd ICCE, Venice, published by ASCE, 1992.

Endoh, K., and Takahashi, S., Numerically Modelling Personnel Danger on Promenade Breakwater due to Overtopping Waves, Proc. International Conference on Coastal Engineering, Kobe, Japan, 1994.

Franco, C., Wave Overtopping and Loads on Caisson Breakwaters under Three Dimensional Sea States, Delft Hydraulics, complete reference unobtainable to date, 1996.

Franco, L. Comments to paper 4. Coastline Structures and Breakwaters, 19-20 March 1998, ICE London, Published by Thomas Telford.

Franco, L., Overtopping of Vertical Faced Breakwaters : Results of Model Tests and Admissible Overtopping Rates, Paper presented to 1st MCS Workshop, Milan, 1993.

Franco, L., de Gerloni, M., and van der Meer, J.W., Wave Overtopping at Vertical and Composite Breakwaters, Proceedings 24th ICCE, Kobe, published by ASCE, 1994.

Goda, Y., Random Seas and Design of Maritime Structures, University of Tokyo, 1985.

Herbert, D.M., Wave Overtopping of Vertical Walls, HR Wallingford, Report SR 316, 1993.

Herbert, D.M., The Overtopping of Seawalls, A Comparison between Prototype and Physical Model Data, HR Wallingford, Report TR22, 1996.

Herbert, D.M and Reeves, M K., Report EX 2433, HR Wallingford Ltd, 1991.

Lowe, J P., Report EX 2310, HR Wallingford Ltd, 1991.

Madurini, L., Laboratory notes, unpublished, HR Wallingford

Owen , M.W., Design of Seawalls Allowing for Wave Overtopping, HR Wallingford, Report EX 924, 1980.

Owen, M.W., Overtopping of Sea Defences, Paper presented to International Conference on the Hydraulic Modelling of Civil Engineering Structures, Coventry, 1992.

Owen, M.W., and Steele, A.A.J., Effectiveness of Recurved Wave Return Walls, HR Wallingford, Report SR 261, 1991.

Simm J.D., (Editor), Manual on the use of rock in coastal and shoreline engineering, CIRIA special publication 83, CUR Report 154, 1991.

Smith, G.M., Seijffert, J.W.W., and van der Meer, J.W., Erosion and Overtopping of a Grass Dike : Large Scale Model Tests, Proc. International Conference on Coastal Engineering, Kobe, Japan, 1994.

van der Meer, J.W., and de Waal, J.P., Summary of Wave Overtopping at Dykes, Technical Note, Delft Hydraulics, 1992.

van der Meer, J.W., and Janssen, J.P.F.M., Wave Run-Up and Wave Overtopping at Dikes, in Wave Forces on Inclined and Vertical Wall Structures, ASCE, 1995.

Figures

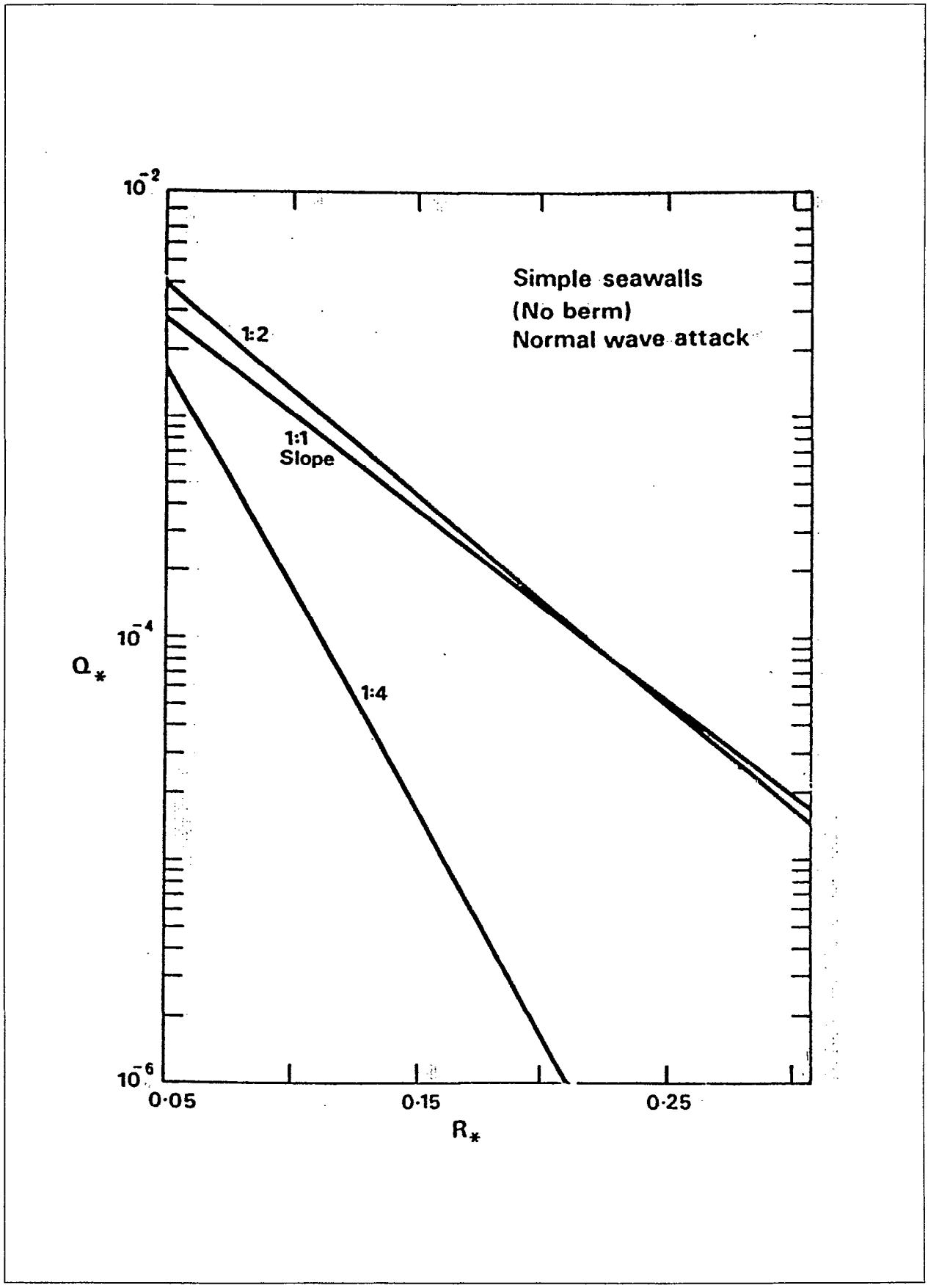

Figure 2.1 Owen (1980) relationship for impermeable simple slopes

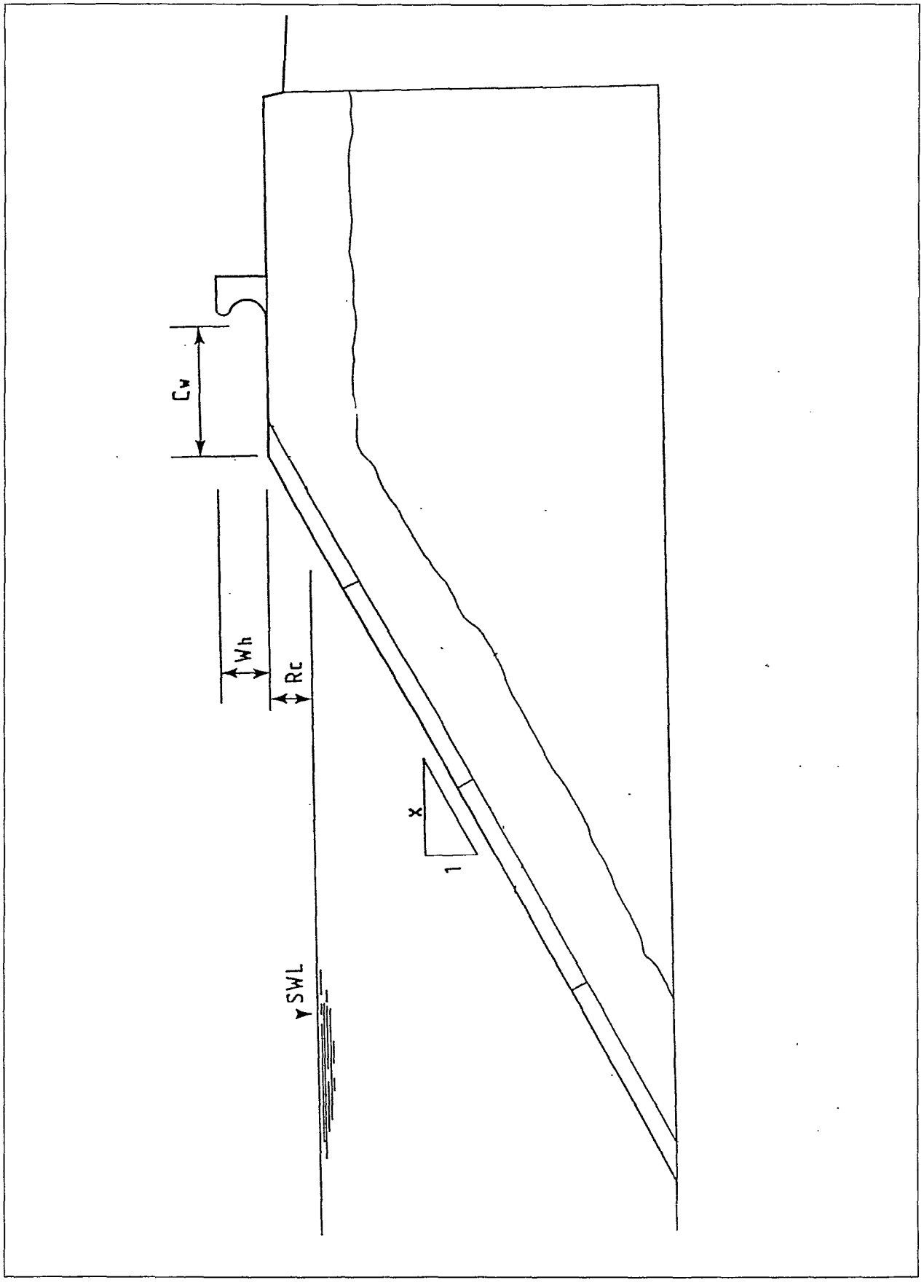

Figure 2.2 Wave return wall

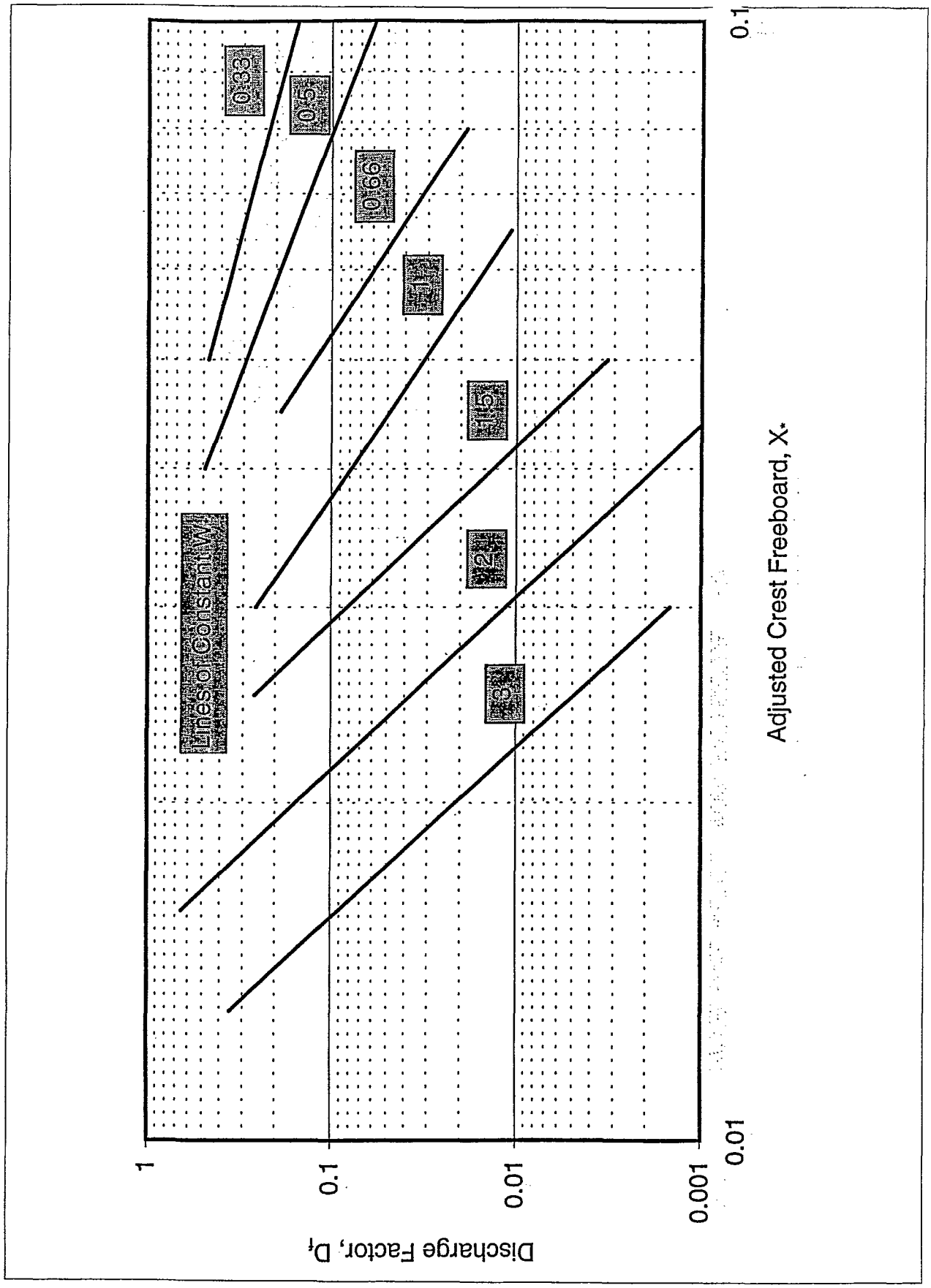

Figure 2.3 **Wave return wall design chart (Owen and Steele(1991))**

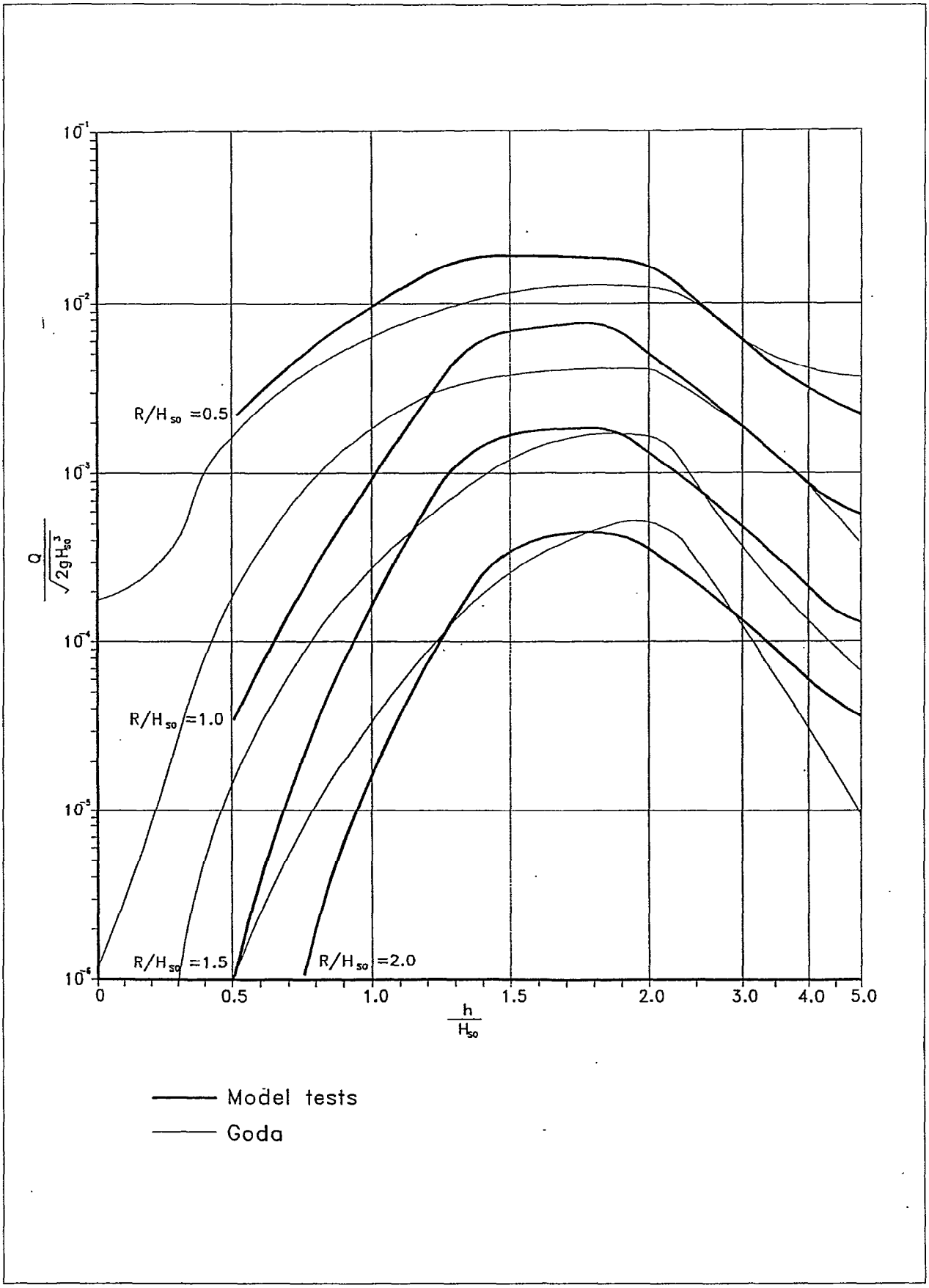

Figure 2.4 Goda's (1985) graphical design method

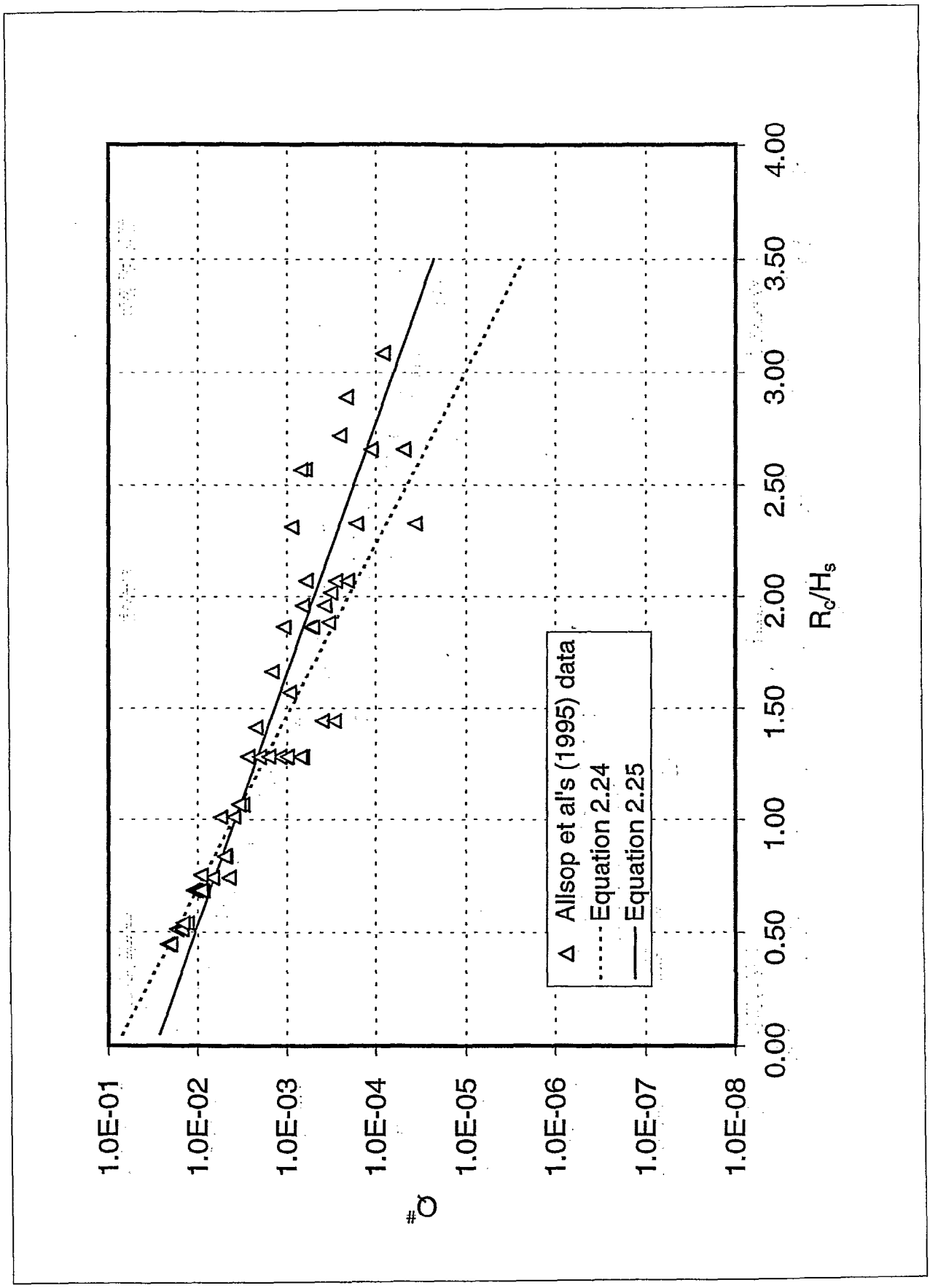

Figure 2.5 Overtopping of vertical wall (Allsop et al (1995))

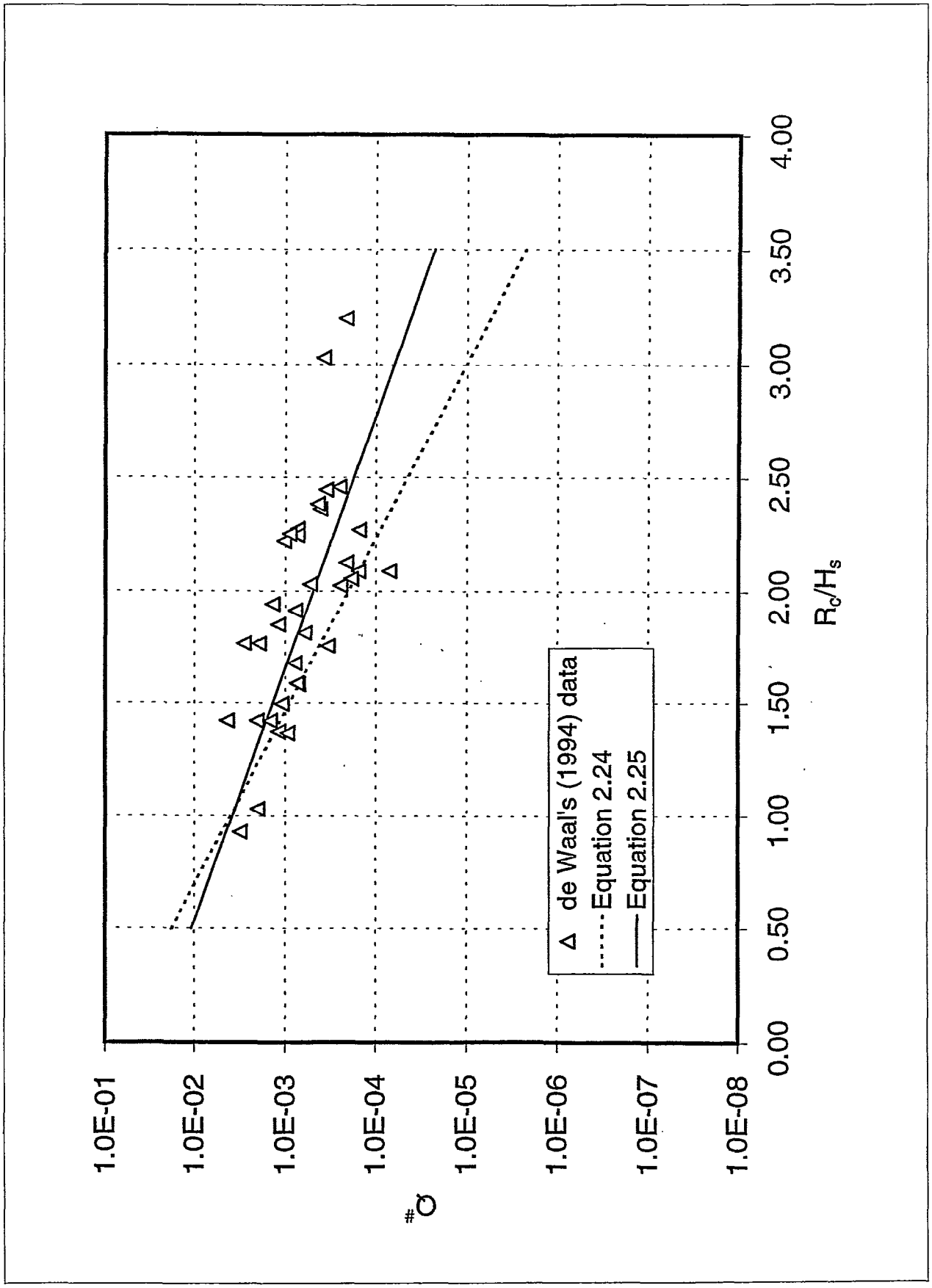

Figure 2.6 De Waal's (1994) vertical wall overtopping data

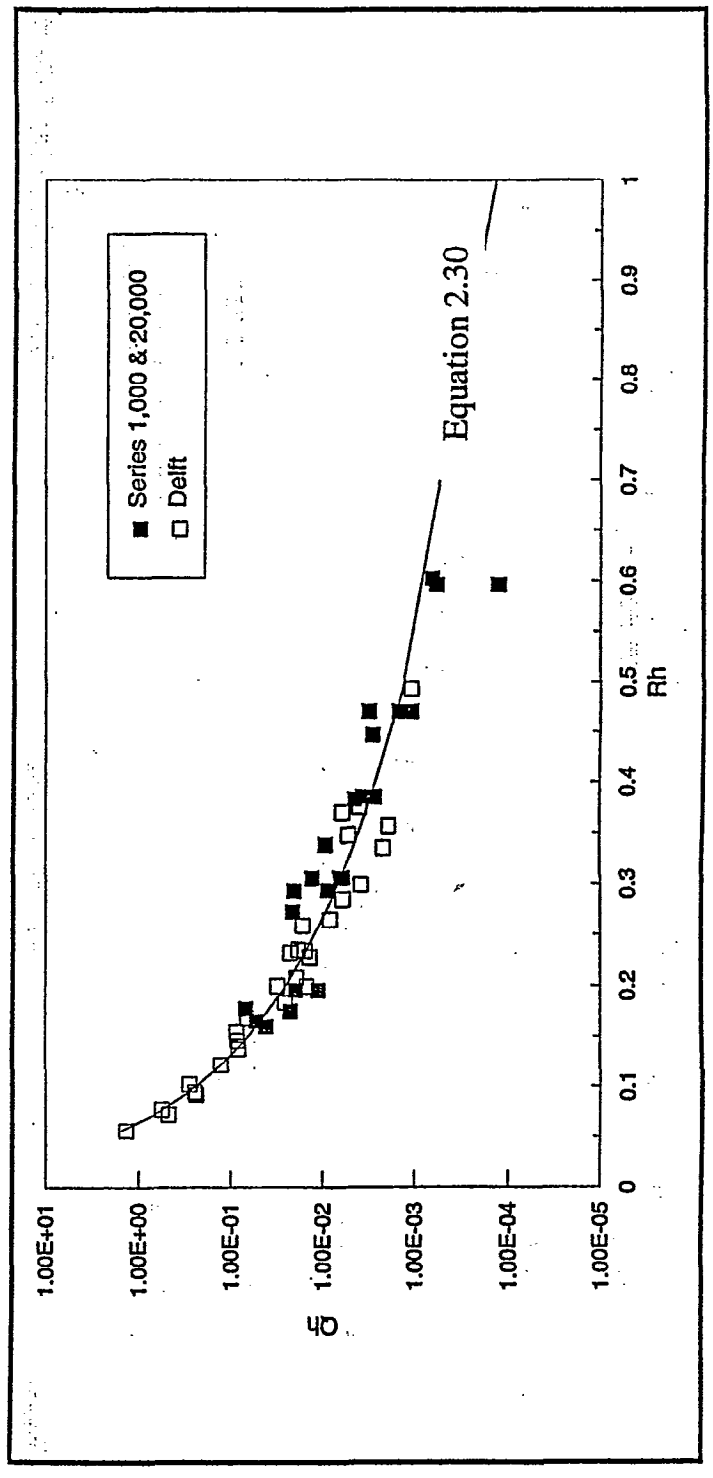

Figure 2.7 Vertical wall under impacting wave attack (Allsop et al (1995)

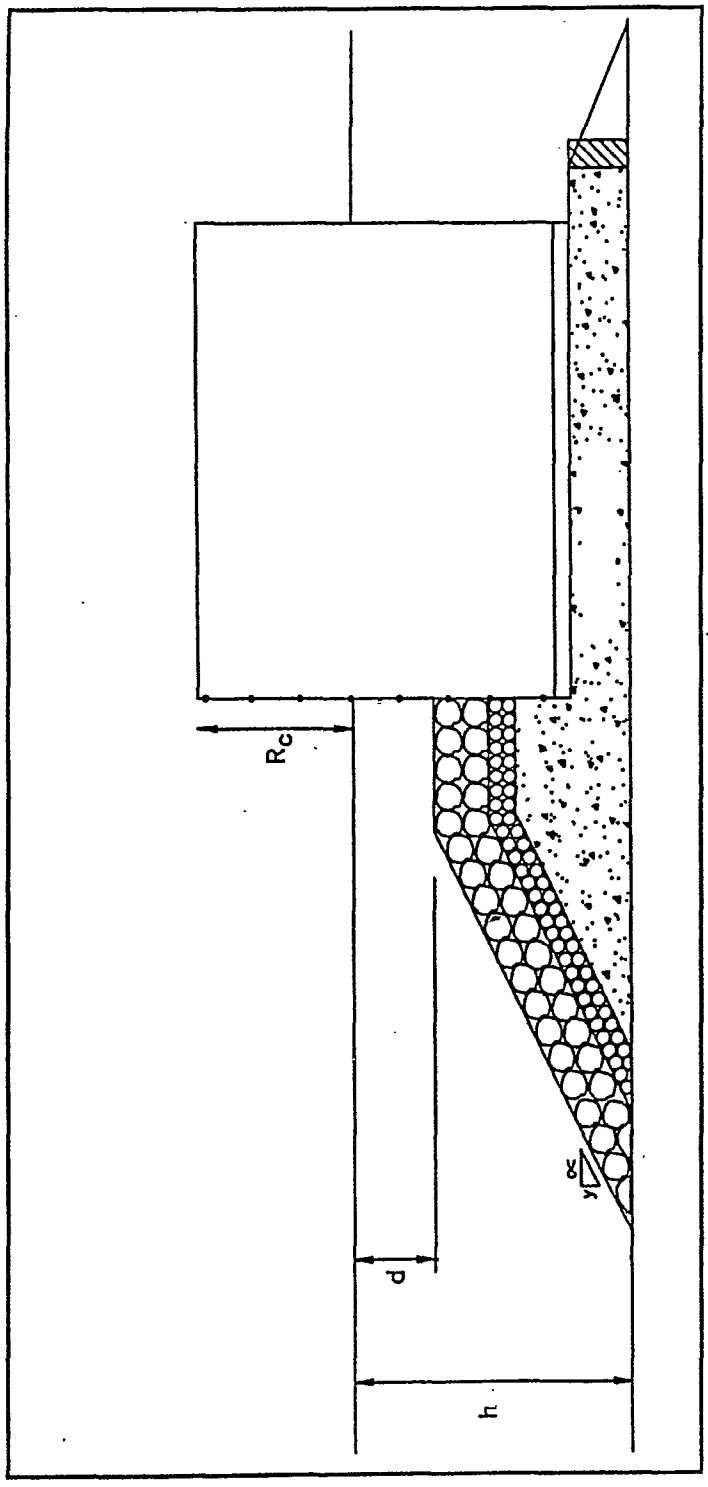

Figure 2.8 Composite structure

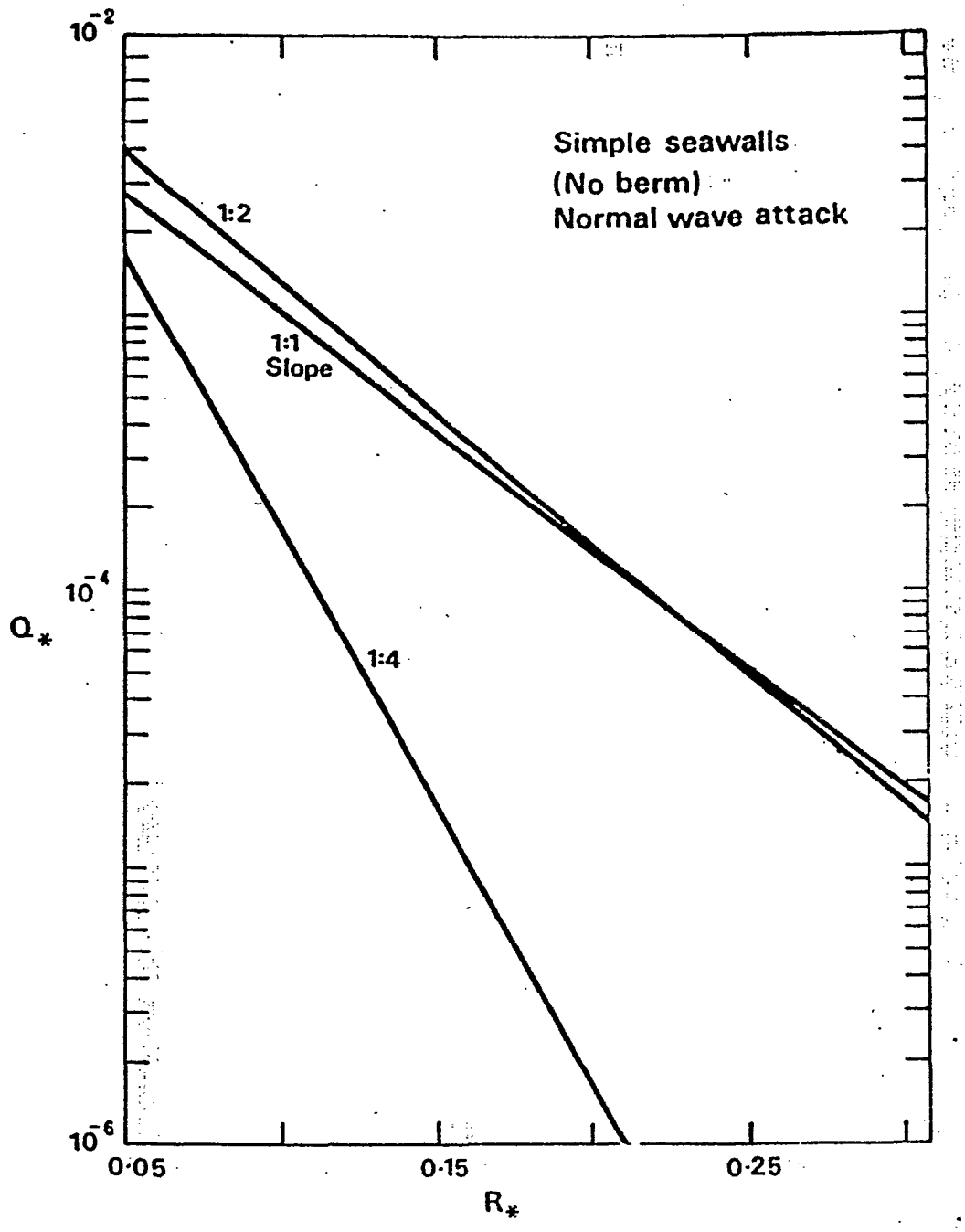

Figure 4.1 Overtopping of simply sloping smooth structure

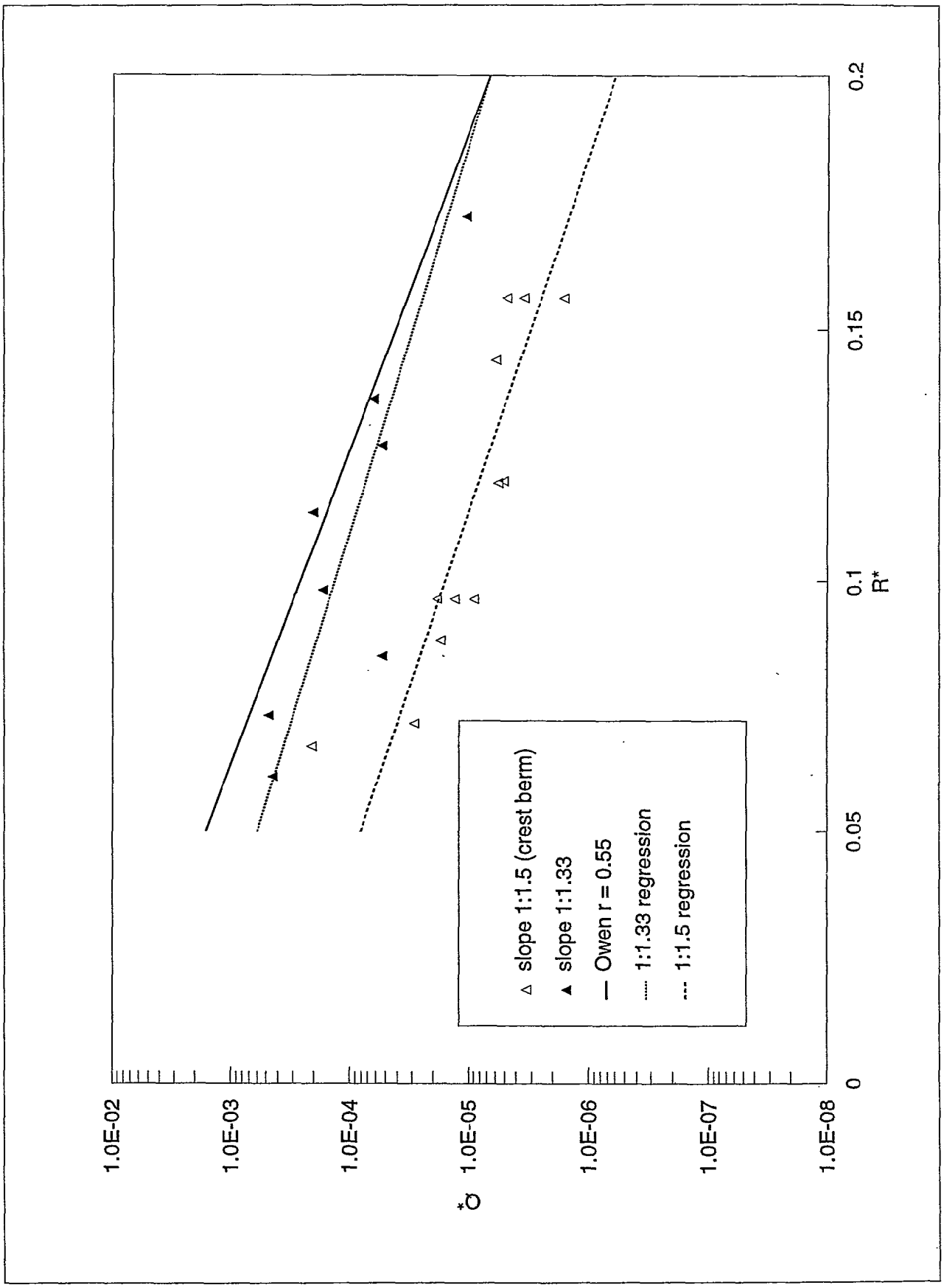

Figure 4.2 Overtopping of SHED armoured slopes with and without crest berm

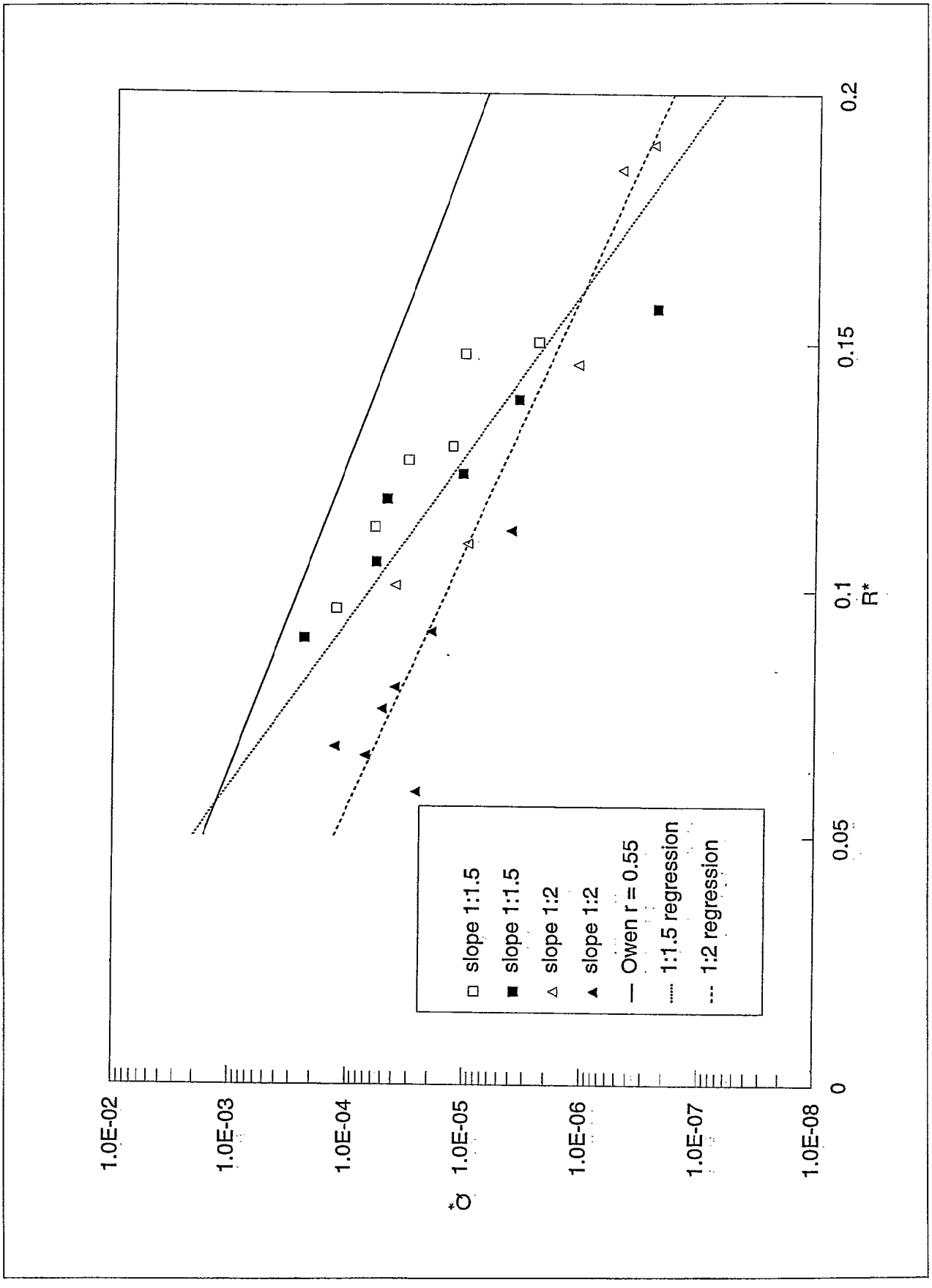

Figure 4.3 Overtopping of Antifer armoured slopes with crest berms

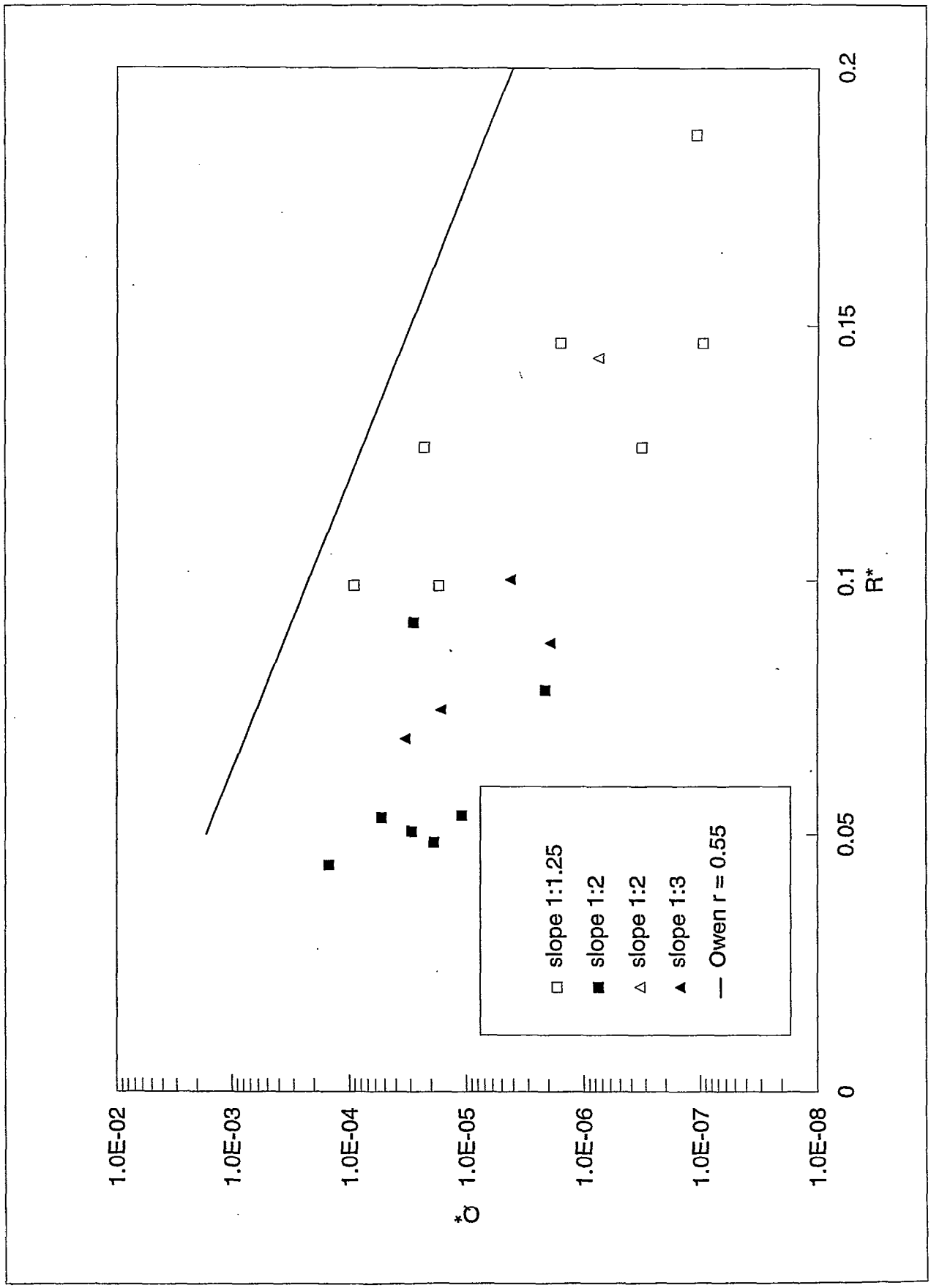

Figure 4.4 Overtopping of rock armoured slopes with crest walls

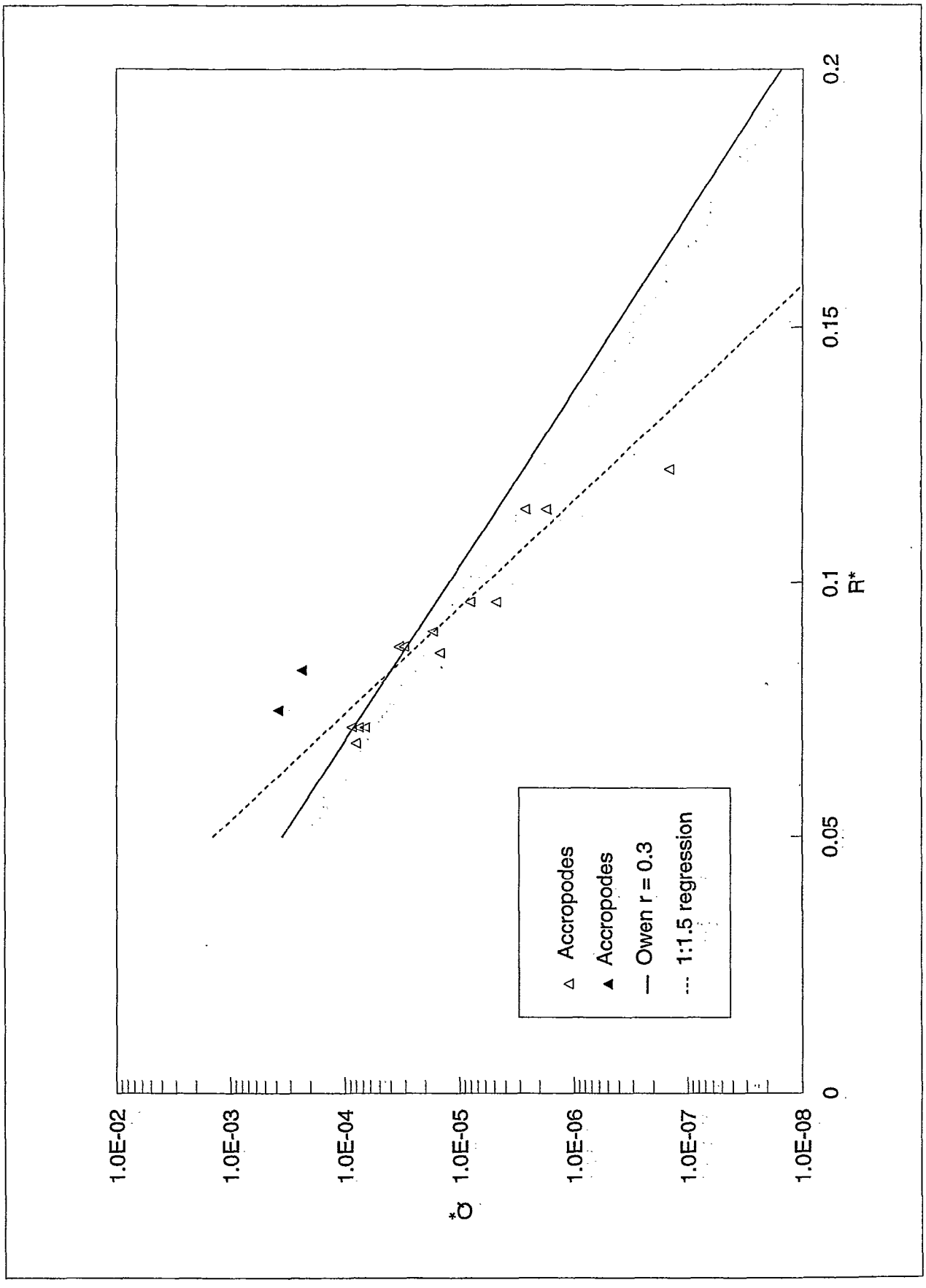

Figure 4.5 Overtopping of Accropode armoured slopes

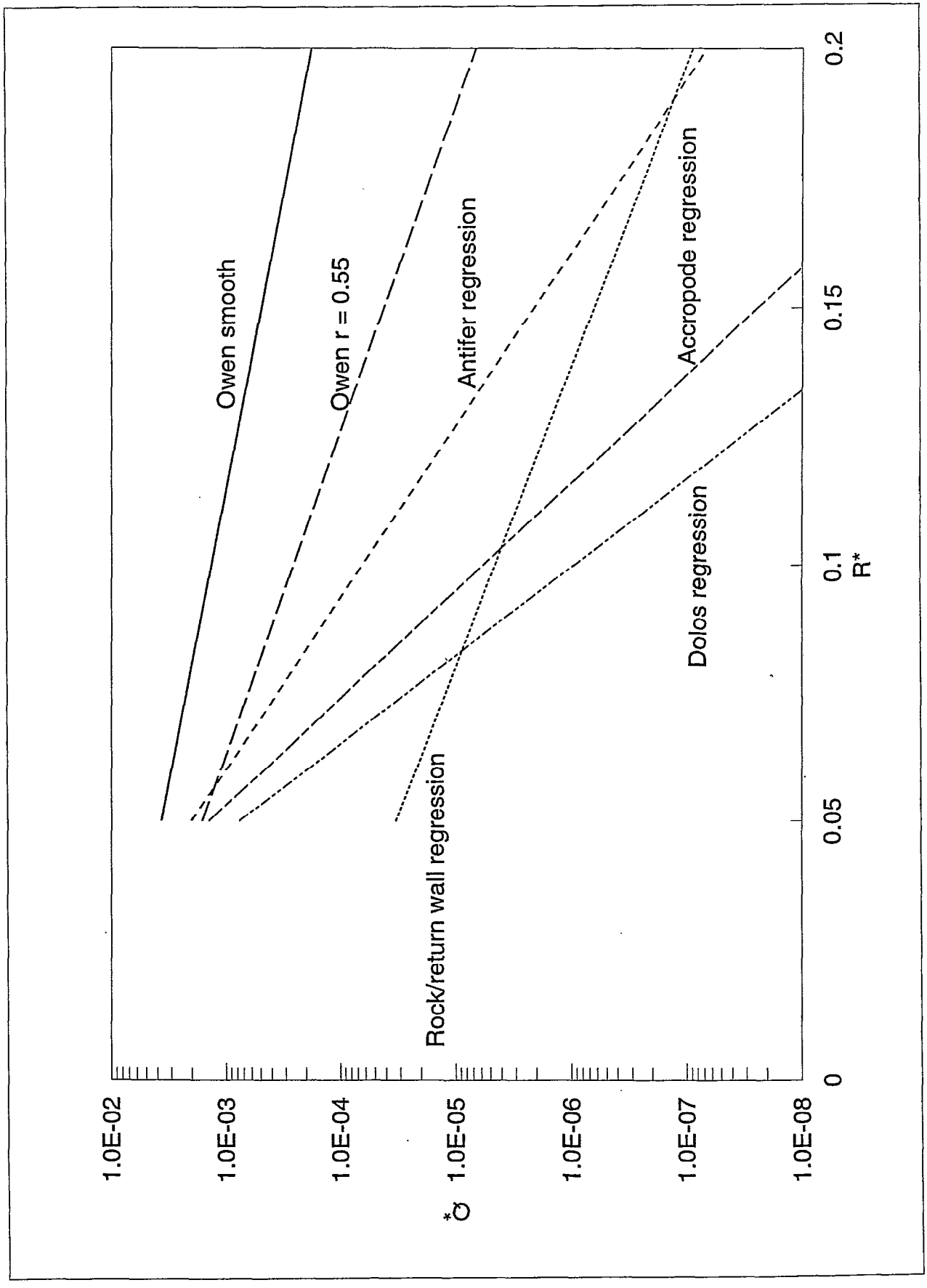

Figure 4.6 Effect of slope roughness on overtopping

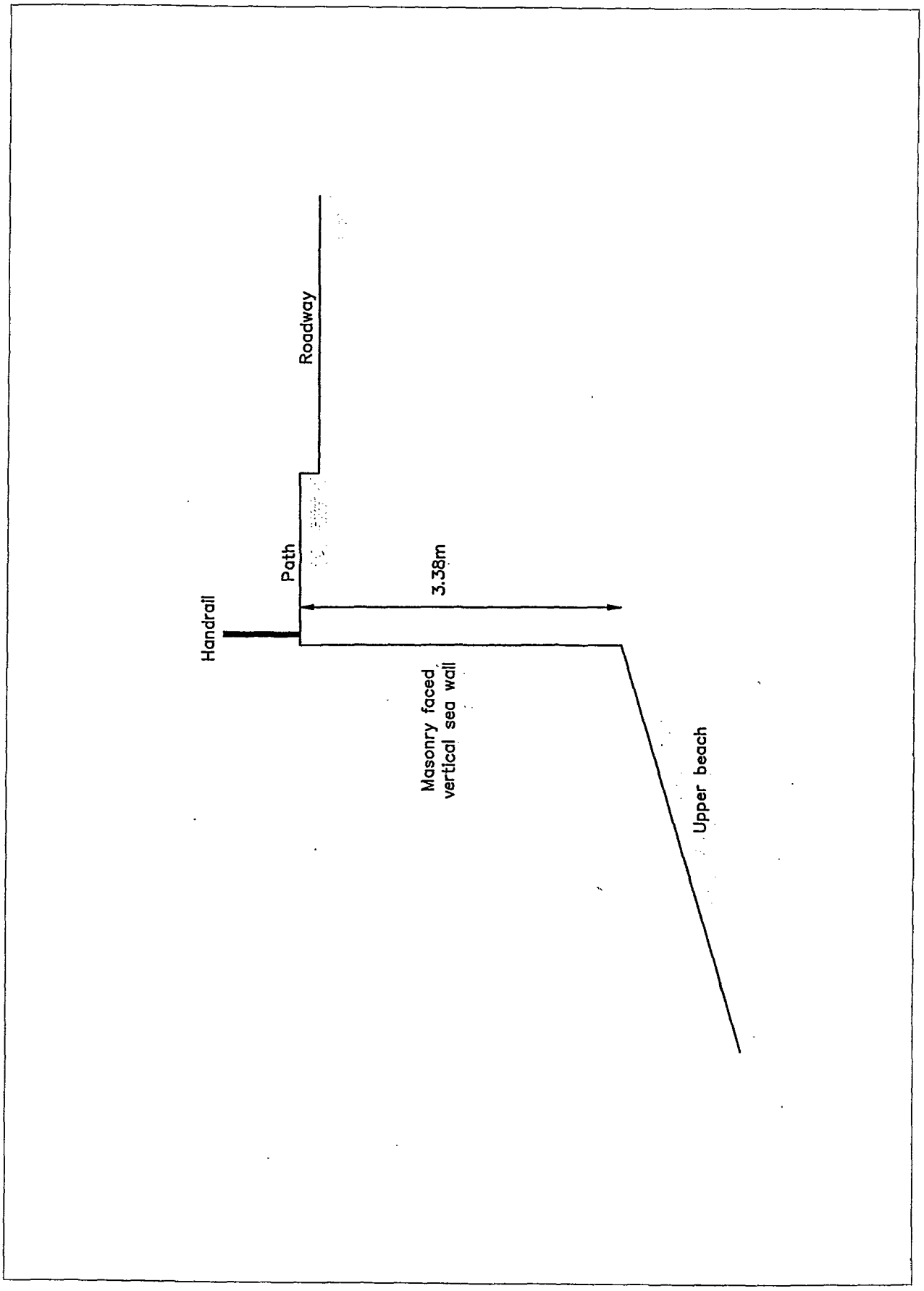

Figure 4.7 Vertical seawall at Colwyn Bay

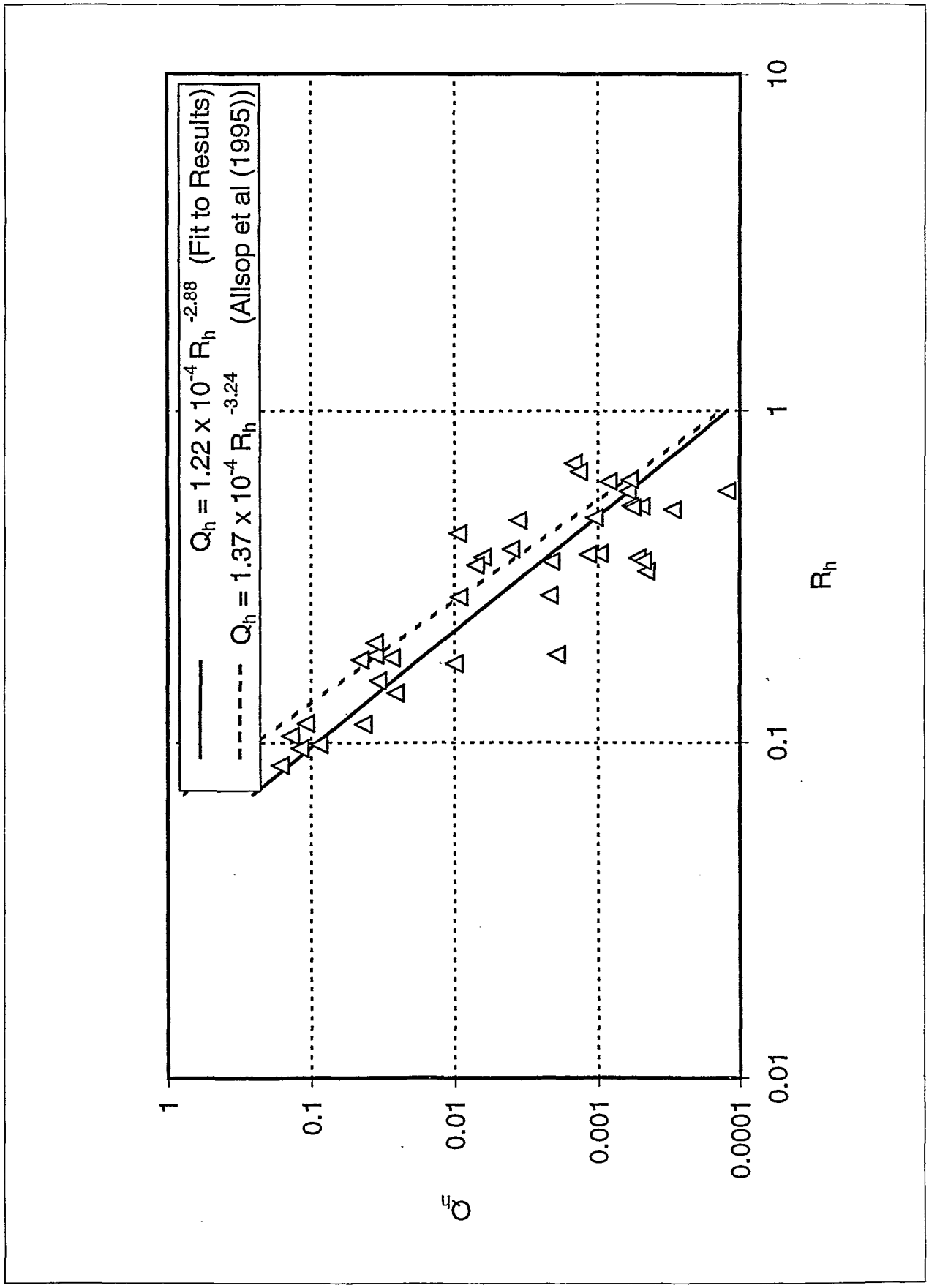

Figure 4.8 Overtopping of vertical seawall at Colwyn Bay

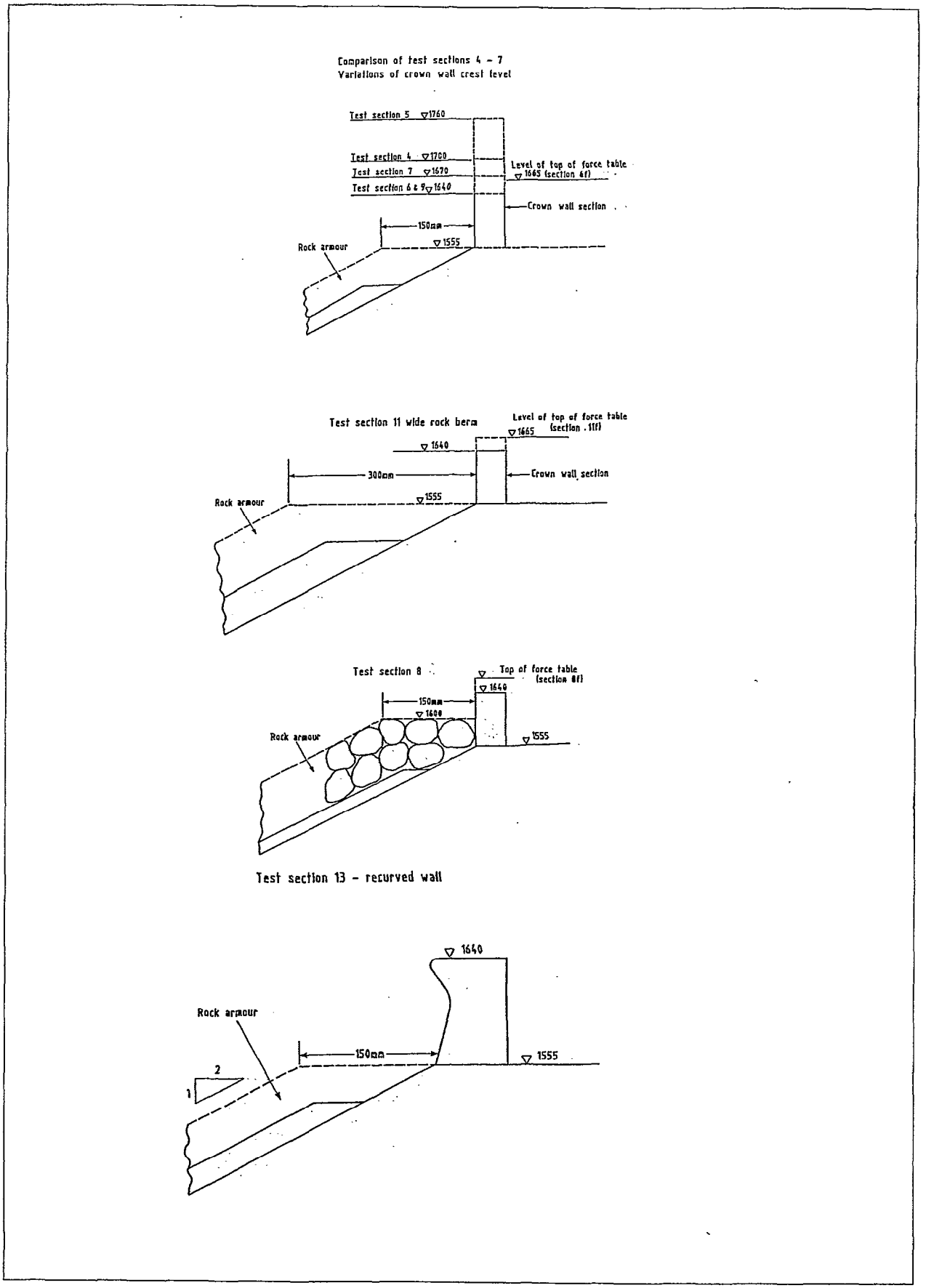

Figure 5.1 Sections tested by Bradbury et al

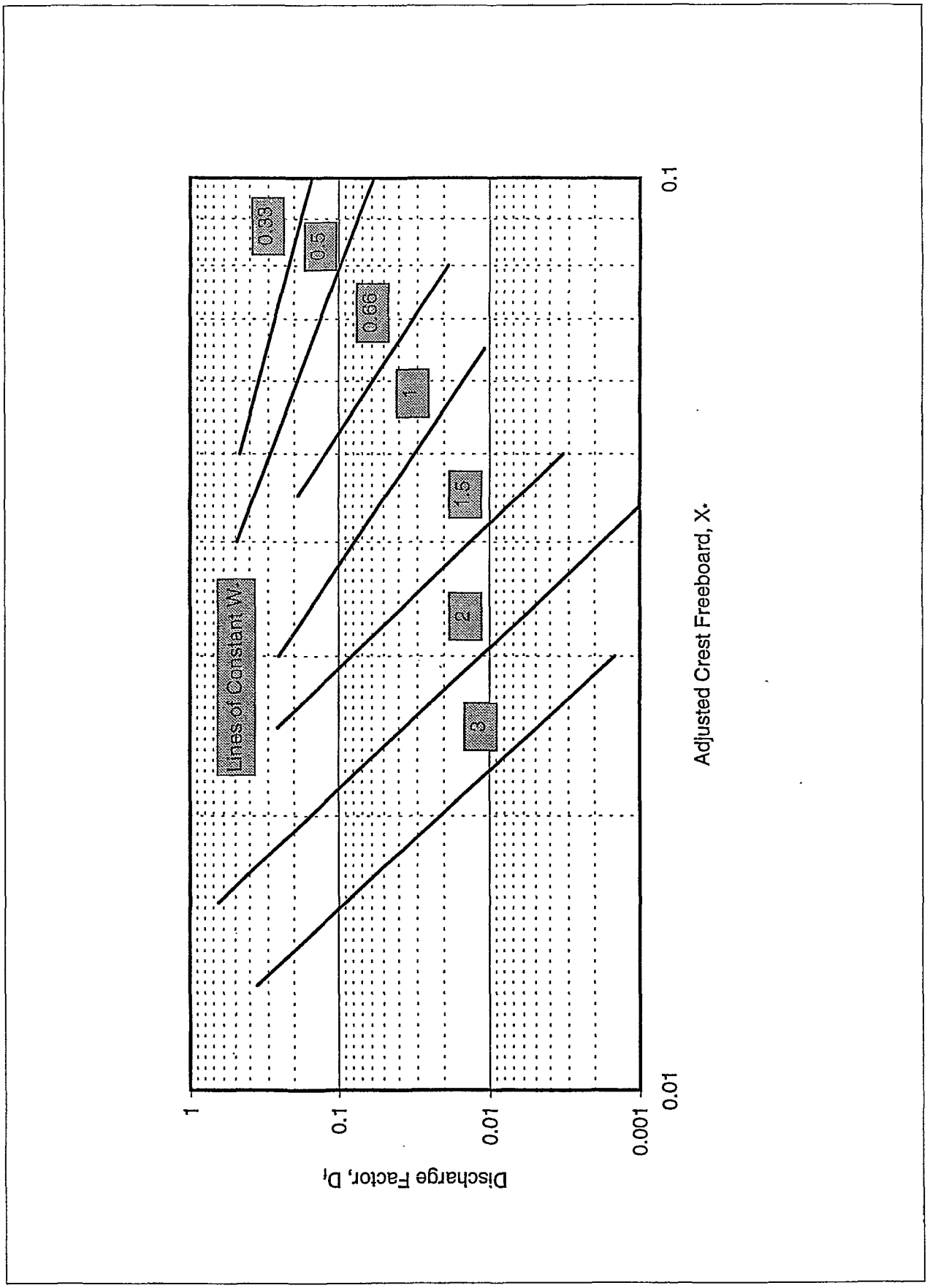

Figure 5.2 Owen and Steele's (1991) design chart

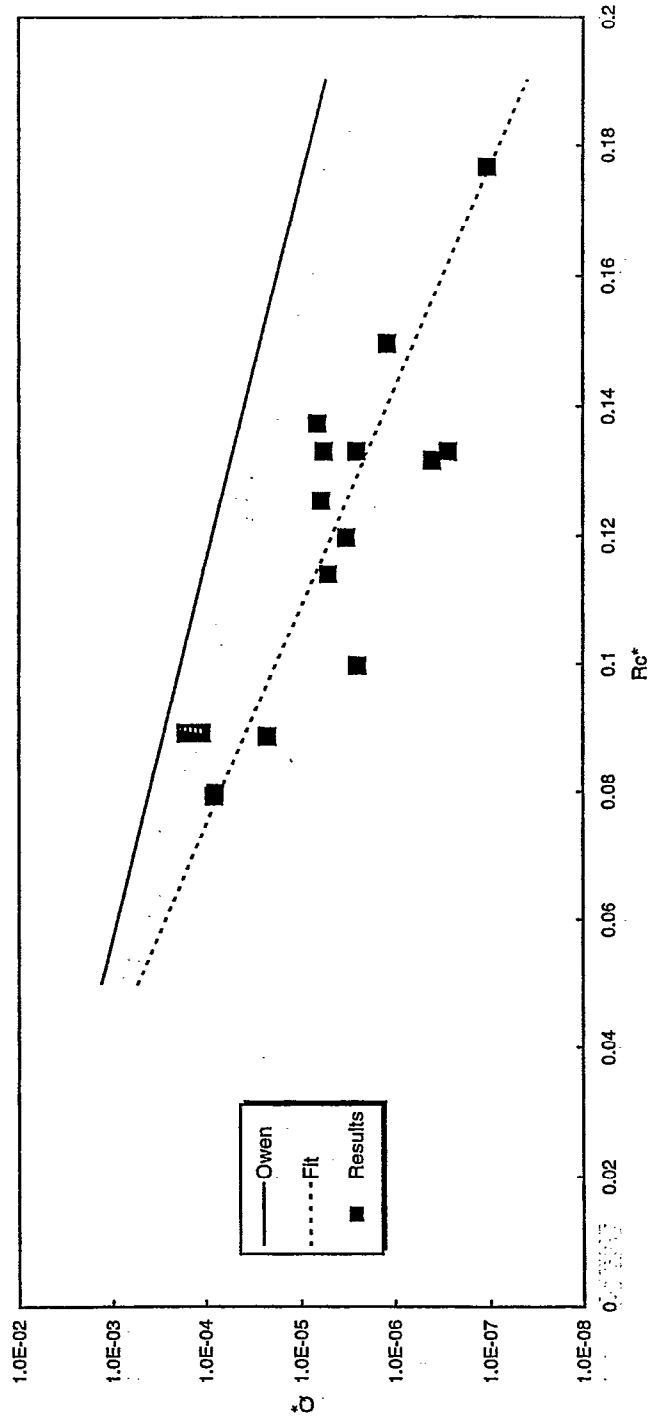

Figure 5.3 Overtopping of section 14

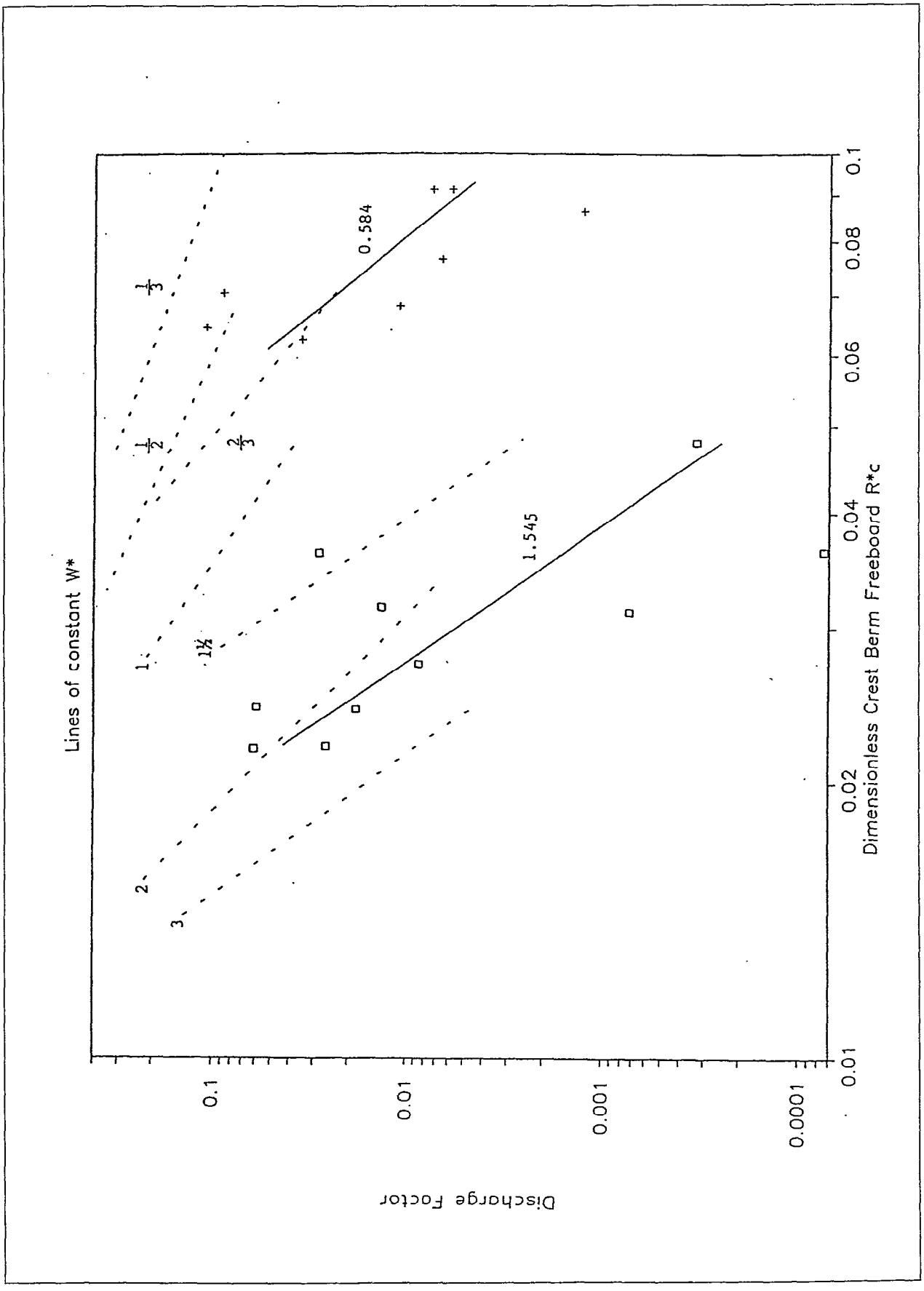

Figure 5.4 Discharge factors of recurved wall on rock armoured slope

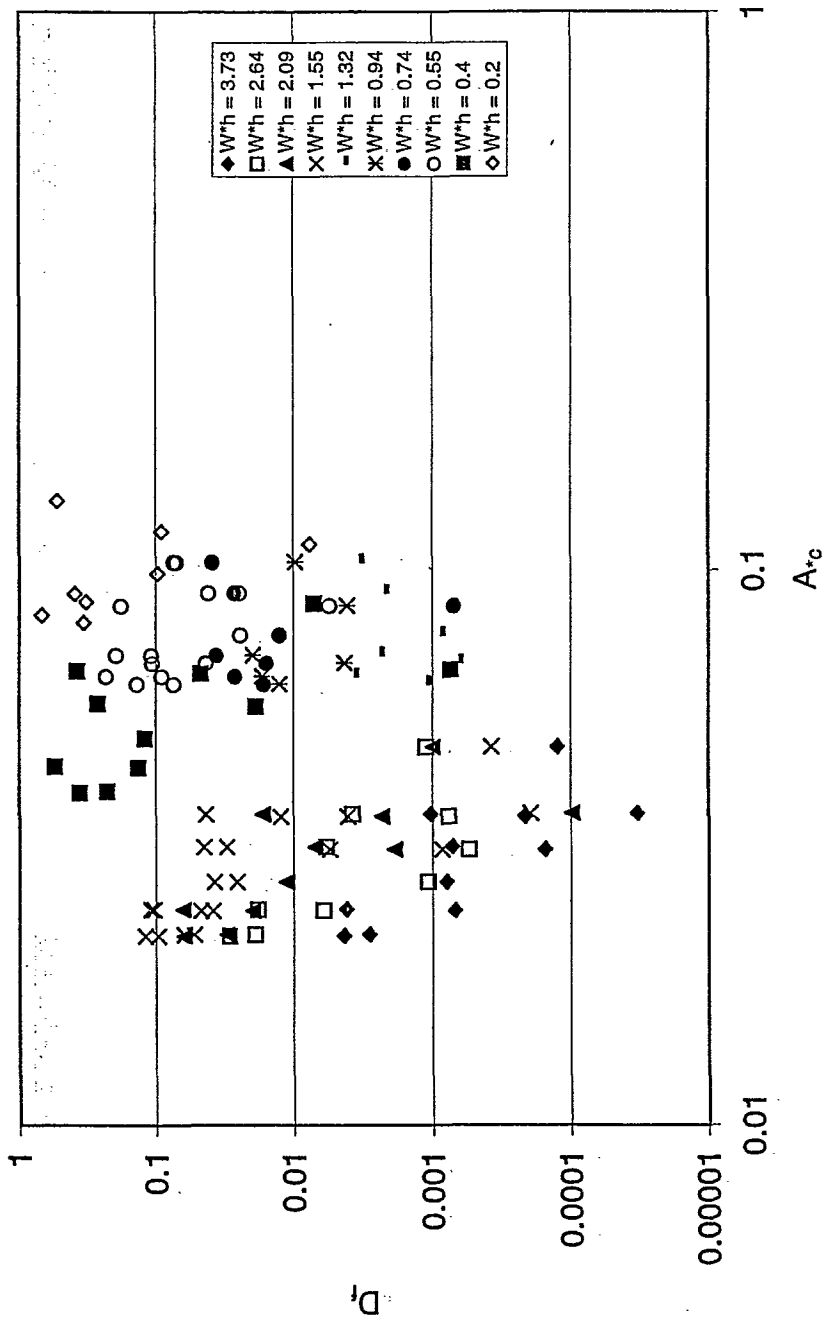

Figure 5.5 Discharge factors of crest walls on rock armoured slopes

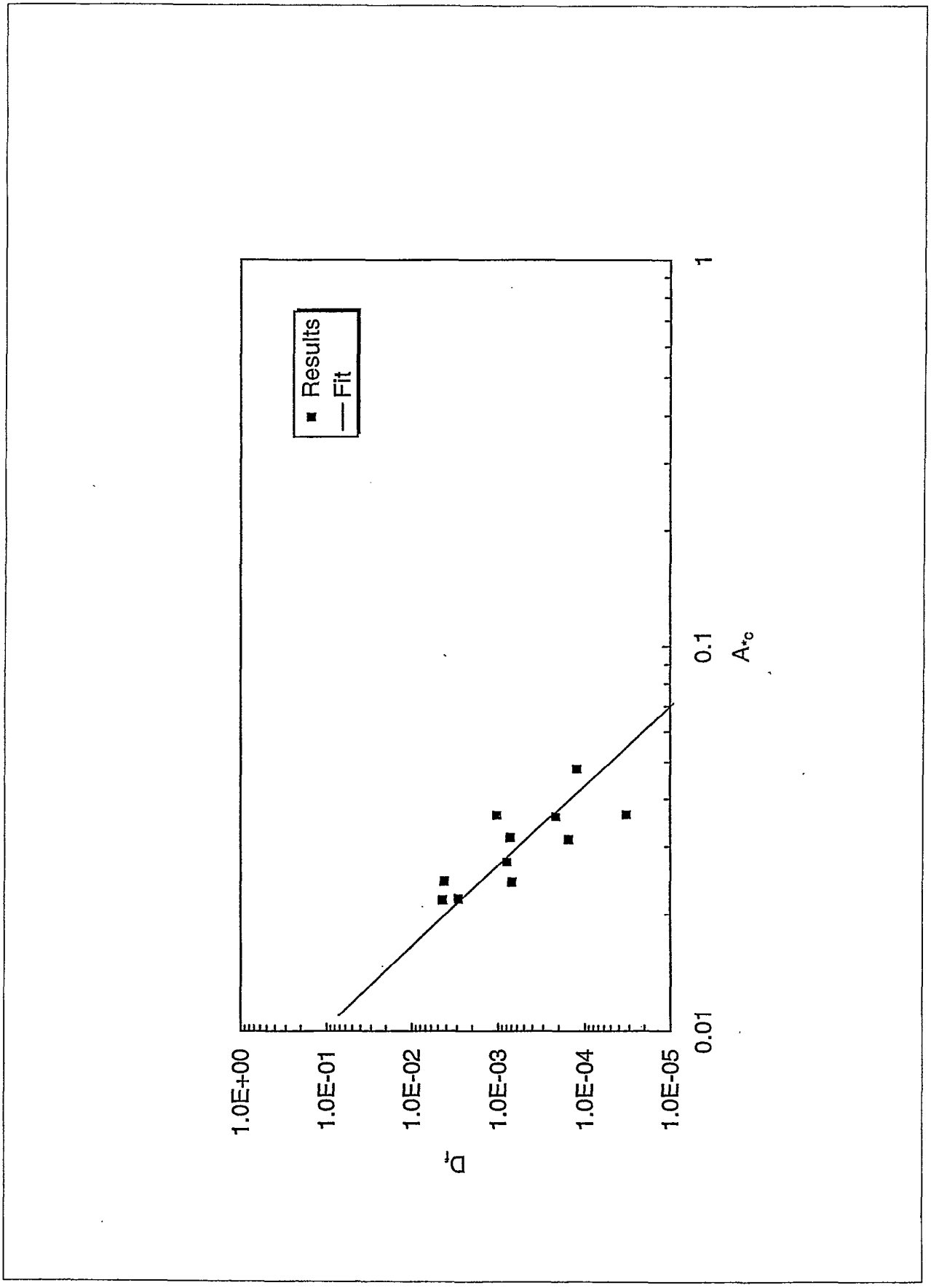

Figure 5.6 Discharge factors for crest wall on rock armoured slope, $W_* h = 3.73$

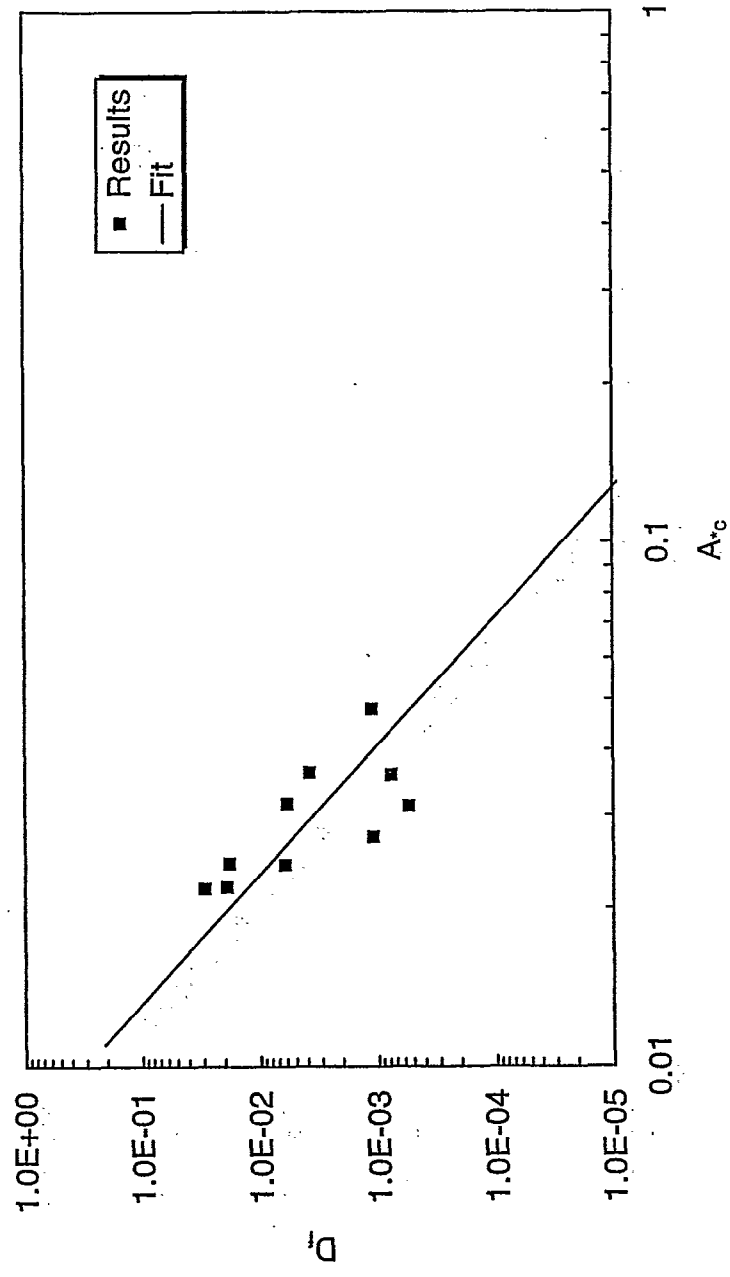

Figure 5.7 Discharge factors for crest wall on rock armoured slope, $W_* h = 2.64$

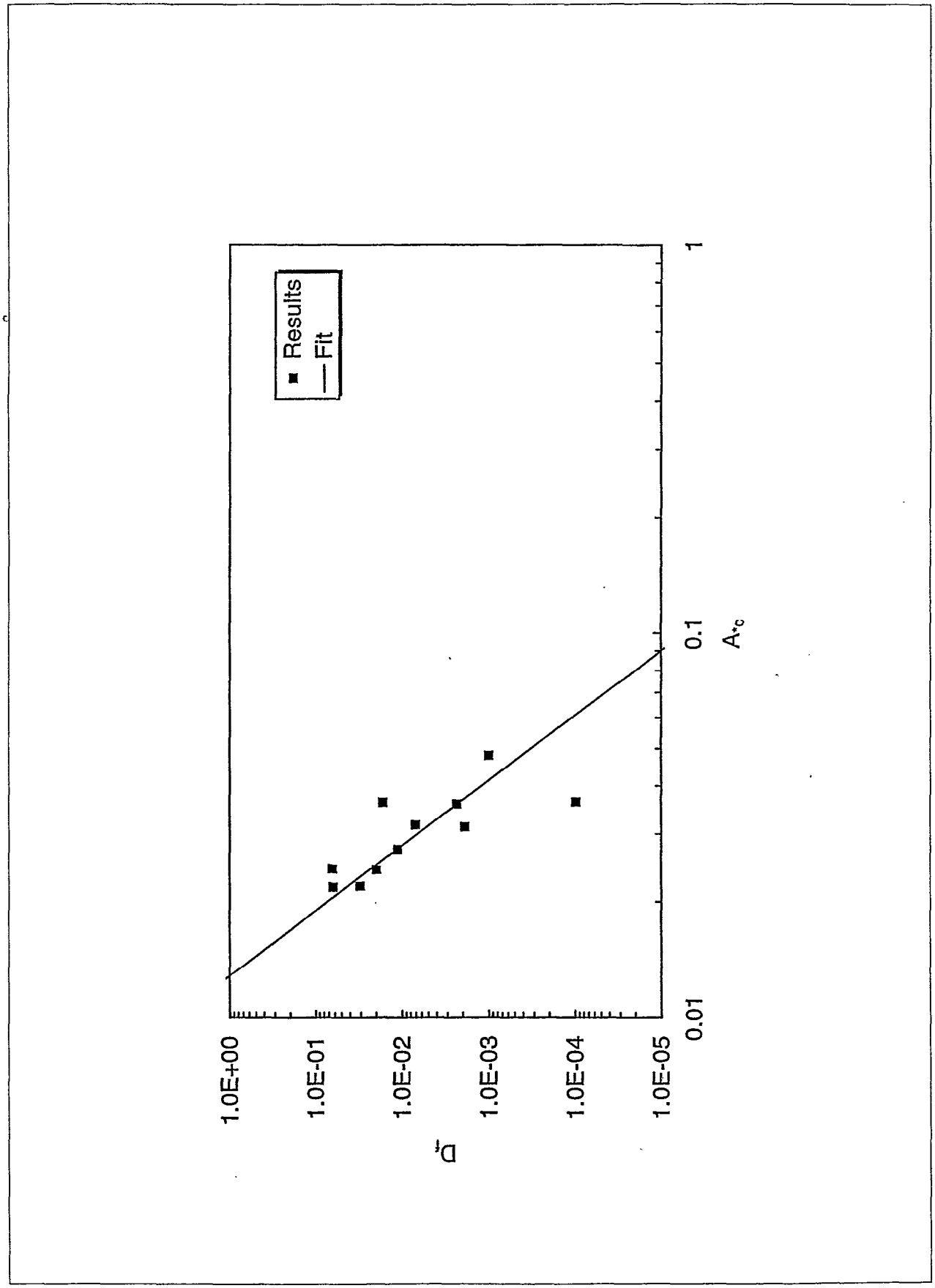

Figure 5.8 Discharge factors for crest wall on rock armoured slope, $W_* h = 2.09$

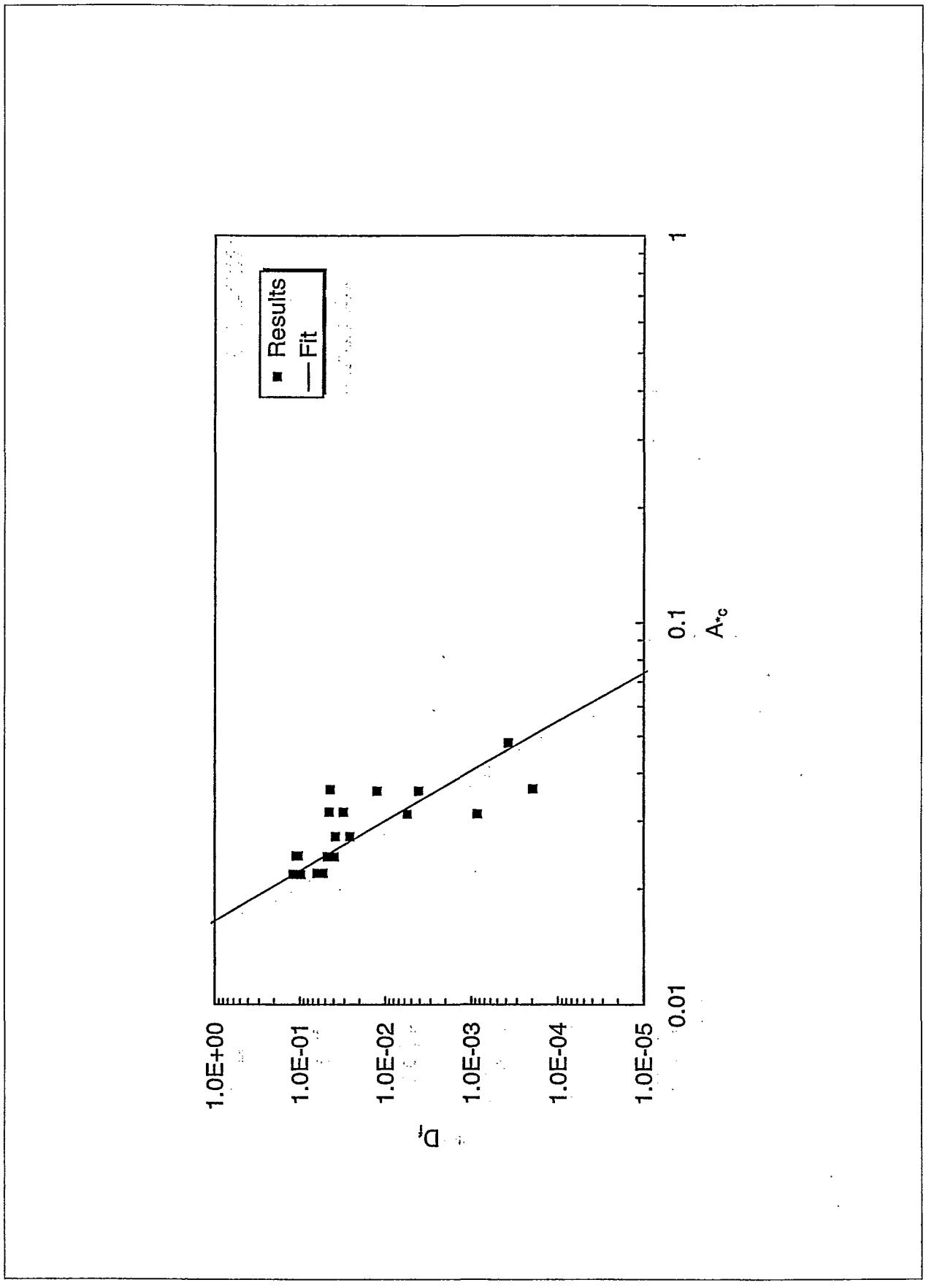

Figure 5.9 Discharge factors for crest wall on rock armoured slope, W*h = 1.55

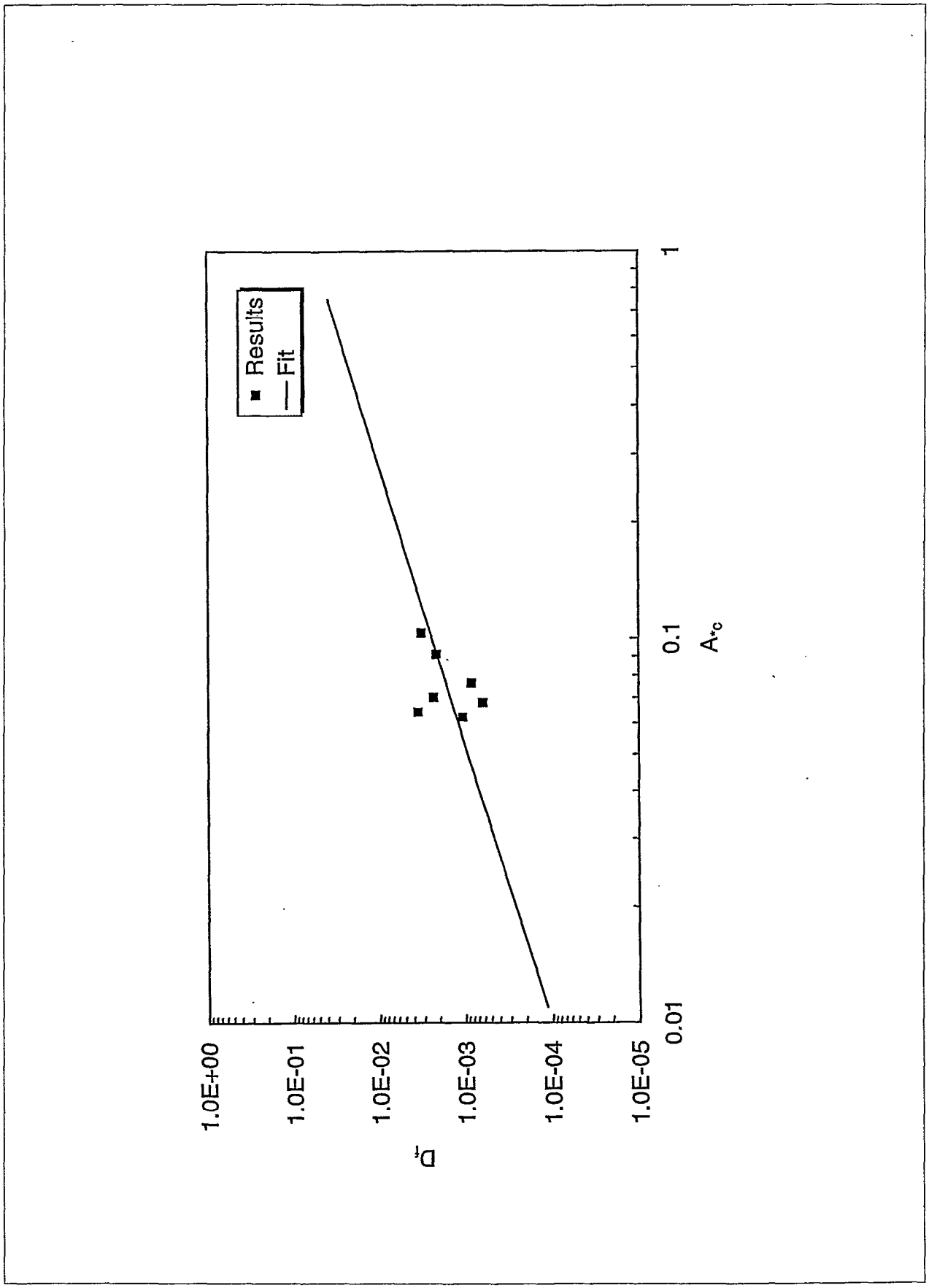

Figure 5.10 Discharge factors for crest wall on rock armoured slope, $W_* h = 1.32$

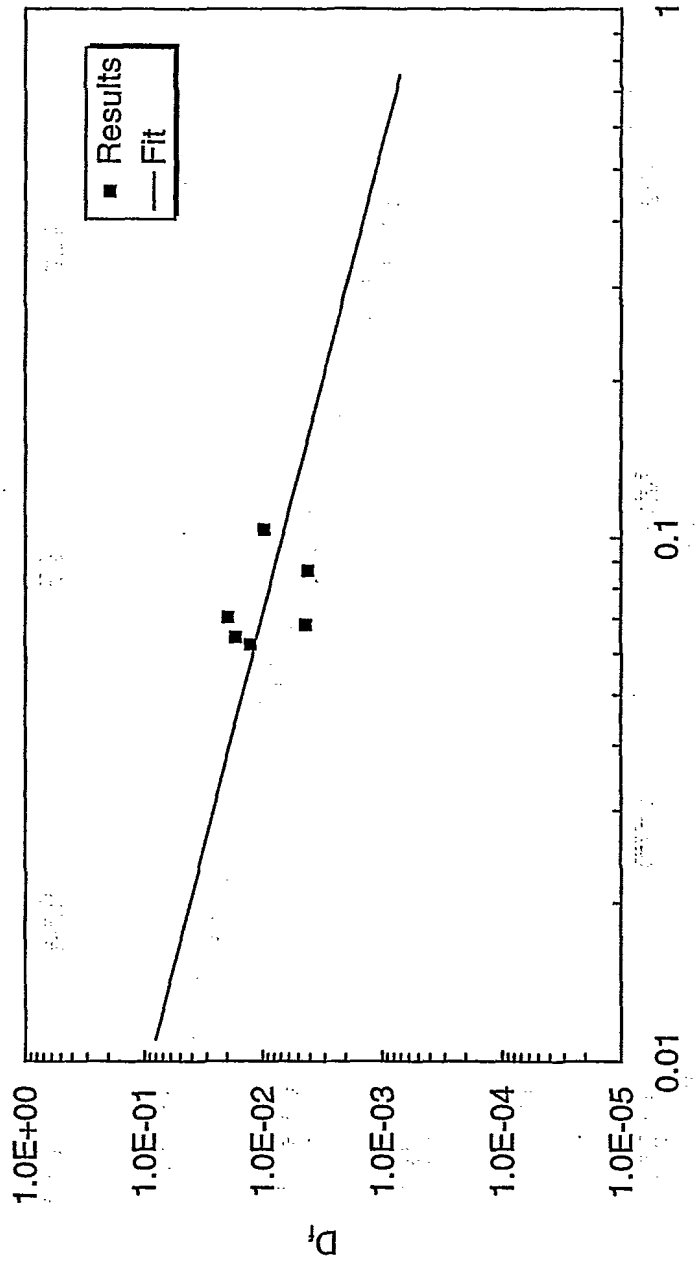

Figure 5.11 Discharge factors for crest wall on rock armoured slope, $W_{*}h = 0.94$

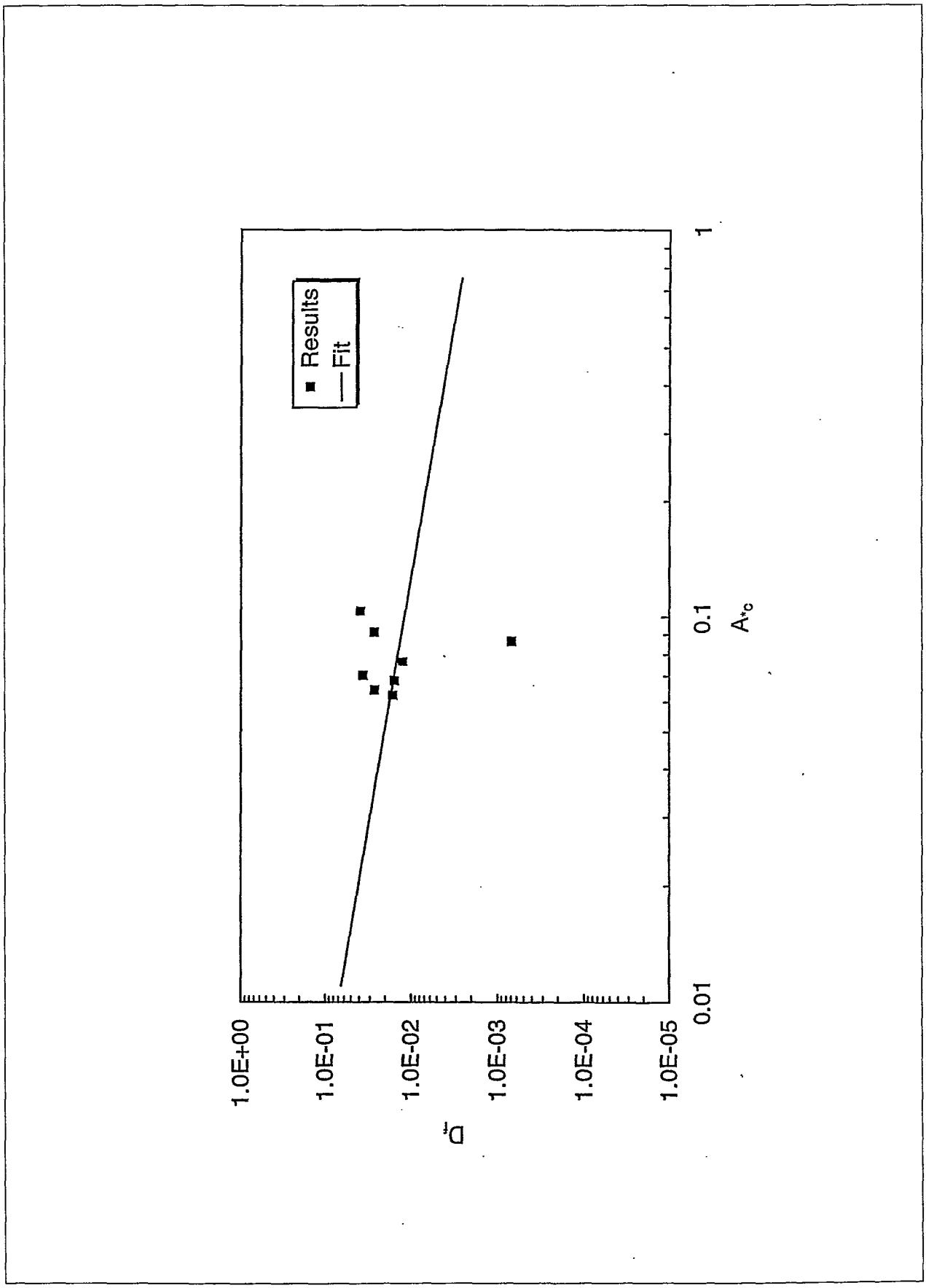

Figure 5.12 Discharge factors for crest wall on rock armoured slope, W*h = 0.74

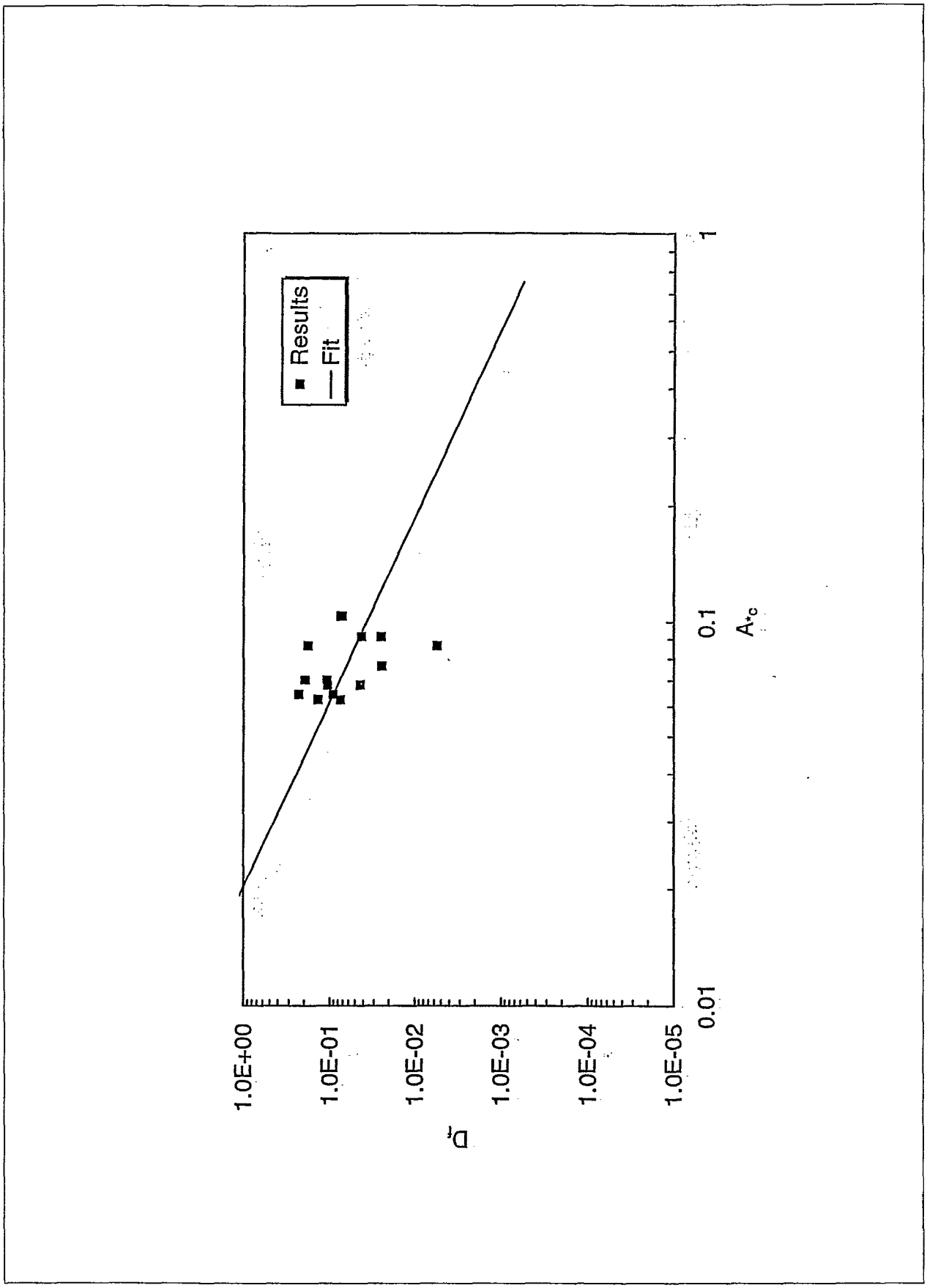

Figure 5.13 Discharge factors for crest wall on rock armoured slope, $W_* h = 0.55$

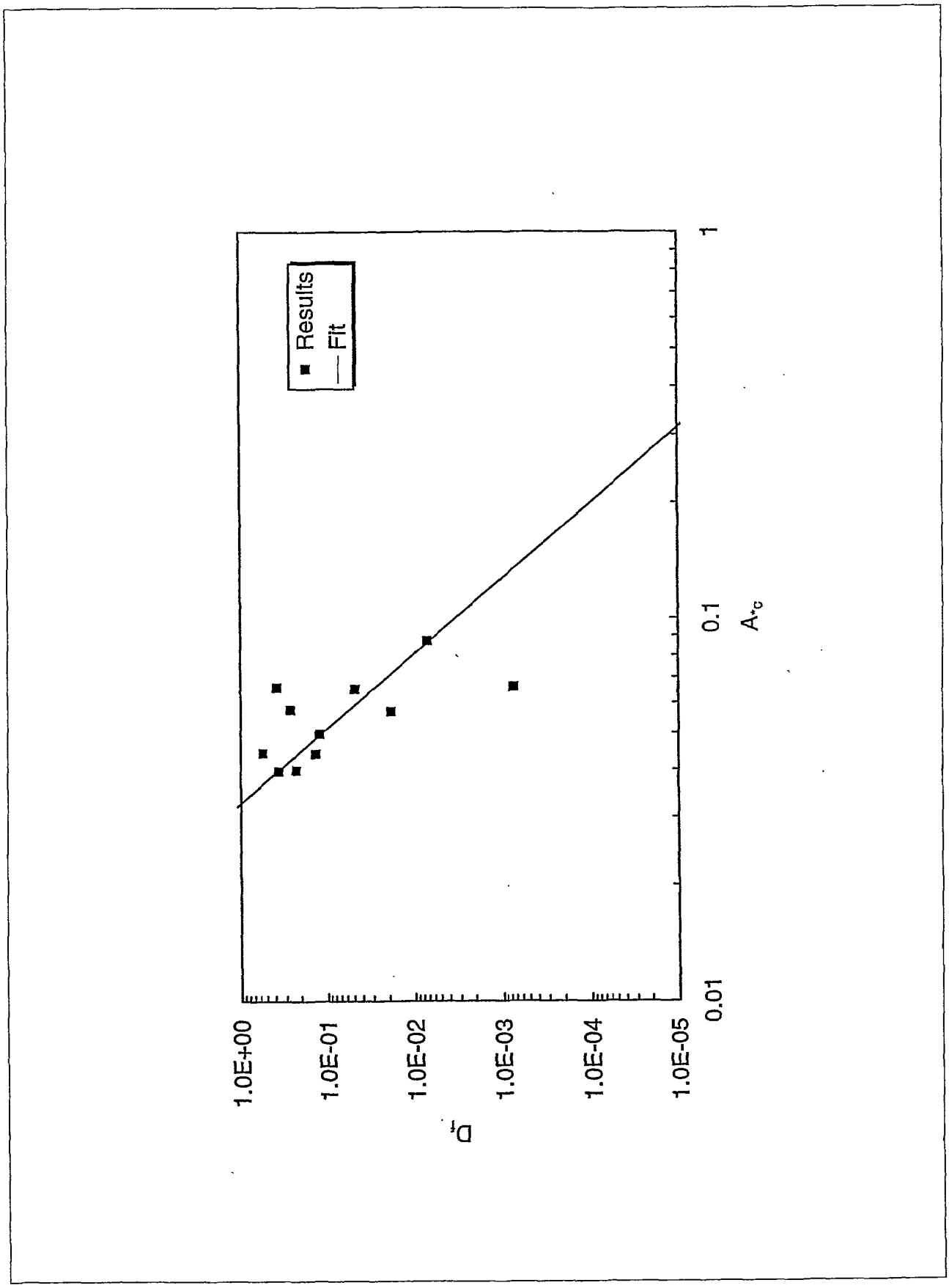

Figure 5.14 Discharge factors for crest wall on rock armoured slope, $W_* h = 0.40$

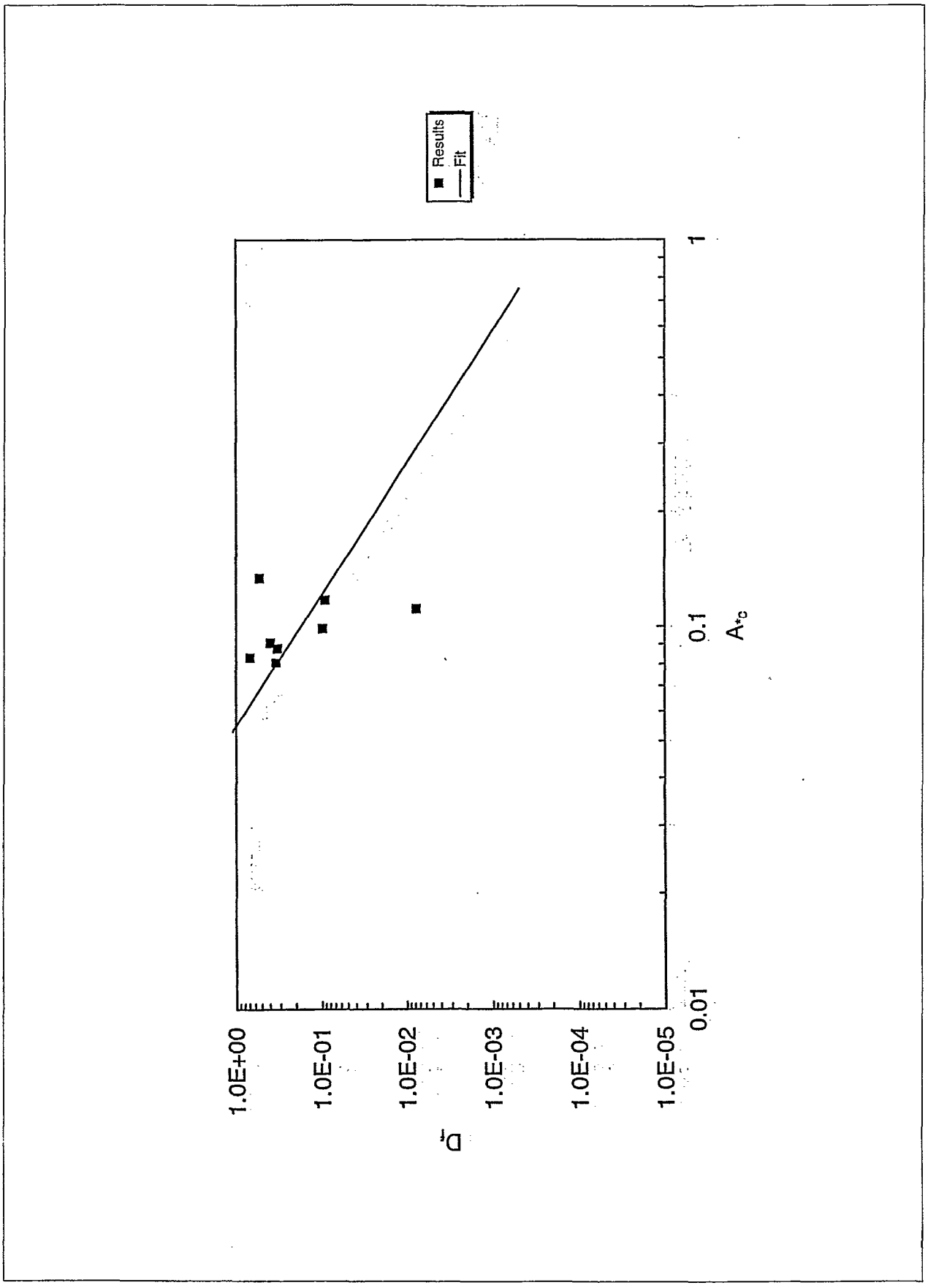

Figure 5.15 Discharge factors for crest wall on rock armoured slope, W*h = 0.20

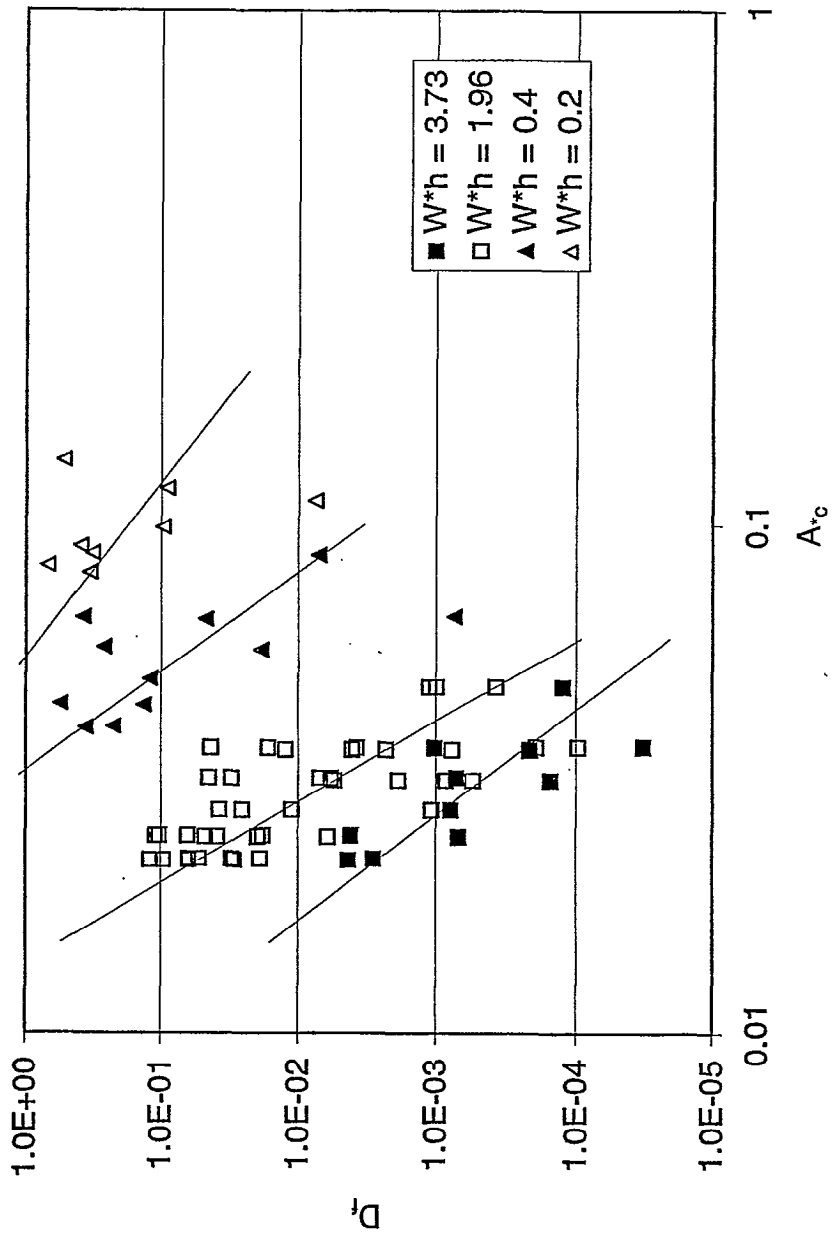

Figure 5.16 **Discharge factors for crest walls on rock armoured slopes, selected values of W^*h**

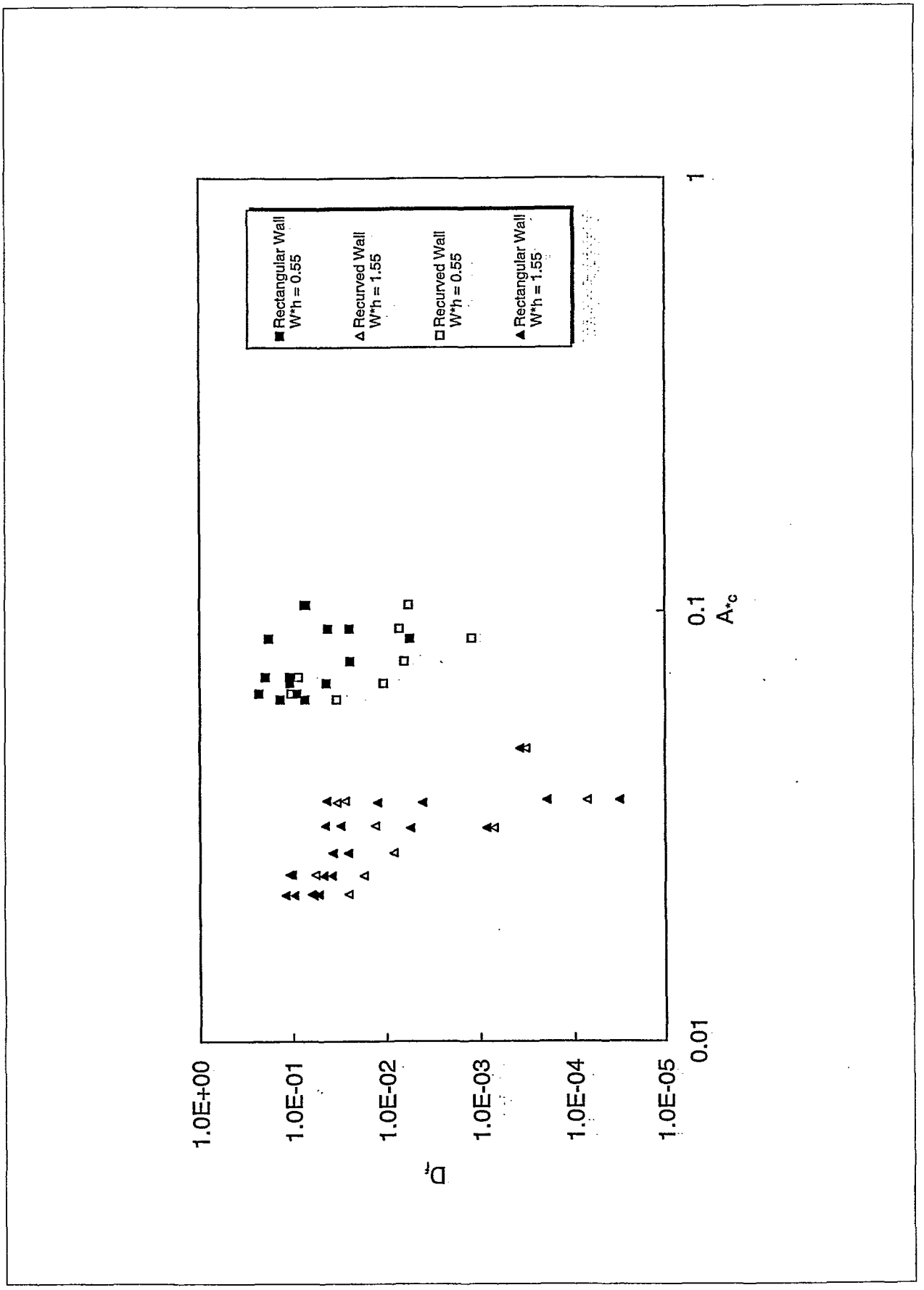

Figure 5.17 Effect of recurved wall on discharge factors

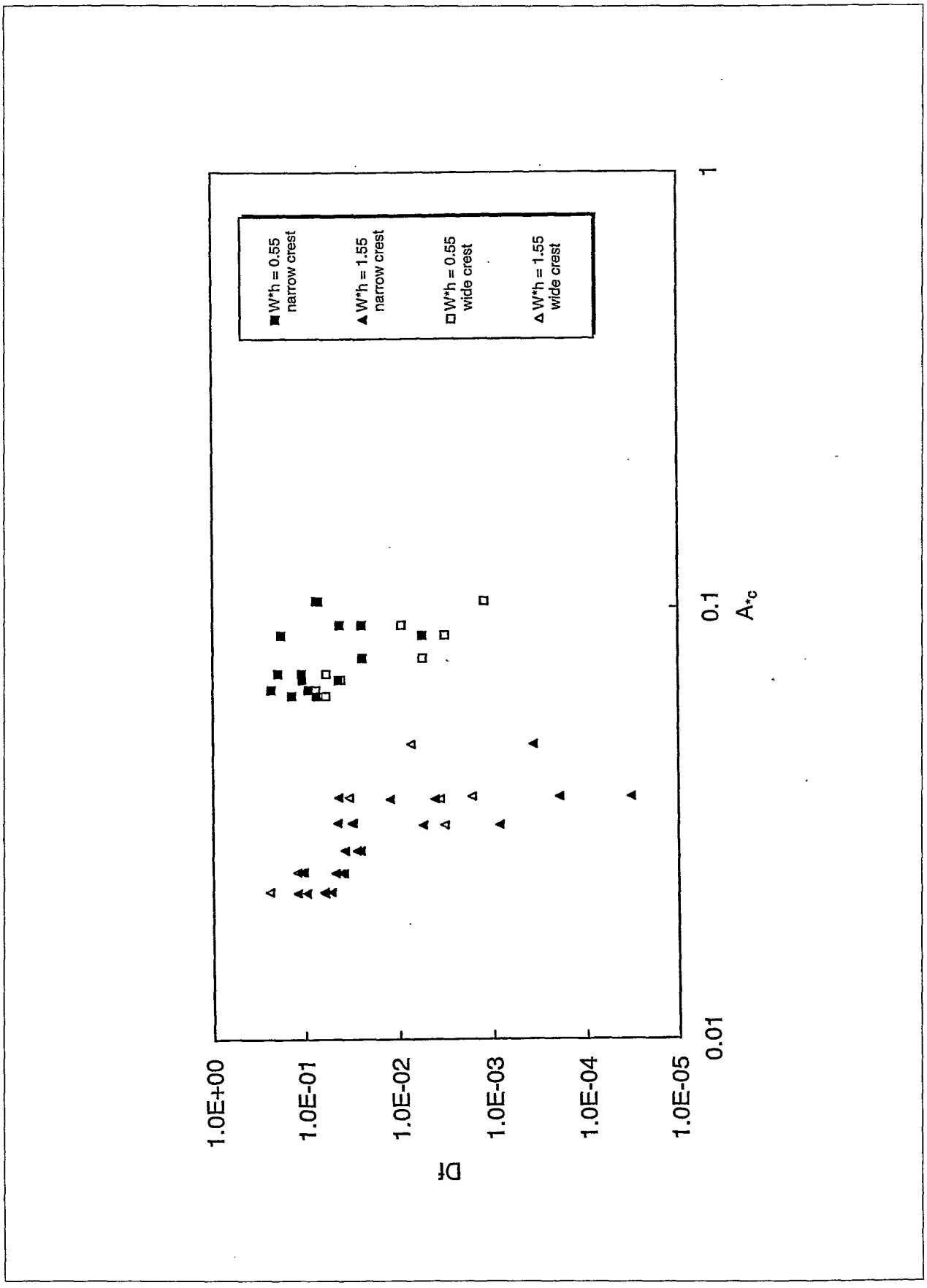

Figure 5.18 Effect of crest berm on discharge factors

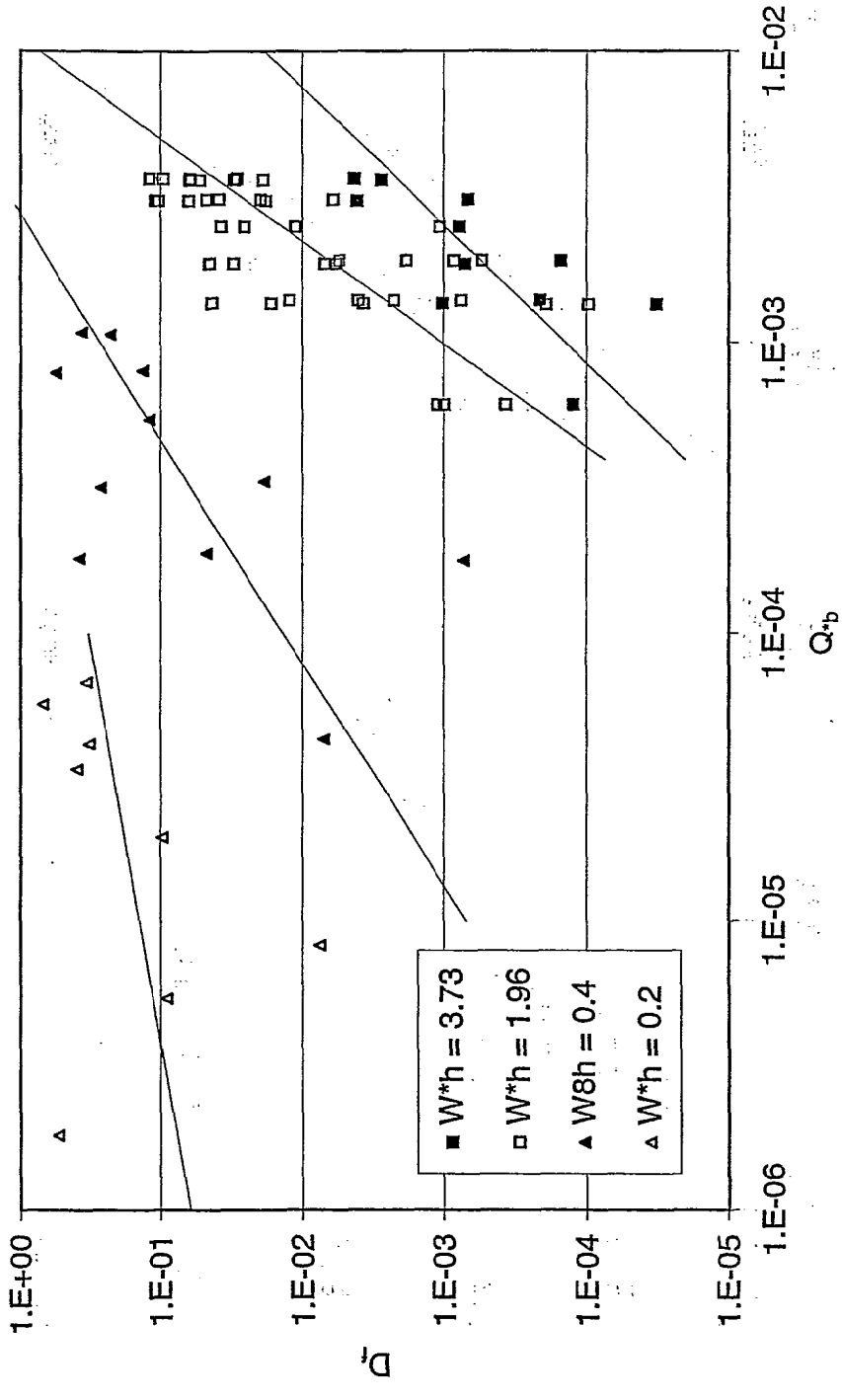

Figure 5.19 Discharge factors for crest walls on rock armoured slopes, selected values of $W_{*}h$

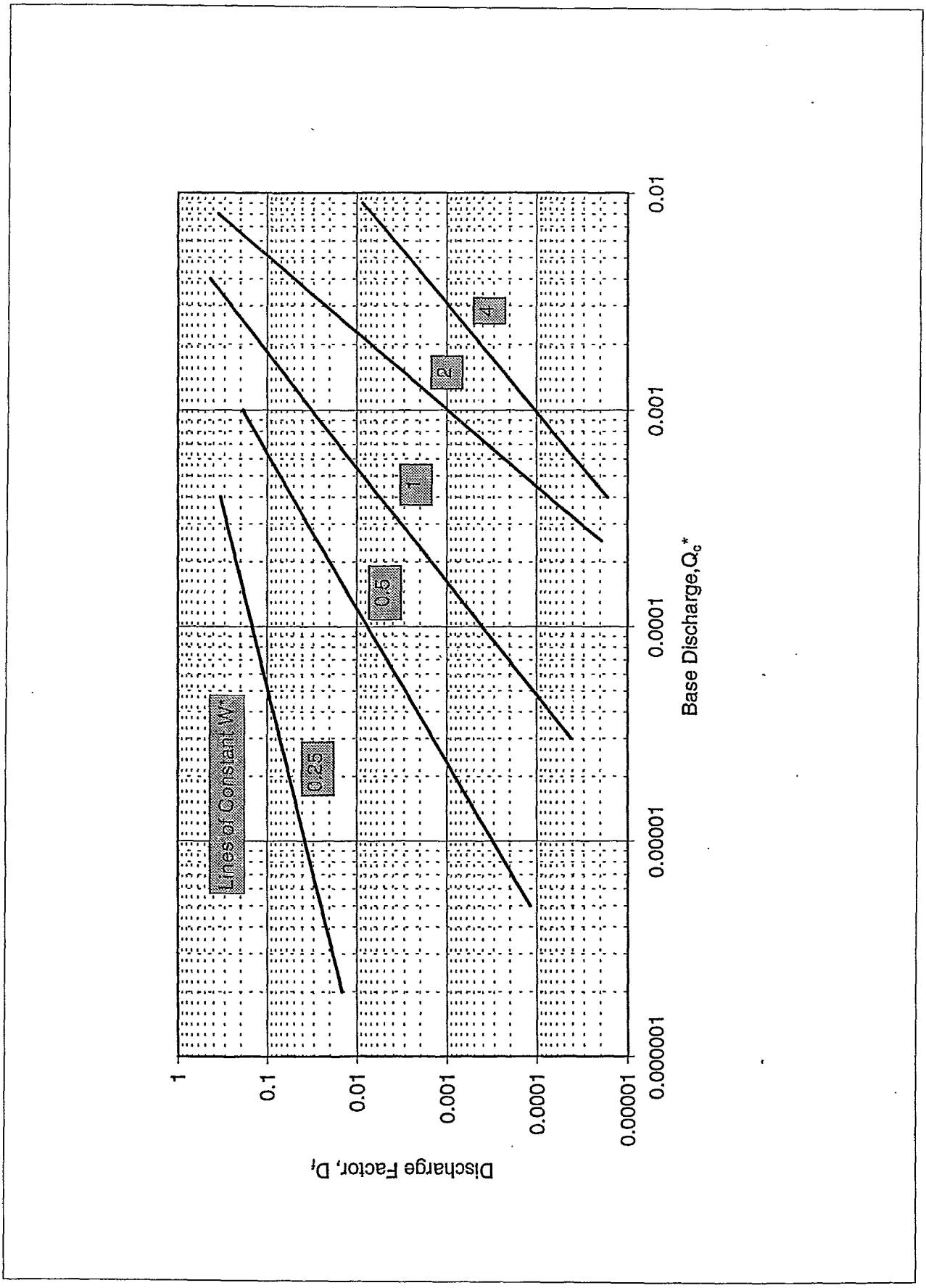

Figure 5.20 Design chart

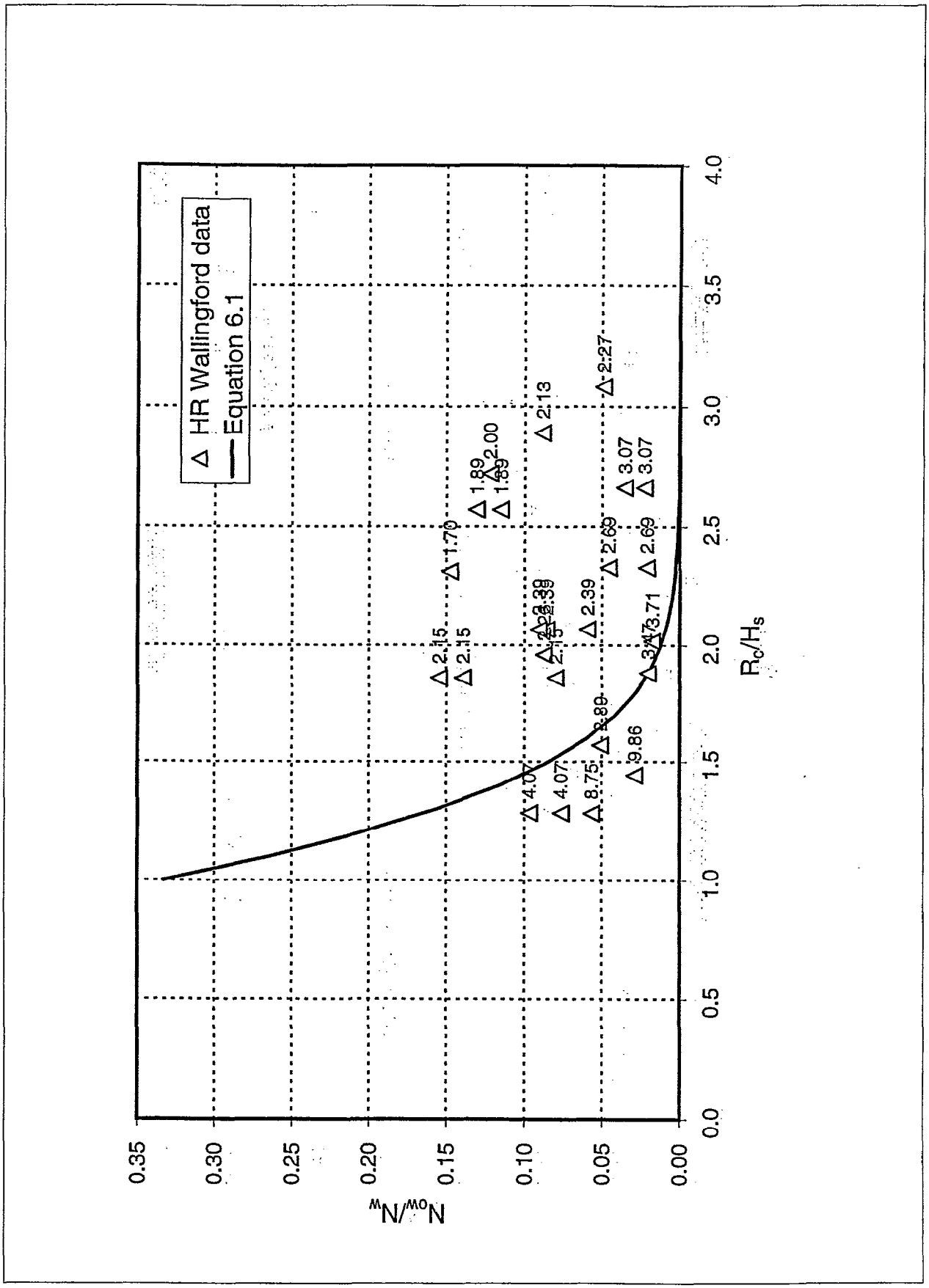

Figure 6.1 Number of waves overtopping a vertical wall, deep and shallow water

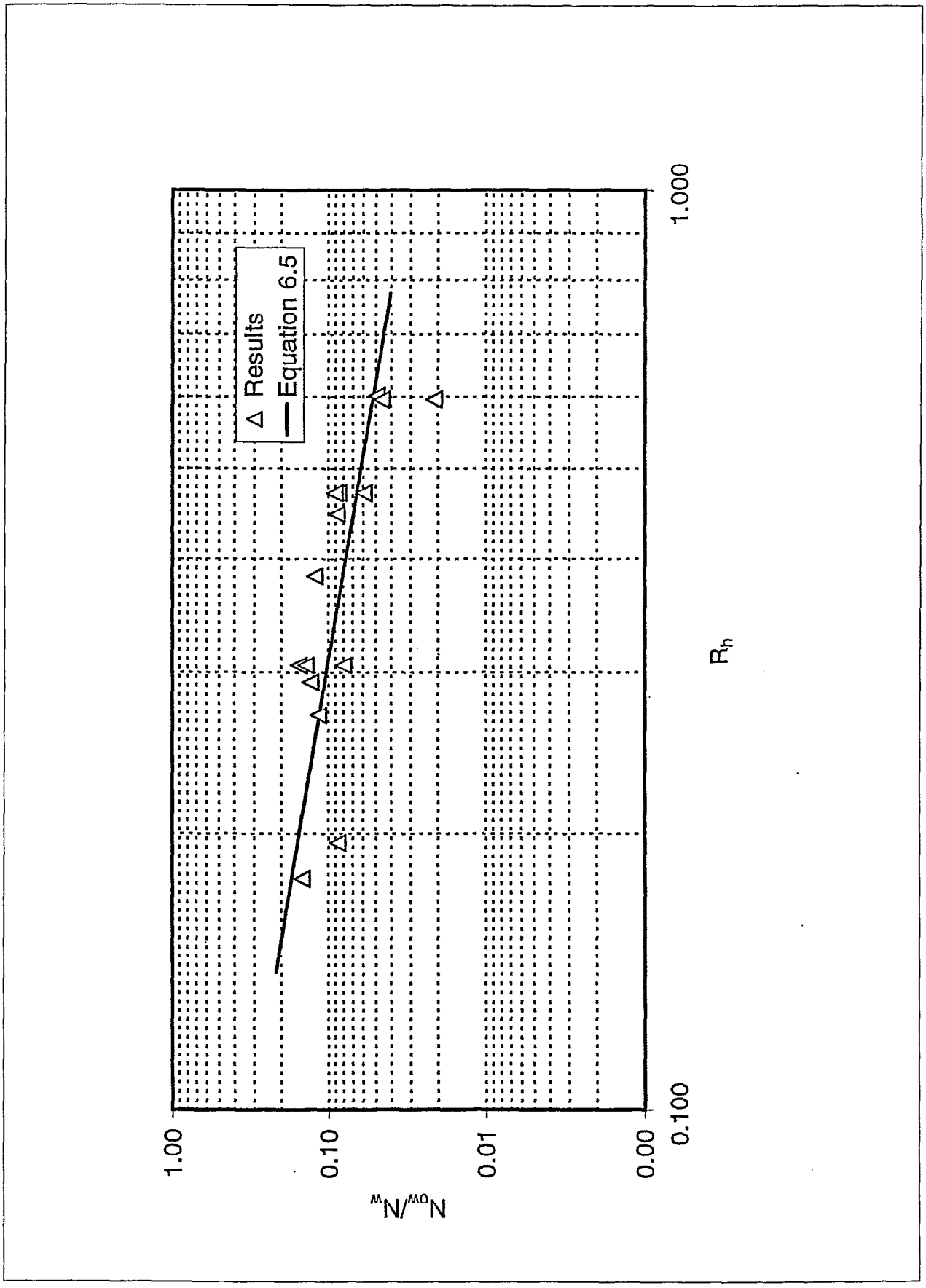

Figure 6.2 Number of waves overtopping a vertical wall, impacting waves only

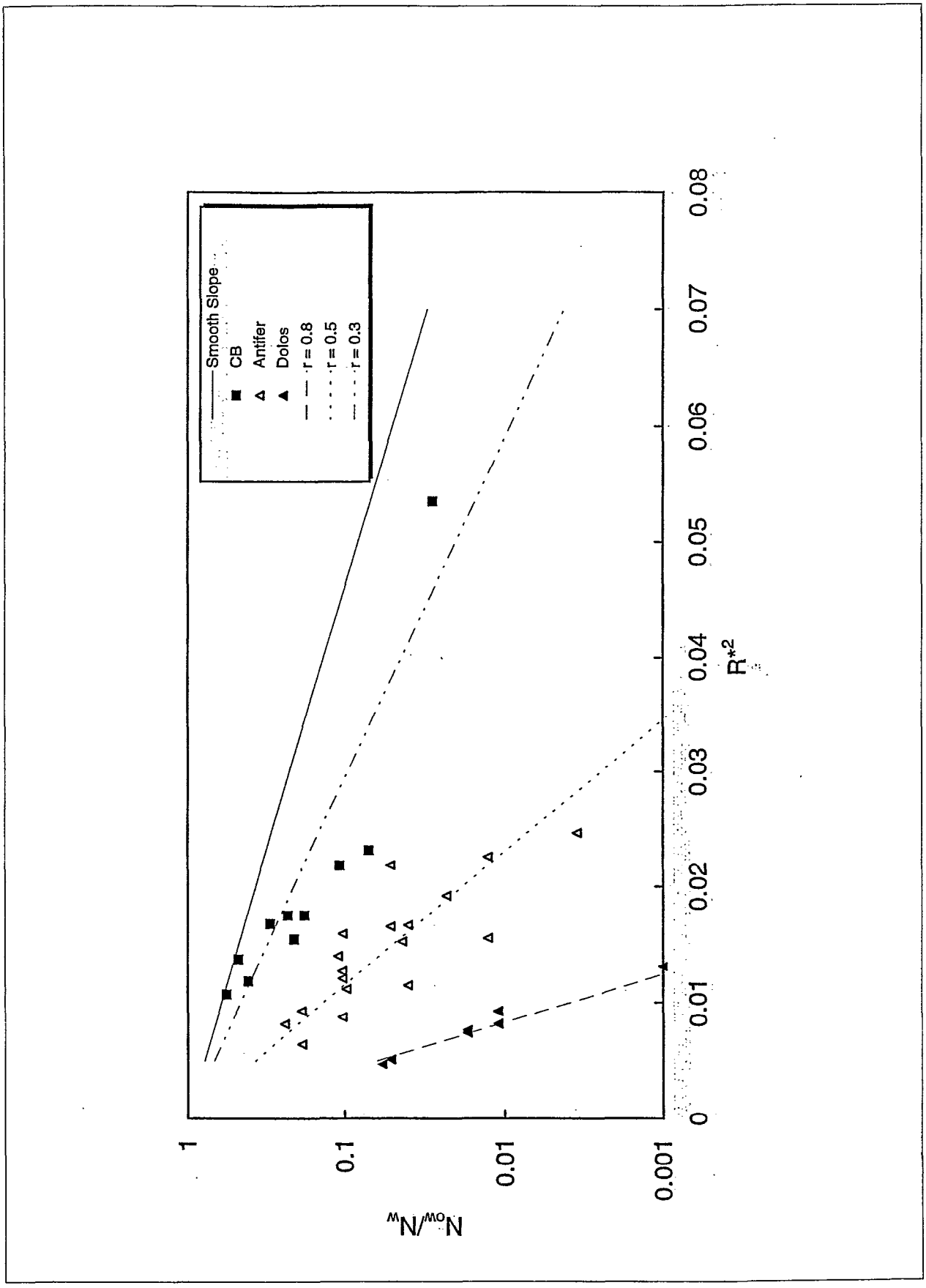

Figure 6.3 Number of waves overtopping simple armoured slopes

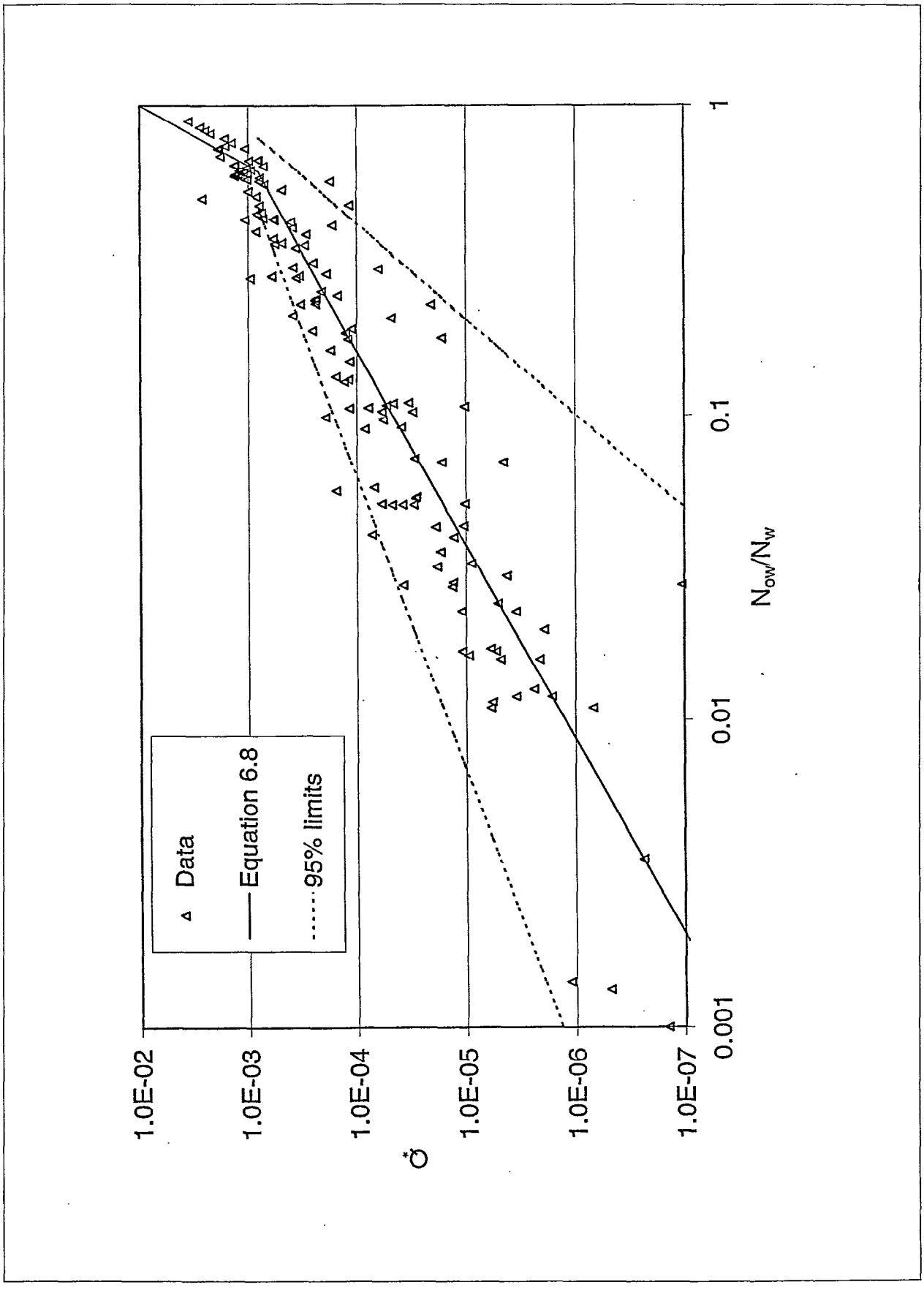

Figure 6.4 Number of waves overtopping sloped structures, all structural types

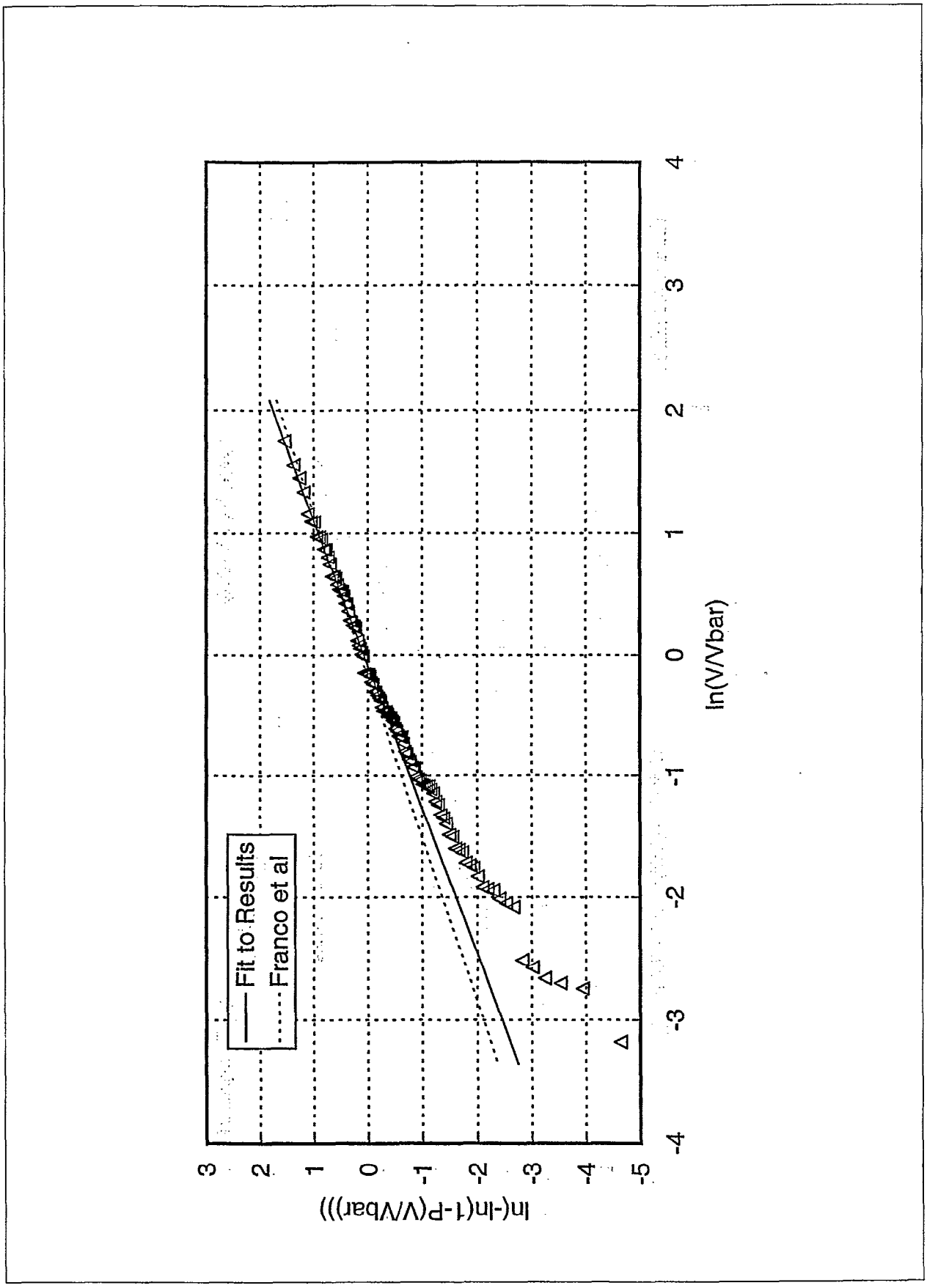

Figure 6.5 Distribution of individual overtopping volumes, reflecting waves

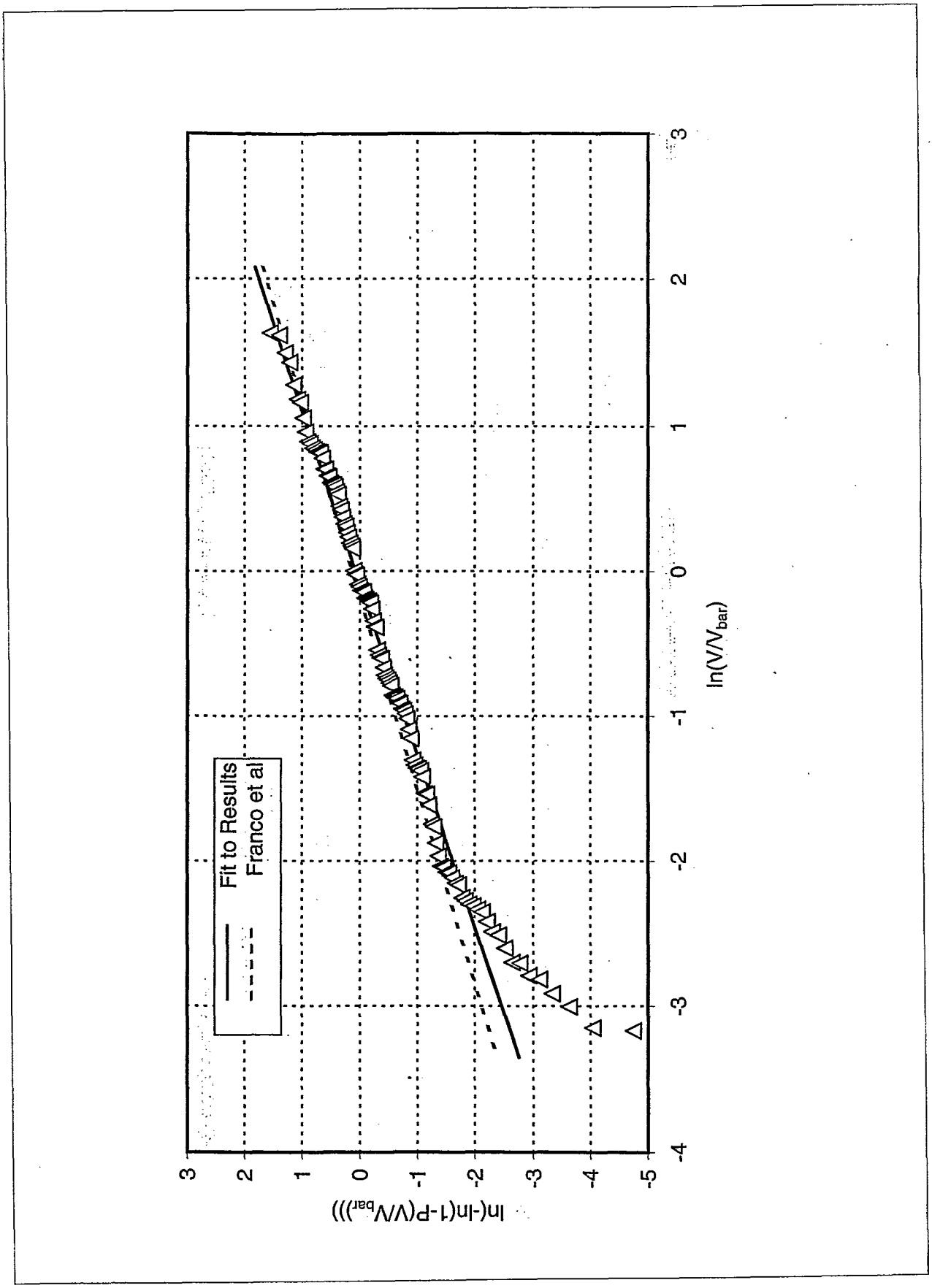

Figure 6.6 Distribution of individual overtopping volumes, impacting waves

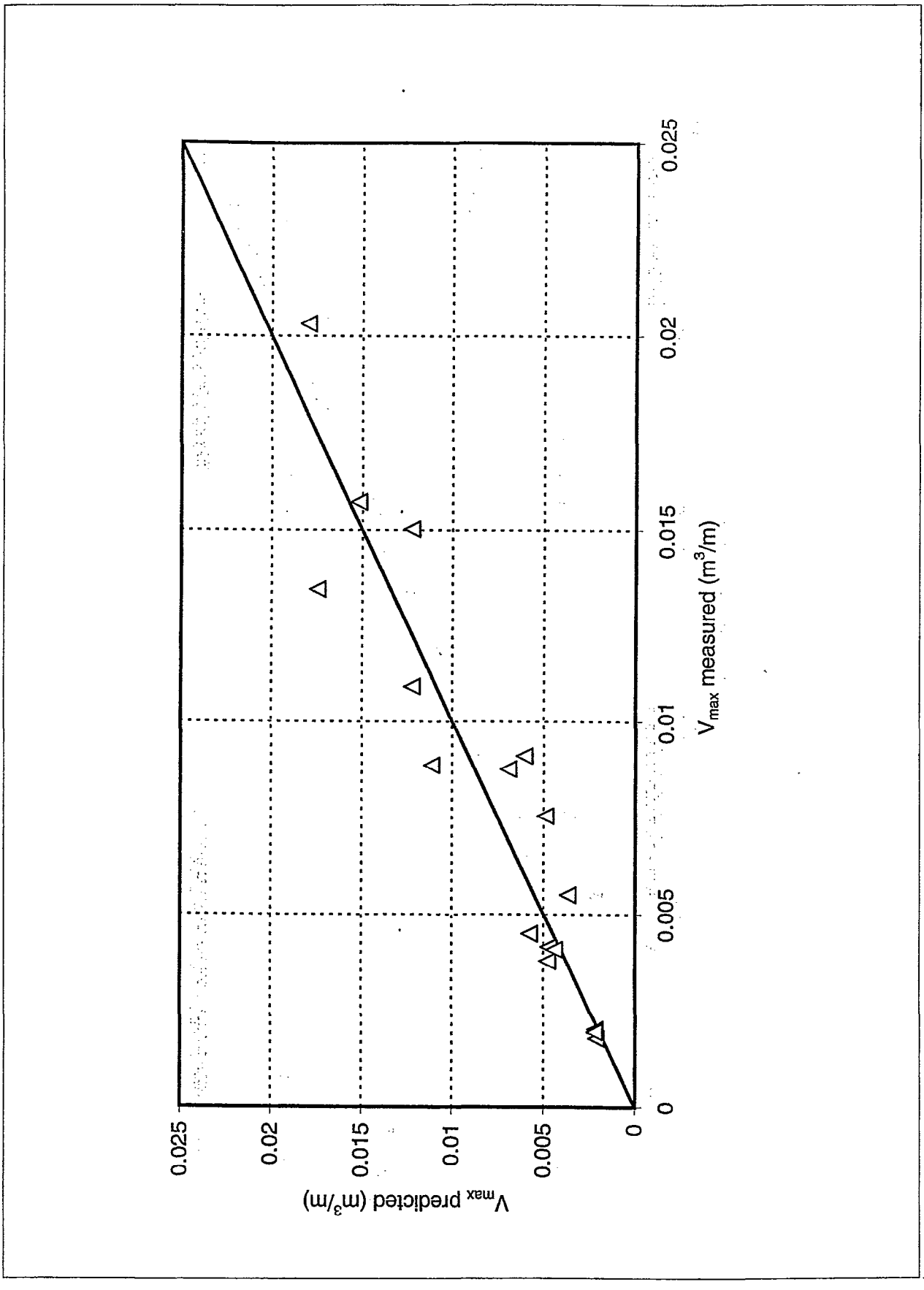

Figure 6.7 Predicted and measured maximum volume

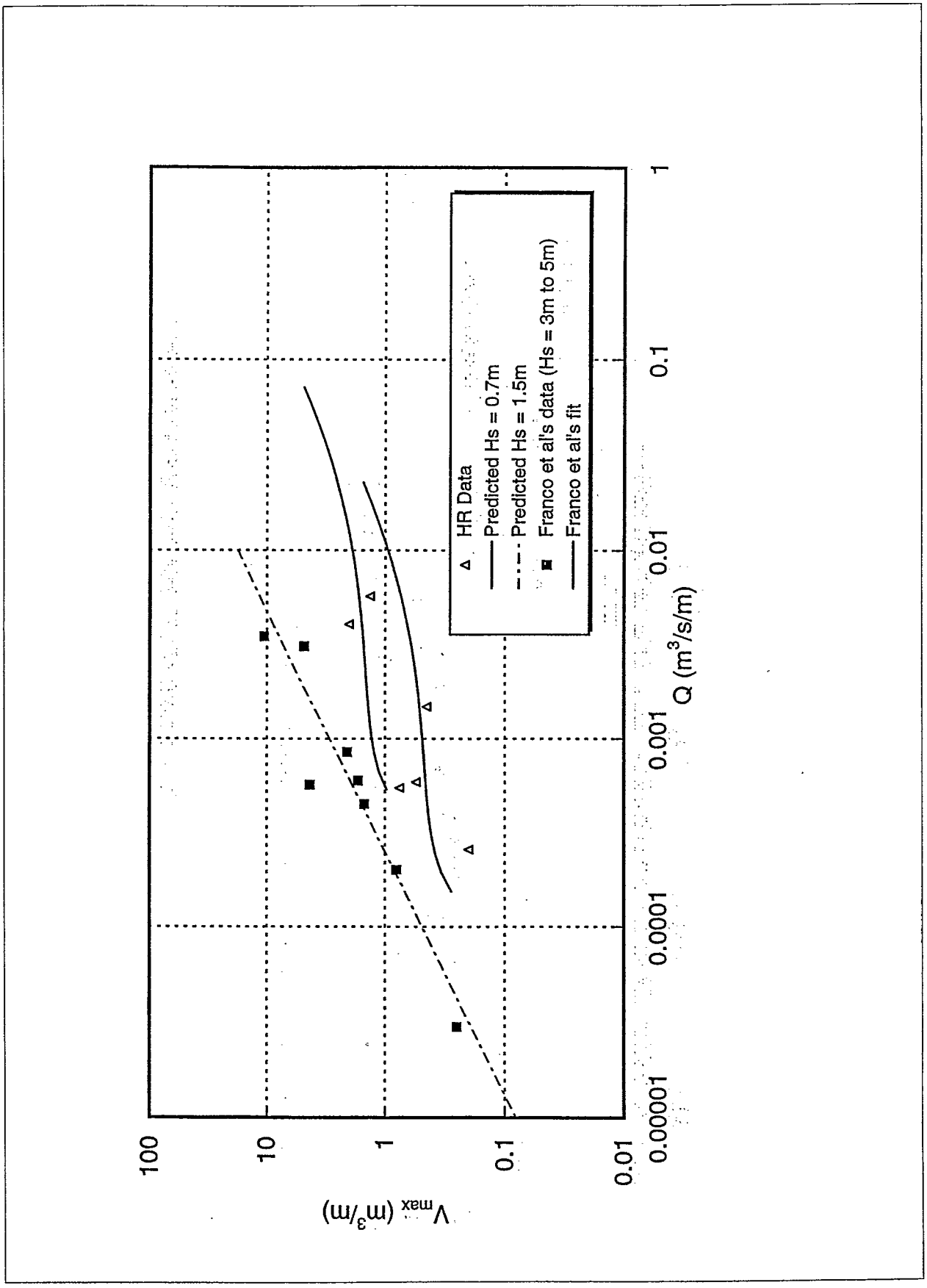

Figure 6.8 Relationship between mean discharge and peak event, (reflecting waves)

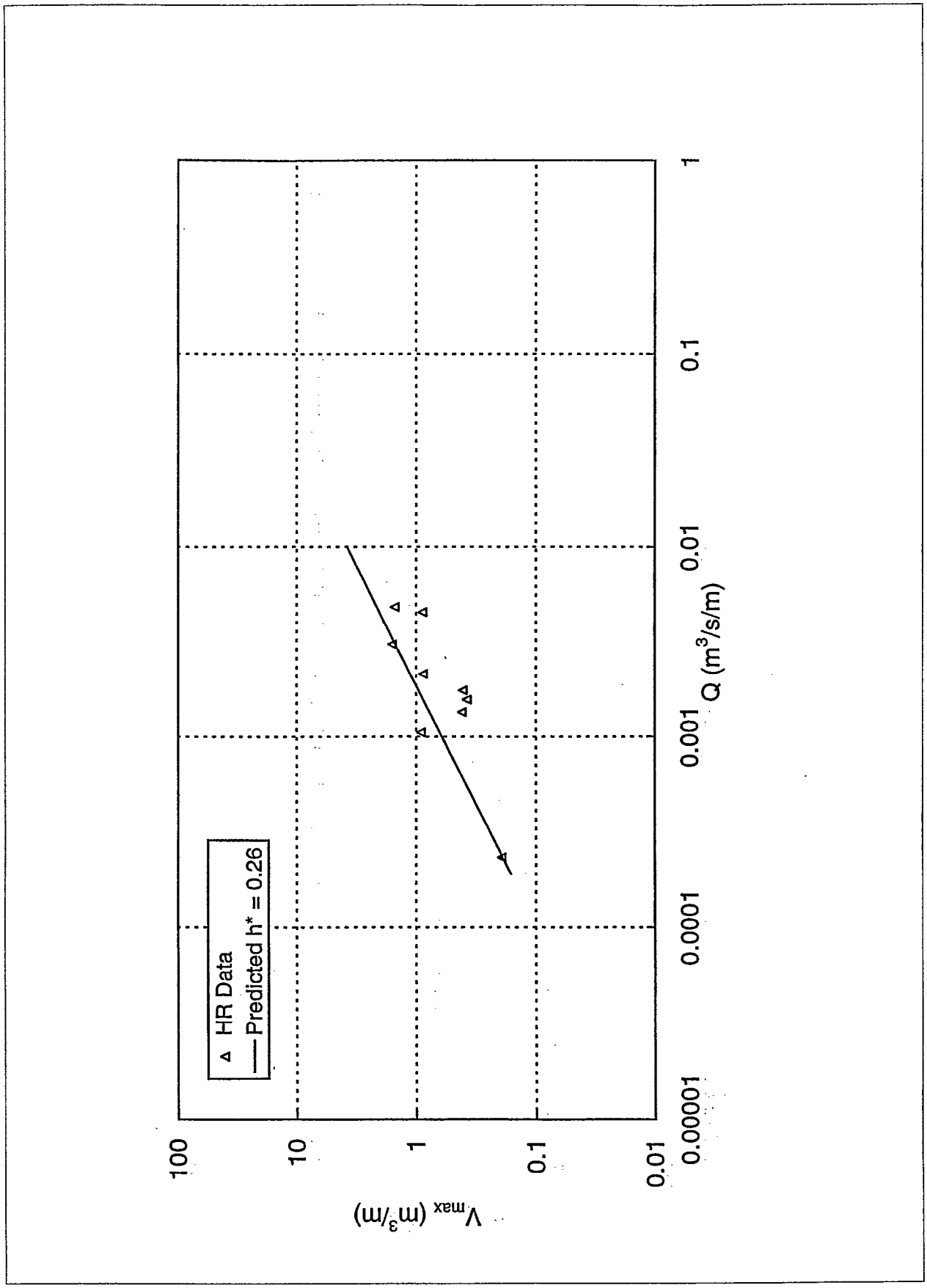

Figure 6.9 Relationship between mean discharge and peak event (impacting waves)

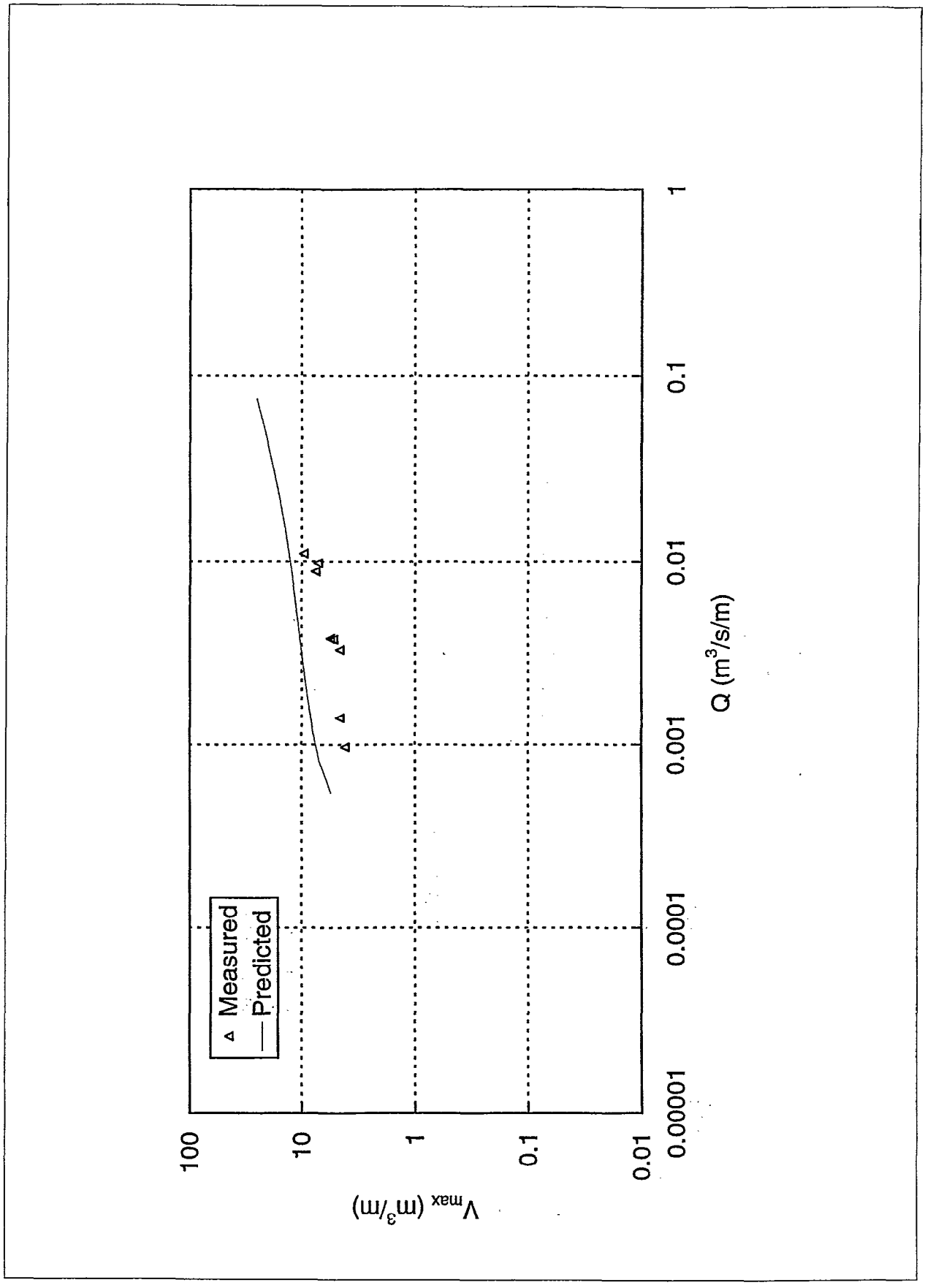

Figure 6.10 Relationship between mean discharge and peak event (structure A)

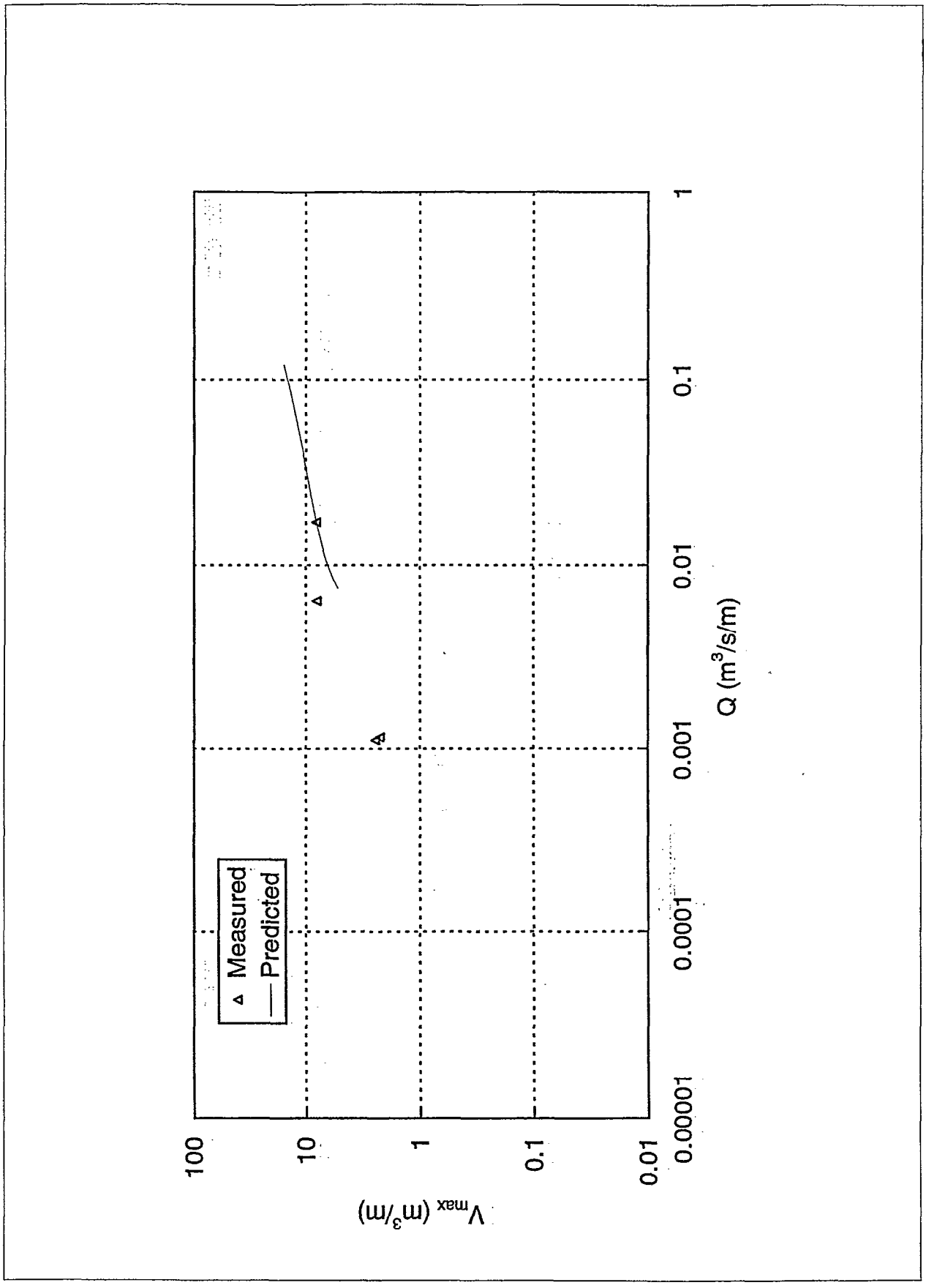

Figure 6.11 Relationship between mean discharge and peak event (structure B)

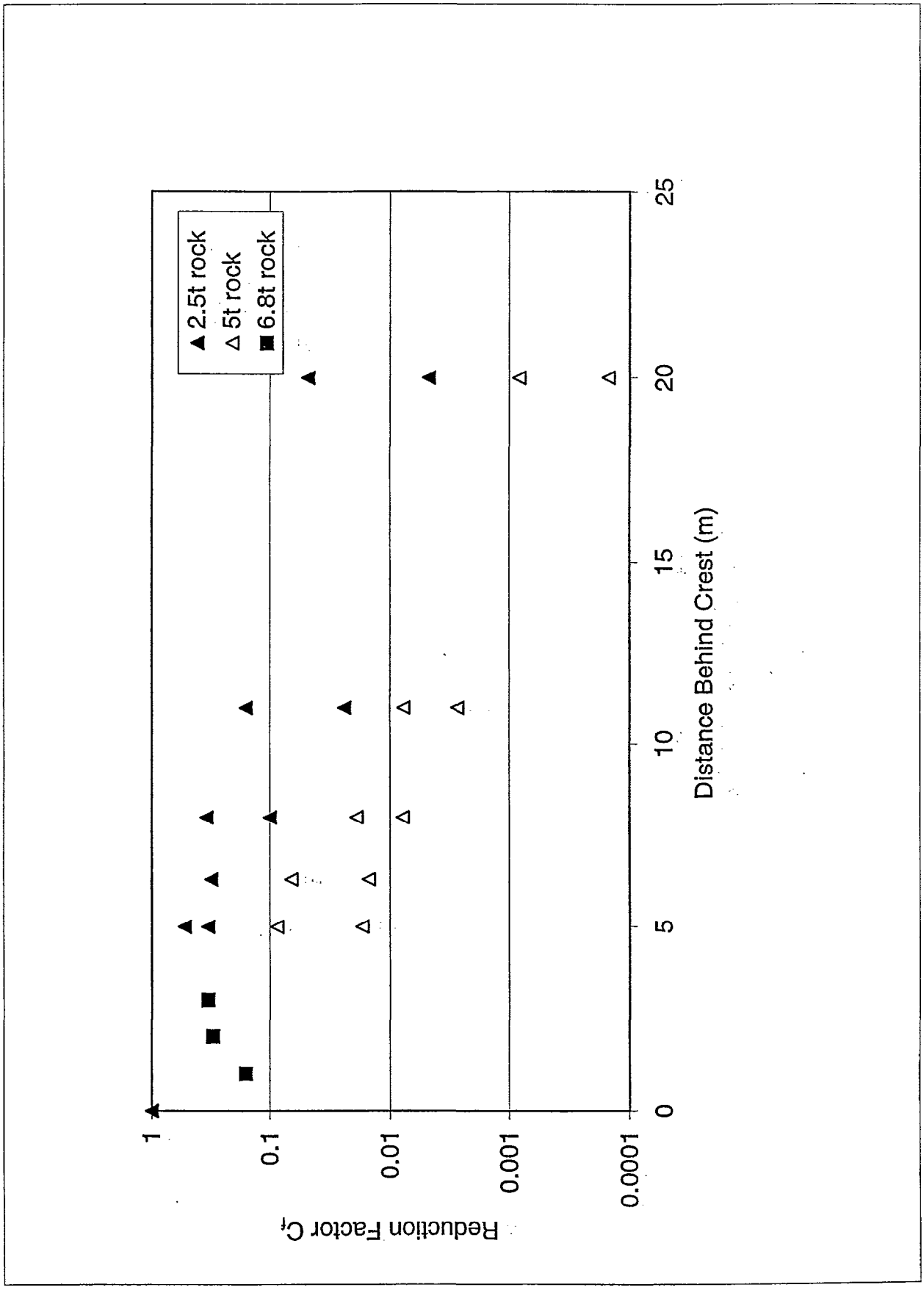

Figure 7.1 Effect of crest width on overtopping, Lowe (1991)

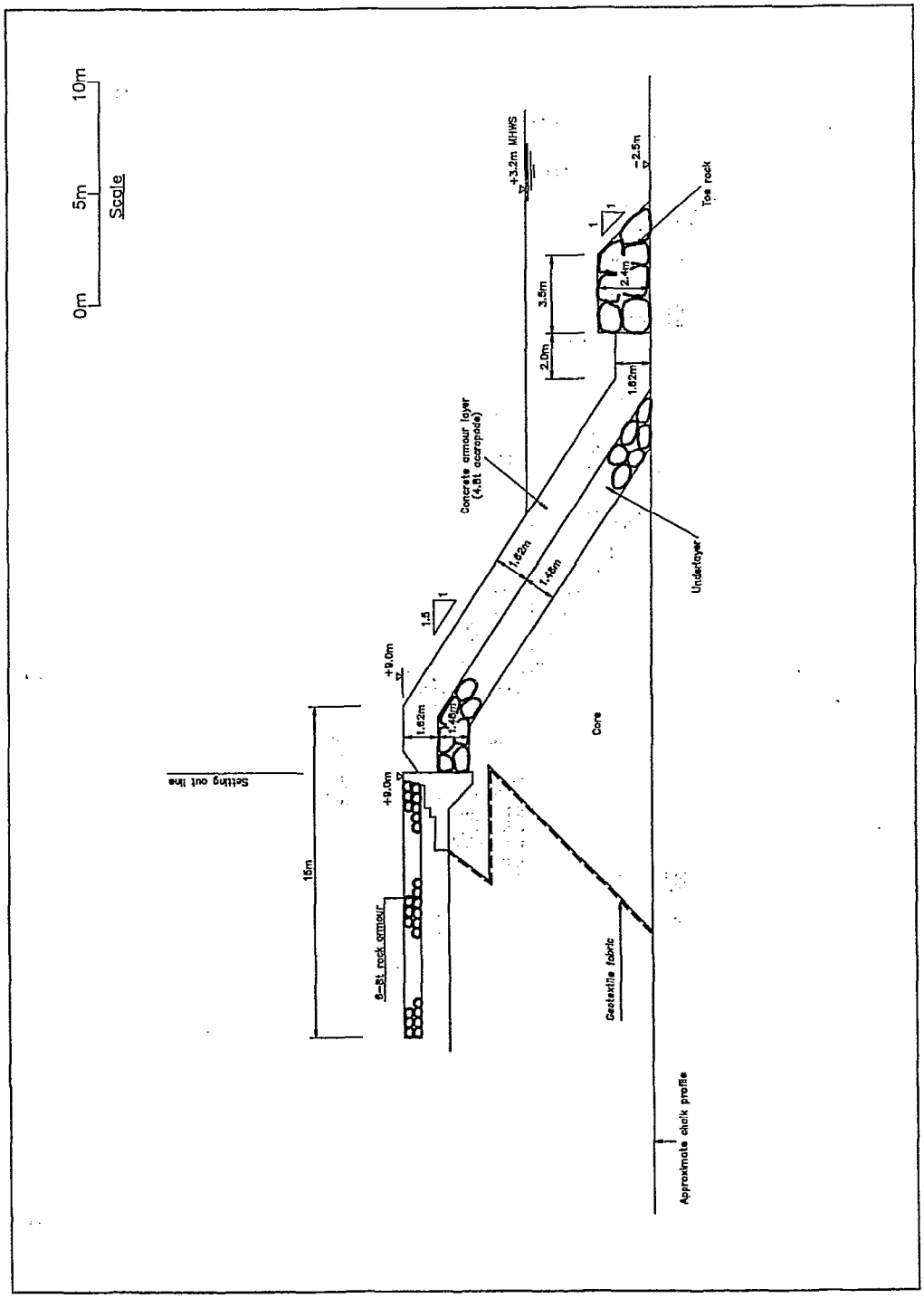

Figure 7.2 Accropode-armoured structure

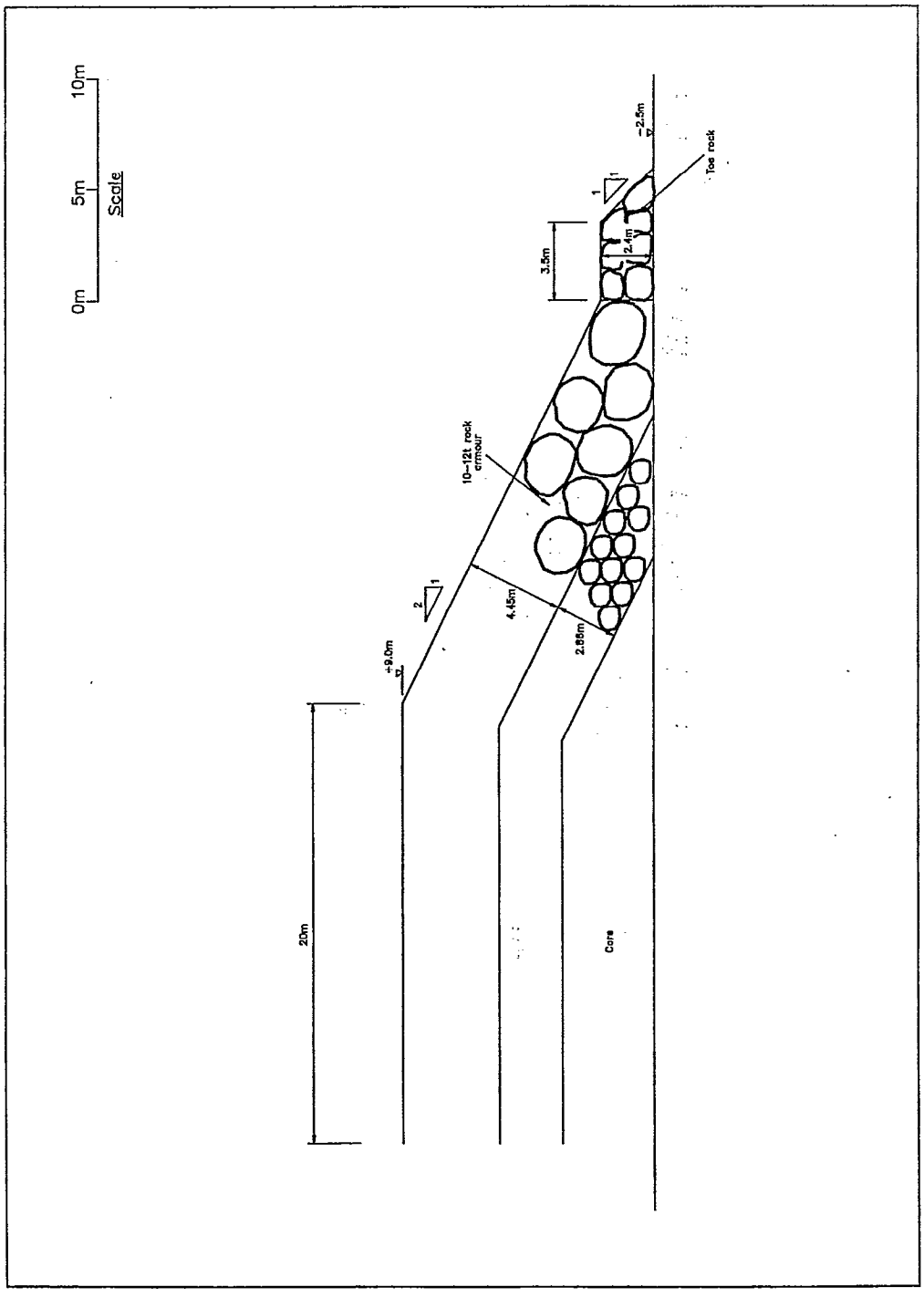

Figure 7.3 Rock armoured structure

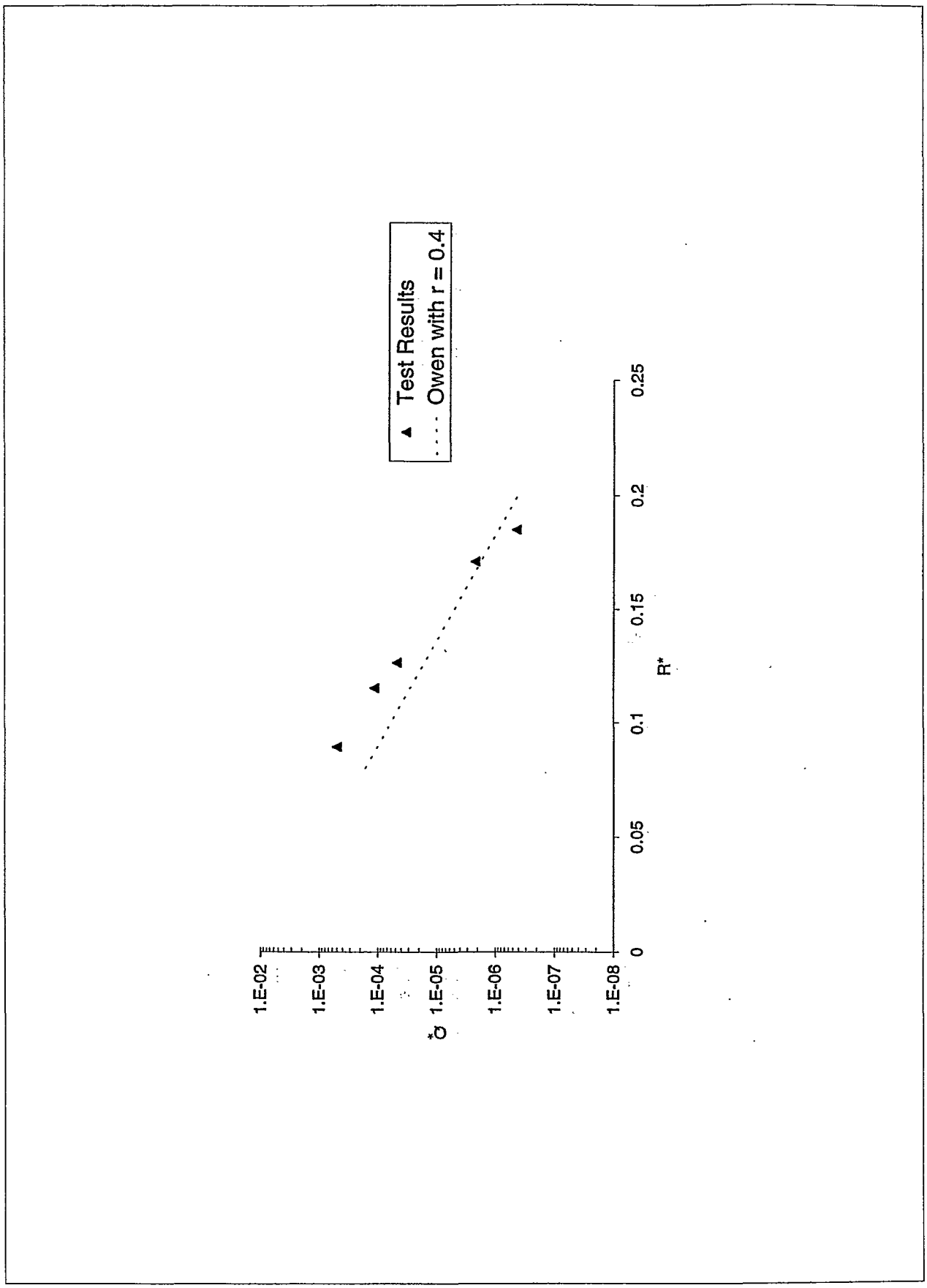

Figure 7.4 Overtopping without crest berm (Accropode armoured structure)

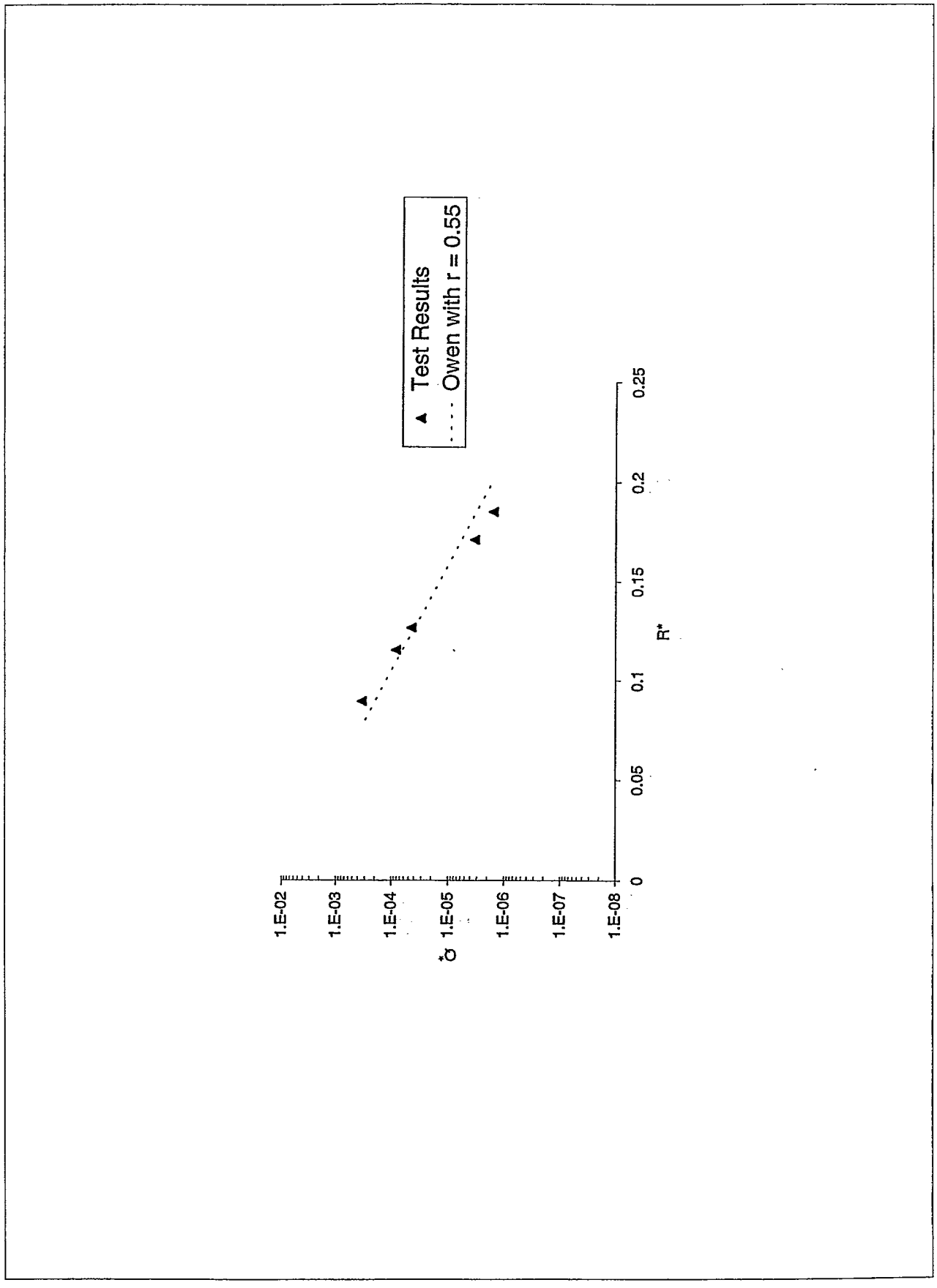

Figure 7.5 Overtopping without crest berm (rock armoured structure)

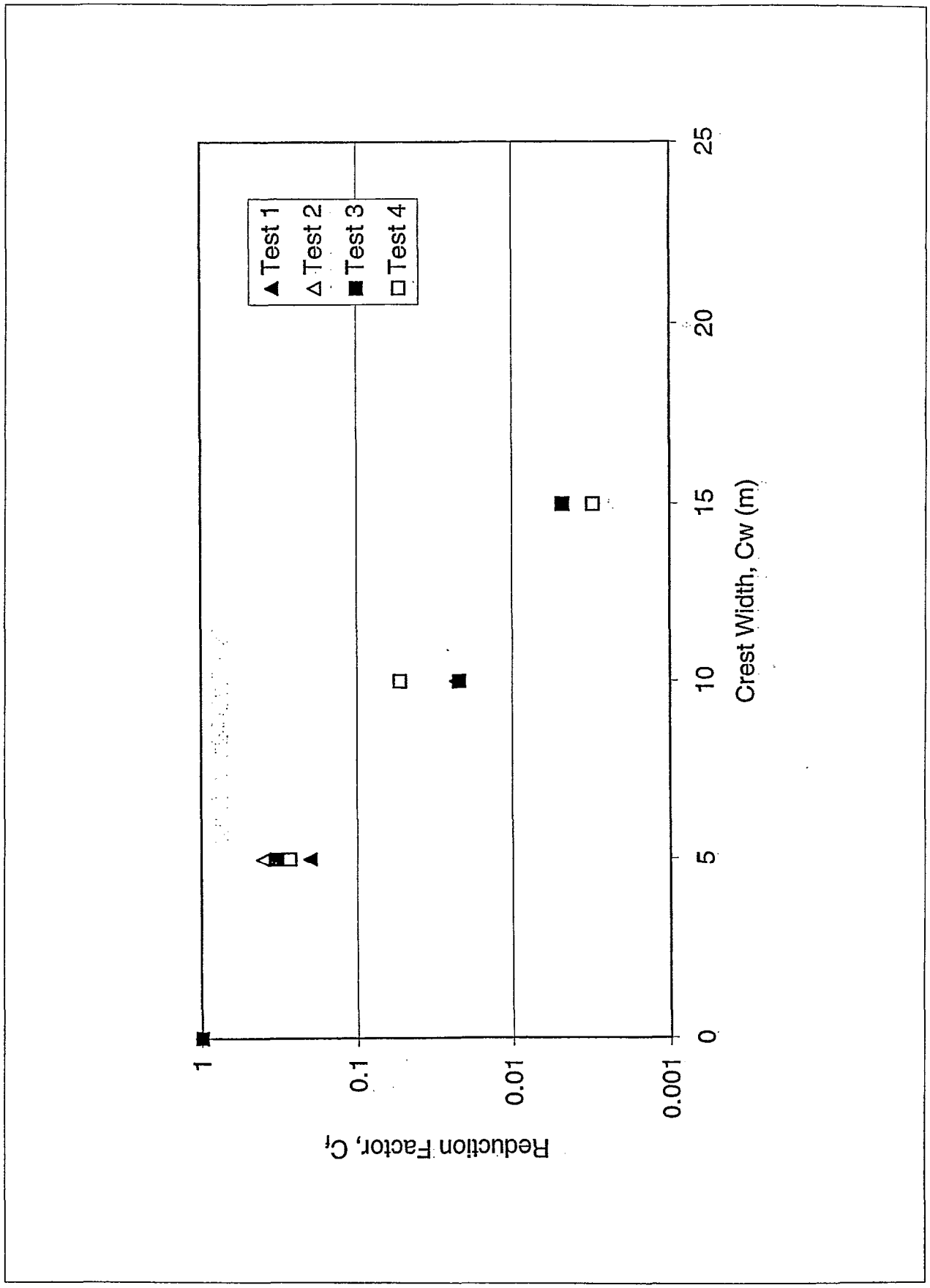

Figure 7.6 Effect of crest width on overtopping (Accropode armoured structure)

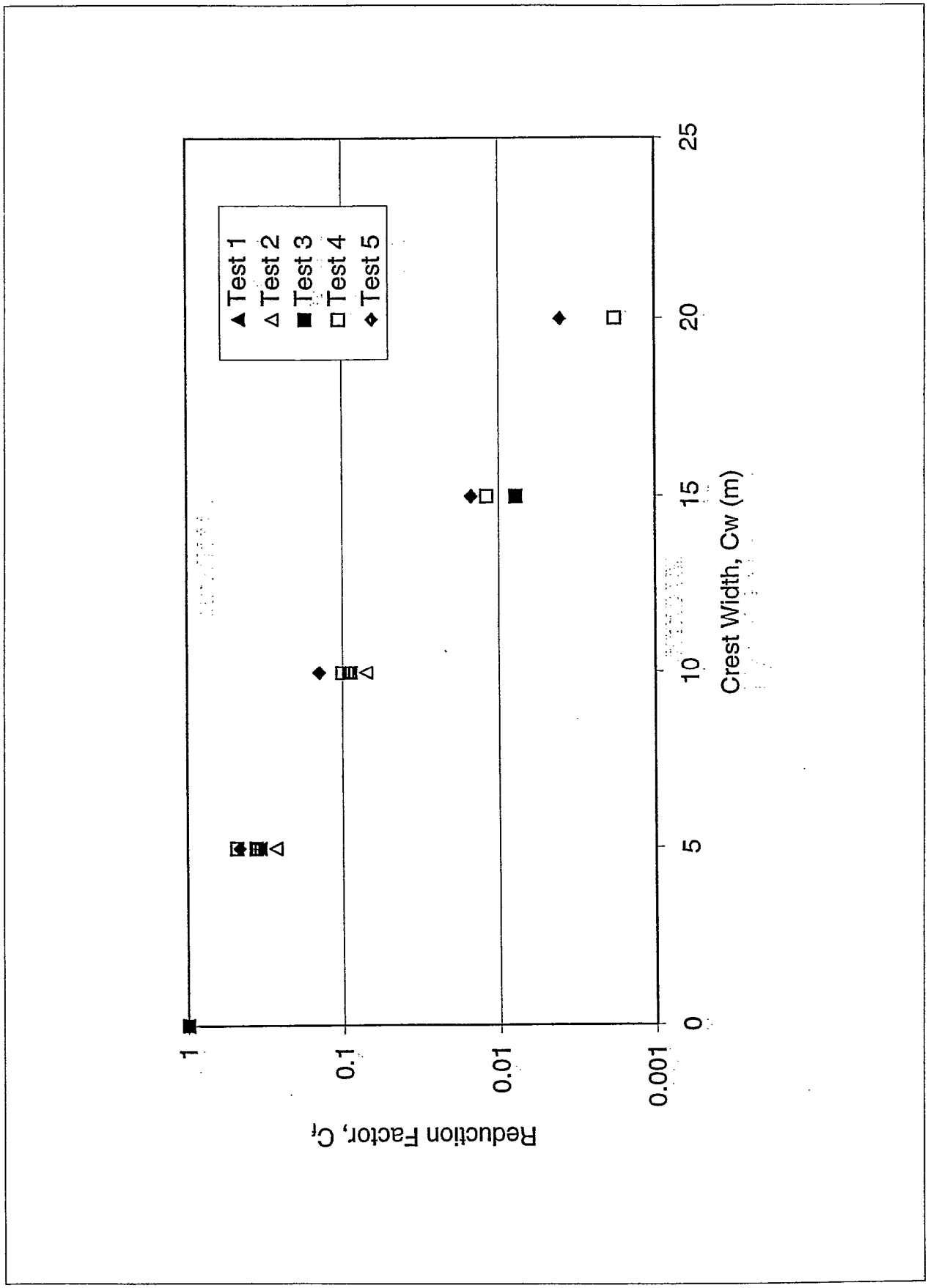

Figure 7.7 Effect of crest width on overtopping (rock armoured structure)

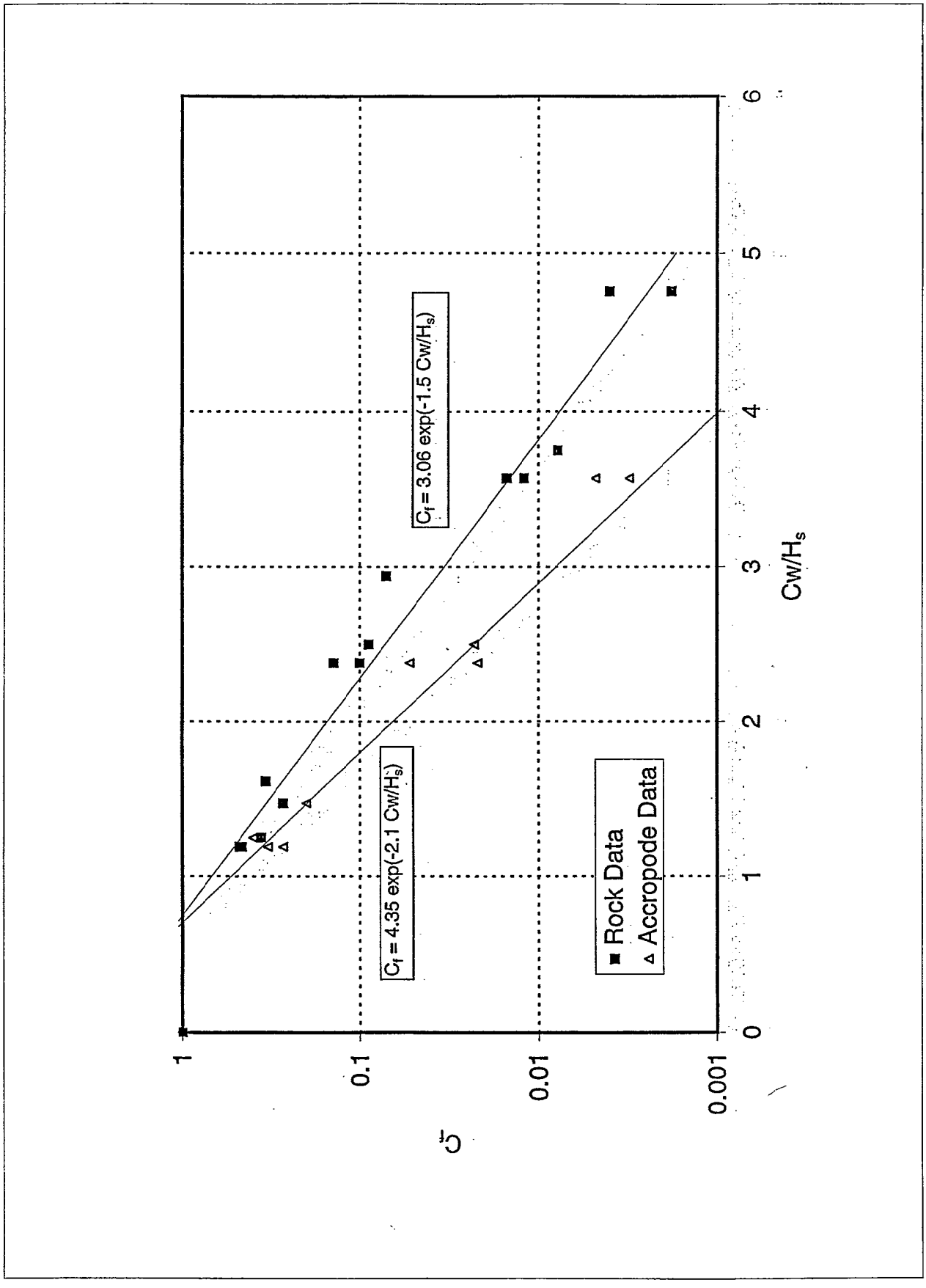

Figure 7.8 Effect of crest width on overtopping (dimensionless data)

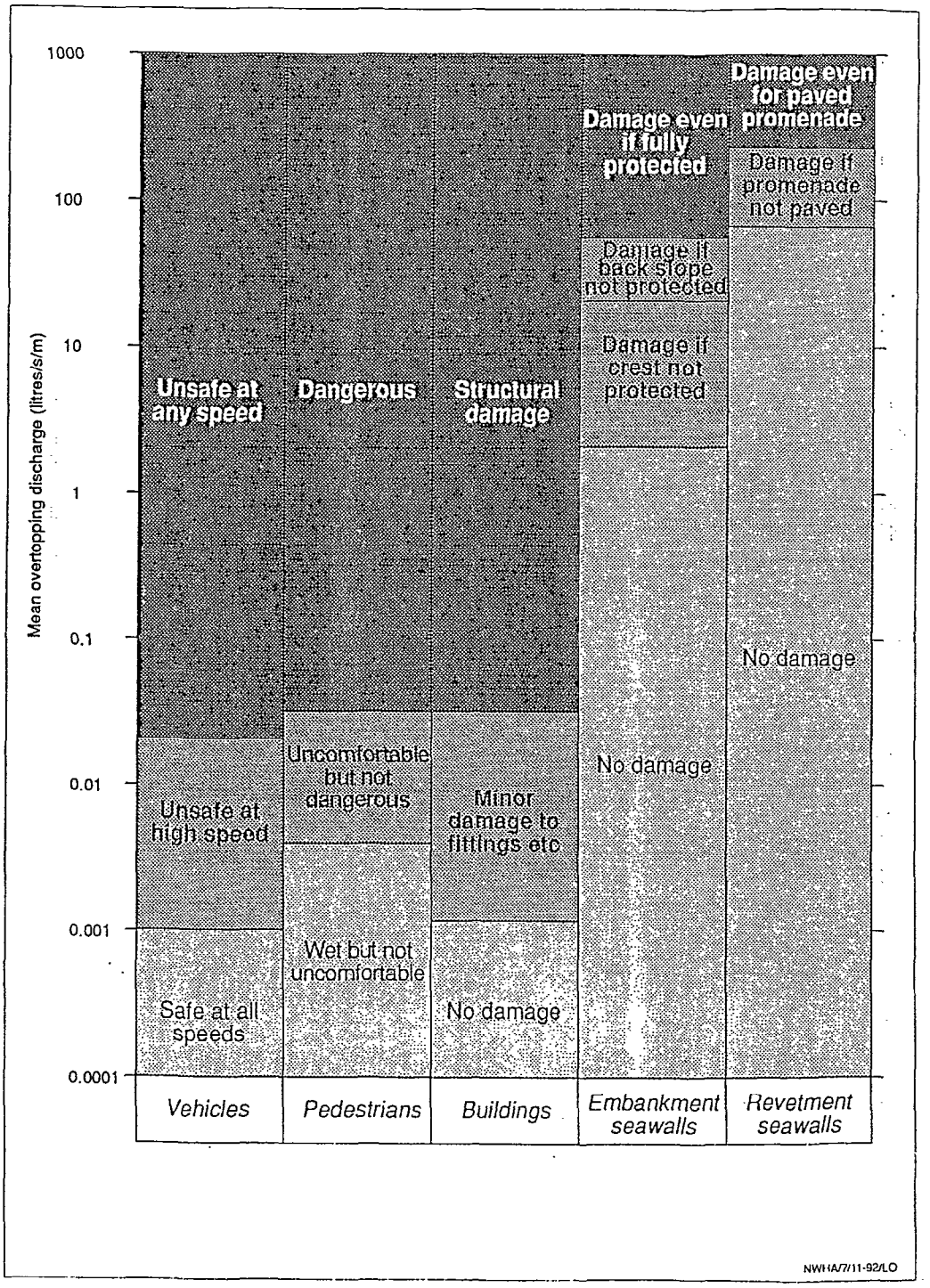

Figure 8.1 Tolerable mean discharges

Tables

Table 2.1 A and B coefficients : simply sloping seawalls

Seawall slope	A	B
1:1	7.94×10^{-3}	20.1
1:1.5	8.84×10^{-3}	19.9
1:2	9.39×10^{-3}	21.6
1:2.5	1.03×10^{-2}	24.5
1:3	1.09×10^{-2}	28.7
1:3.5	1.12×10^{-2}	34.1
1:4	1.16×10^{-2}	41.0
1:4.5	1.20×10^{-2}	47.7
1:5	1.31×10^{-2}	55.6

Table 2.2 A and B coefficients : bermed structures

Seawall Slope	Berm Elevation	Berm Width	A	B
1:1			6.40E-3	19.50
1:2	-4.0	10	9.11E-3	21.50
1:4			1.45E-2	41.10
1:1			3.40E-3	16.52
1:2	-2.0	5	9.80E-3	23.98
1:4			1.59E-2	46.63
1:1			1.63E-3	14.85
1:2	-2.0	10	2.14E-3	18.03
1:4			3.93E-3	41.92
1:1			8.80E-4	14.76
1:2	-2.0	20	2.00E-3	24.81
1:4			8.50E-3	50.40
1:1			3.80E-4	22.65
1:2	-2.0	40	5.00E-4	25.93
1:4			4.70E-3	51.23
1:1			2.40E-4	25.90
1:2	-2.0	80	3.80E-4	25.76
1:4			8.80E-4	58.24
1:1			1.55E-2	32.68
1:2	-1.0	5	1.90E-2	37.27
1:4			5.00E-2	70.32
1:1			9.25E-3	38.90
1:2	-1.0	10	3.39E-2	53.30
1:4			3.03E-2	79.60
1:1			7.50E-3	45.61
1:2	-1.0	20	3.40E-3	49.97
1:4			3.90E-3	61.57
1:1			1.20E-3	49.30
1:2	-1.0	40	2.35E-3	56.18
1:4			1.45E-4	63.43
1:1			4.10E-5	51.41
1:2	-1.0	80	6.60E-5	66.54
1:4			5.40E-5	71.59
1:1			8.25E-3	40.94
1:2	0.0	10	1.78E-2	52.80
1:4			1.13E-2	68.66

Table 2.3 Roughness coefficients

Type of seawall	Roughness coefficient, r
Smooth concrete or asphalt	1.0
Smooth concrete blocks with little or no vertical drainage	1.0
Stone blocks, pitched or mortared	0.95
Stepped	0.95
Turf	0.9-1.0
One layer of rock armour on impermeable base	0.8
One layer of rock armour on permeable base	0.55-0.60
Two layers of rock armour	0.50-0.55

Table 4.1 Wave overtopping studies at HR Wallingford and other European Laboratories

Wave overtopping studies at HR Wallingford and other European Laboratories.

Structure	Title		Date	Additional design details
Smooth sloping	101 Wave overtopping EX 924		Sept 1979	Plain, bermed
	102		Mar 1985	Crown wall, with wind duct/hood
	103		Feb 1990	Steps, recurve walls, berms
	104		April 1992	Recurve wall, crest berm
	105		July 1996	recurve wall
	106 Breakwater crown walls SR 146		Mar 1988	Plain, wave return walls
	107 Recurve wave return walls SR 261		Feb 1991	Crest berm, recurve walls
	108 3-d wave attack SR 396		Nov 1994	Berm, recurve
	109		Aug 1994	Plain
Rock armour	201		Mar 1985	Crown wall, with wind duct/hood
	202		June 1985	Plain
	203		April 1987	Plain
	204		Jan 1988	Crown wall, crest berm
	205		Dec 1989	Berm
	206		Dec 1990	
	207		Nov 1991	Berm
	208		Mar 1991	Rock armour detached mound protecting sea wall
	209		June 1991	Crest berm
	210		Sept 1991	Concave corner
	211		Oct 1991	Berm and wave return wall
	212		Oct 1991	Crest berm
	213		June 1992	Plain
	214		Sept 1993	Vertically composite
	215		Nov 1993	Composite slope
	216		Sept 1995	Vertically composite
	217		Jan 1996	Crown wall
	218		Oct 1995	Recurve wall
	219 Breakwater crown walls SR 146		Mar 1988	Plain, wave return & recurve walls
	220		July 1993	Various structure
	221		July 1993	Various structures
	222		July 1993	Various structures

Table 4.1 (continued)

Structure			Date	Additional design details
Concrete units				
	301		May 1985	Tetrapods / Antifers, crest berm,
	302		Aug 1985	Antifers
	303		Mar 1989	Seabees
	304		Dec 1989	Cubes
	305			Accropode / rock armour
	306		Dec 1991	T-blocks
	307		Dec 1991	Wavewalker / Efficient armour units
	308		July 1992	Dolos
	309		Oct 1992	New revetment block
	310		Dec 1993	Accropods, various structures and crown walls
	311		June 1994	Antifers
	312		Oct 1994	SHEDs
	313		Jan 1996	Accropodes, Dolosse, crown wall
	314		April 1996	Antifer
	315		Feb 1993	Cobs / Sheds
	316			Antifers
	317		July 1993	Conctrete
	318		July 1993	Antifers
	319		July 1993	Cubes, Dolos, Blocks, Cobs
	320		July 1993	Tetrapodes
	321		July 1993	Antifers
	322		July 1993	Antifers
Vertical walls	401		July 1990	Stepped / colonnade
	402		Dec 1990	
	403		May 1991	Vertical, berm and recurve
	404		July 1996	Stepped at base
	405		Feb 1993	Vertical wall
	406		Sept 1994	Vertical wall with and without wave screens
	407		Nov 1994	3-d wave attack
	408			Vertcal walls behind submerged rubble berms
Beach	501		Sept 1994	promenade 0.5m crown wall

Table 4.2 Type and scale of overtopping measurements undertaken during previous studies

Type and scale of overtopping measurements undertaken during previous studies

Title	bathymetry	slopes	No. tests	d / L min	d / L max	2d	3d	angle	spread	q bar	Now	w by w	q peak
101 Wave overtopping EX 924	1:20	1:1, 1:2, 1:4	200 ?	0.06	0.31	■	■	■		■	■		
102	1:10	1:3	12	0.15	0.21	■				■			
103	1:50	1:2.5, 1:2	30	0.03	0.06	■				■			
104	?	1:3	6	0.07	0.09		■			■			
105	1:20 beach	1:5	50	0.01	0.04	■				■			
106 Breakwater crown walls SR 146	1:52	1:2	20?	0.06	0.22	■				■			
107 Recurve wave return walls SR 261	?	1:2, 1:4	200	?	?	■				■			
108 3-d wave attack SR 396	1:50	1:2, 1:4	?	0.01	0.83		■			■			
109	1:32	1:2	9	0.047	0.18	■				■	■	■	
201	1:10	1:1.25	24	0.15	0.21	■				■			
202	?	1:1.5	4	0.05	0.08		■			■			
203	1:52	1:1.5, 1:2	8	0.08	0.09	■					■		
204	1:120	1:4	12	0.01	0.03	■				■			
205	1:50	1:2	17	0.04	0.07	■	■			■	■		
206	1:10	1:3, 1:4	20	0.02	0.03	■					■		
207	horizontal	1:3	20	0.23	0.42	■				■	■		
208	1:50	1:1.5, 1:2	33	0.02	0.05	■					■		
209	1:200	1:2	145	0.11	0.26	■				■			
210	1:200	1:2, 1:2.5	150	0.17	0.25		■	■		■			
211	1:200	1:2.5, 1:3	25	0.02	0.05	■				■			
212	?	1:4, 1:5	19	0.04	0.09	■				■			
213	1:100	1:5	8	0.03	0.05	■	■			■			■
214		1:3	195	0.04	0.11		■	■		■	■		
215	1:100	composite	205	0.04	0.28	■				■	■		
216	1:80	1:3	35	0.05	0.09		■	■		■			
217	?	1:1.5	50	0.002	0.02		■	■		■			
218	?	1:2	8	0.03	0.03	■				■			
219 Breakwater crown walls SR 146	1:52	1:2	80?	0.06	0.22	■				■			
220		1:1.5	90							■			
221		1:1.5	5								■		
222		1:1.5, 1:2, 1:2.5, 1:3	48							■			

Table 4.2 (continued)

	bathymetry	slopes	No. tests	d / L min	d / L max	2d	3d	angle	spread	q bar	Now	w by w	q peak
301		1:2.5. 1:1.67	120 ?										
302	1:20-1:35	1:133	35	0.05	0.12								
303	1:10	1:1.5	10	0.06	0.15								
304	1:50	1:1.5	5	0.04	0.07								
305			6										
306	1:100	1:1, 1:2 1:4	23	0.04	0.12								
307	?	1:1.5	64	0.02	0.17								
308	?	1:1.5	35	0.02	0.07								
309	1:100	1:2	3	0.08	0.16								
310			9										
311	1:90	1:2	5	0.06	0.09								
312	1:75	1:1.5	55	0.04	0.10								
313	?	1:1.5	36	0.002	0.02								
314	?	1:2	10	0.03	0.07								
315	1:50	1:1.33	100 ?										
316		various	25 ?										
317		1:1.33, 1:1.75, 1:2	25										
318		1:2	21										
319		1:1.5, 1:3	168										
320		1:1.5	54										
321		1:4	5										
322		1:1.5	2										
401	1:100	vertical	21	0.08	0.09								
402	1:10	vertical	?	0.02	0.03								
403	?	vertical	30	0.06	0.13								
404	?	vertical	15	0.01	0.04								
405	1:10, 1:30, 1:100	vertical	?	?	?								
406		vertical											
407	1:50	vertical	?	0.01	0.83								
408													
501	?	1:7.5 beach	18										

Key: yes / no / ? uncertain

angle wave obliquity tested
spread wave spreading tested
d/L approx depth / wave length
w by w wave by wave
Now number of overtopping waves
q bar mean overtopping discharge

Table 5.1 Sections tested by Bradbury et al

Test Section	Crest Wall Level (m)	Armour Crest Level(m)	Cw
4	1.70	1.555	0.15
5	1.76	1.555	0.15
6	1.64	1.555	0.15
7	1.67	1.555	0.15
8	1.64	1.600	0.15
9	1.64	1.555	0.15
11	1.64	1.555	0.30
13	1.64	1.555	0.15
14 (Owen & Steele)	2.00	2.000	0.15

Table 5.2 Regression analysis to equation of form $D_f = X A_{*c}^{Y}$

W*h	Number of results	X	Y	r^2
3.73	11	2.82e-11	-4.80	0.592
2.64	10	2.25e-09	-4.07	0.510
2.09	11	6.49e-11	-5.92	0.565
1.55	20	2.12e-14	-7.67	0.540
1.32	7	5.67e-02	1.37	0.142
0.94	6	5.17e-04	-1.12	0.110
0.74	8	2.08e-03	-0.76	0.011
0.55	16	3.07e-04	-2.07	0.138
0.40	11	2.72e-08	-5.09	0.392
0.20	8	2.11e-04	-2.91	0.129

Table 5.3 Regression analysis to equation of form $Df = X\ Q_{*b}^{\ Y}$

W*h	Number of results	X	Y	r^2
3.73	11	3.21e02	2.12	0.543
2.64	10	1.72e02	1.73	0.440
2.09	11	8.85e04	2.63	0.525
1.55	20	7.26e07	3.65	0.538
1.32	7	1.39e-04	-0.26	0.160
0.94	6	5.33e-02	0.19	0.092
0.74	8	3.59e-02	0.09	0.005
0.55	16	1.69e00	0.35	0.117
0.40	11	2.00e03	1.29	0.389
0.20	8	9.01e00	0.36	0.097

Table 7.1 Herbert & Reeves (1991) overtopping results

Test code (rock size)	H_{so} (m)	T_{mo} (s)	Q_0 (l/s/m)	Q_{10} (l/s/m)	C_f
A1a (6-10t)	3.84	8.31	0.00	0.00	-
A1b	5.99	10.33	0.33	0.04	0.12
A1c	6.10	10.57	1.05	0.07	0.067
A2a	5.98	11.38	0.81	0.08	0.10
A2b	6.03	11.75	1.62	0.16	0.10
A3a	6.02	12.18	0.61	0.07	0.11
A3b	5.87	12.54	1.22	0.15	0.12
B1a (9-13t)	3.84	8.31	0.00	0.00	-
B1b	5.99	10.33	0.08	0.01	0.13
B1c	6.10	10.57	0.28	0.06	0.21
B2a	5.98	11.38	0.20	0.05	0.25
B2b	6.03	11.75	0.32	0.05	0.16
B3a	6.02	12.18	0.12	0.04	0.33
B3b	5.87	12.54	0.37	0.06	0.16

Table 7.2 Lowe (1991) overtopping results

Test code (rock size)	SWL (mCD)	H_{so} (m)	T_{mo} (s)	Cw (m)	Q_w (l/s/m)	C_f
Test 1 (2.5t)	4	3.21	5.7	0	30	1.00
				5	10	0.33
				6.3	9.4	0.31
				8	2.9	0.10
				11	0.71	0.024
				20	0.14	0.0047
Test 2 (2.5t)	4	3.68	5.98	0	50	1.00
				5	26	0.52
				6.3	-	-
				8	17	0.34
				11	8.2	0.16
				20	2.4	0.048
Test 3 (5t)	3.25	3.26	6.08	0	82	1.00
				5	1.4	0.017
				6.3	1.2	0.015
				8	0.64	0.0078
				11	0.22	0.0027
				20	0.012	0.00015
Test 3 (5t)	4	3.21	5.7	0	53.1	1.00
				5	4.6	0.087
				6.3	3.5	0.066
				8	0.99	0.019
				11	0.41	0.0077
				20	0.044	0.00083

Test 1 (6.8t)	2.50	3.23	5.82	0	0.38	1.00
				5	0.062	0.16
				6.3	0.047	0.12
				8	0.029	0.076
				11	0.0082	0.022
				20	0	0.00
Test 2 (6.8t)	3.25	2.57	5.46	0	0.054	1.00
				5	0.016	0.30
				6.3	0.013	0.24
				8	0.008	0.15
				11	0.0015	0.028
				20	0.00037	0.0069
Test 3 (6.8t)	4.00	2.64	5.48	0	0.6017	1.00
				5	0.2	0.33
				6.3	0.11	0.18
				8	0.06	0.010
				11	0.023	0.038
				20	0.003	0.0050

Table 7.3 Overtopping test wave conditions

Test code	SWL (mOD)	H_s (m)	T_m (s)
1	3.18	3.10	6.00
2	3.18	3.40	6.20
3	4.23	4.00	6.40
4	4.49	4.20	6.50
5	5.34	4.20	6.90

Table 7.4 Overtopping test results

Test	Crest Width (m)	Accropode Q (l/s/m)	Accropode C_f	Rock Q (l/s/m)	Rock C_f
1	0	0.00	-	0.29	1.00
	5	0.00	-	0.10	0.34
	10	0.00	-	0.00	-
	15	0.00	-	0.00	-
	20	-	-	0.00	-
2	0	0.46	1.00	0.70	1.00
	5	0.09	0.20	0.19	0.27
	10	0.00	-	0.05	0.071
	15	0.00	-	0.00	-
	20	-	-	0.00	-
3	0	12.00	1.00	11.48	1.00
	5	4.76	0.40	4.14	0.36
	10	0.27	0.023	1.02	0.089
	15	0.00	-	0.09	0.0078
	20	-	-	0.00	-
4	0	31.00	1.00	22.50	1.00
	5	10.30	0.33	10.86	0.48
	10	0.69	0.022	2.34	0.10
	15	0.15	0.0048	0.26	0.012
	20	-	-	0.04	0.0018
5	0	145.30	1.00	97.26	1.00
	5	39.00	0.27	44.75	0.46
	10	7.70	0.053	14.08	0.14
	15	0.45	0.0031	1.47	0.015
	20	-	-	0.39	0.0040